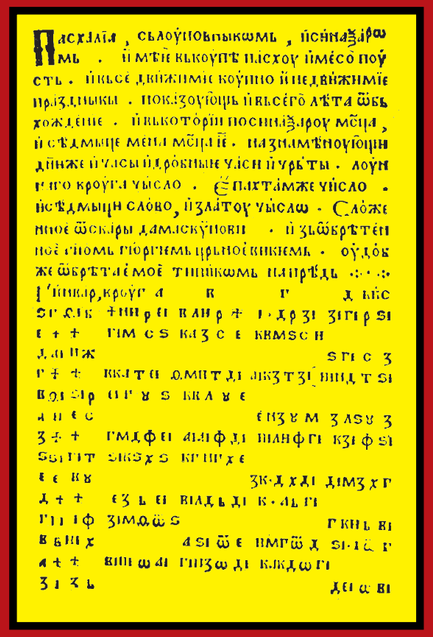

VOLUME XLII-2018

MATHEMATICA MONTISNIGRI

# MATHEMATICA MONTISNIGRI

VOLUME XLII-- 2018

The journal Mathematica Montisnigri is published by the Society of mathematicians and physicists of Montenegro and Department of Mathematics of The University of Montenegro.

Editors:

V. DAŠIĆ
University of Montenegro,
Podgorica, Montenegro

R. MEŠTROVIĆ
University of Montenegro,
Kotor, Montenegro

F. P. VASILJEV
Lomonosov Moscow State University,
Moscow, Russia

S. PILIPOVIĆ
University of Novi Sad,
Novi Sad, Serbia

S. A. KARABASOV
Queen Mary, University of London,
London, United Kingdom

RICARD BORRELL POL
Computer Applications in Science and Engineering (CASE), Barcelona Supercomputing Center (BSC-CNS, Barcelona, Spain

O.N. KOROLEVA
Keldysh Institute of Applied Mathematics
of RAS, Moscow, Russia

U. SEMMLER
Fraunhofer-Institut
für Werkzeugmaschinen und Umformtechnik,
Chemnitz, Deutschland

M. JAĆIMOVIĆ
University of Montenegro,
Podgorica, Montenegro

V. A. SADOVNICHIY
Lomonosov Moscow State University,
Moscow, Russia

V. N. CHUBARIKHOV
Lomonosov Moscow State University,
Moscow, Russia

M. MARJANOVIĆ
University of Belgrade,
Belgrade, Serbia

R. ŠĆEPANOVIĆ
University of Montenegro,
Podgorica, Montenegro

Editor in Chief:

Ž. PAVIĆEVIĆ
University of Montenegro,
Podgorica, Montenegro

V. I. MAZHUKIN
Keldysh Institute of Applied Mathematics
of RAS, Moscow, Russia

Editorial Secretary:

G. POPIVODA
University of Montenegro,
Podgorica, Montenegro

S. TOMOVIĆ
University of Montenegro,
Podgorica, Montenegro

L. BULATOVIĆ
University of Montenegro,
Podgorica, Montenegro

At the front page there is a detail from the first known text in astronomy-mathematics that appeared in Montenegro. It was published in the book Psaltir in 1495. Psaltir was printed on September 22, 1495 in the printing shop of Djurdje Crnojević which was the first printing shop of South Slavs. In the book six, volume 23, Djurdje Crnojević, the sovereign of Montenegro, adapted the Tables of Jovan Damaskin and wrote the Paschalia with lunar calendar. He worked out a series of rules regarding the counting of days of Easter celebrations. Djurdje's Paschalia Tables can be found in numerous written and printed books of later period.

The journal *Mathematica Montisnigri* publishes original scientific works from all fields of mathematics and mathemat ical modelling which comprise new and significant results with complete proofs, which are of interest for a larger mathematical community. It also contains expository articles. The journal does not publish works of polemical or methodological interest, as well as works that have been offered for publishing in other journals. The journal publishes papers in English, Russian, French and German. It is usually issued thrice a year.

*Instructions to the authors:*

Authors should submit the Manuscript electronically at the address:

**zarkop@ac.me,**
**borkov@ac.me,**
**orgcom@LPpM3.ru.**

The paper should be prepared in MS Word by the instructions, which can be found at the web page: **lppm3.ru/en/pub/manusc** .

The file has to be translated into Portable Document Format (PDF) before submission to the Editorial board of the journal.

The papers should have a precise and informative title. 2010 Mathematics Subject Classification and Key words and Phrases should be included at the bottom of first page of the paper.

Theorems, other statements and formulae must be clearly marked, separating the results of the authors from the already known results. The list of references has to be enclosed in alphabetical or chronological order at the end of the paper as well as the affiliation of the author.

Subscription for one volume is 40 USA dollars for institutions and 20 USA dollars for individuals.

For subscriptions and exchange please refer to the above address.

Computer processing of the press Olga Koroleva, Moscow, Russia.
Print: AP Print, Podgorica, Montenegro.

CIP – Каталогизација у публикацији
Централна народна библиотека, Цетиње, 51(05)

MATHEMATICA Montisnigri = Математика Црне Горе/ главни и одговорни уредник Жарко Павићевић. - Књ. 1 (1993) - Подгорица (Џорџа Вашингтона бб) : Друштво математичара и физичара Црне Горе: Природно – математички факултет Универзитета Црне Горе, 1993 – (Подгорица: АП Принт). - 30 cm

Три пута годишње. – Текст на руском и енг. језику.

ISSN 0345-2238 – Mathematica Montisnigri
COBISS.CG-ID 150244359

ДРУШТВО МАТЕМАТИЧАРА И ФИЗИЧАРА ЦРНЕ ГОРЕ
ПРИРОДНО-МАТЕМАТИЧКИ ФАКУЛТЕТ
УНИВЕРЗИТЕТА ЦРНЕ ГОРЕ

# МАТЕМАТИКА ЦРНЕ ГОРЕ

КЊИГА XLII

# MATHEMATICA MONTISNIGRI

VOLUME XLII

UDK 51 ISSN 0354 2238

ПОДГОРИЦА, 2018.

MATHEMATICA MONTISNIGRI
Vol XLII (2018) 5-115

# CONTENTS

## Mathematics

Saber Omidi and Bijan Davvaz. Some characterizations of right weakly prime $\Gamma$-hyperideals of ordered $\Gamma$-semihypergroups…… 5

## Computational mathematics

Yu.A. Kriksin, P.A. Kuchugov, M.E. Ladonkina, O.A. Nekliudova, V.F. Tishkin and V.P. Varin. Construction of exact solutions of some equations of hyperbolic type containing discontinuity moving on a non uniform background …….. 12

V.I.Mazhukin, A.V. Shapranov, E.N. Bykovskaya. Comparative analysis of the quality of two-and three-layer difference schemes of the second order……. 31

## Mathematical modeling

A.E. Bondarev. On the construction of the generalized numerical experiment in fluid dynamics..... 52

A. V. Korchuganov. Hybrid molecular dynamics and Monte Carlo modeling to study physical-mechanical properties of high-entropy alloy CoCrFeMnNi …..…….. 65

## Equations of mathematical physics

A.V. Kolesnichenko. Two-parameter functional of entropy Sharma-Mittal as the basis of the family of generalized thermodynamices of non-extensive systems..... 74

## Academic life

V.I. Mazhukin. 17th International Seminar on Mathematical models and modeling in the laser-plasma processes & advanced science technologies (LPPM3-2018)…….. 102

MATHEMATICA MONTISNIGRI
Vol XLII (2018)

# SOME CHARACTERIZATIONS OF RIGHT WEAKLY PRIME $\Gamma$-HYPERIDEALS OF ORDERED $\Gamma$-SEMIHYPERGROUPS

**SABER OMIDI[*] AND BIJAN DAVVAZ[†]**

[*] Department of Mathematics
Yazd University
Yazd, Iran
e-mail: omidi.saber@yahoo.com

[†] Department of Mathematics
Yazd University
Yazd, Iran
Email: davvaz@yazd.ac.ir - Web page: https://pws.yazd.ac.ir/davvaz/

**Summary.** In this paper, we deal with ordered $\Gamma$-semihypergroups. In particular, we study right weakly prime $\Gamma$-hyperideals and maximal $\Gamma$-hyperideals in ordered $\Gamma$-semihypergroups. Moreover, we give some results on ordered $\Gamma$-semihypergroups.

## 1 INTRODUCTION AND PREREQUISITES

Hyperstructure theory was first introduced in Marty's classical paper [1]. Semihypergroup is the generalization of semigroup theory with the wide range of usages in theory of hyperstructures [2,3]. In [4], Heidari and Davvaz studied a semihypergroup $(S,\bullet)$ besides a binary relation $\leq$, where $\leq$ is a partial orderrelation such that satisfies the monotone condition. This structure is called an ordered semihypergroup. As a reference for more definitions and results on ordered semihypergroups we refer to [3,5,6]. Omidi and Davvaz [7] investigated on the relation $N$ in ordered semihypergroups. We refer to [5] for a survey of some results on the pseudo orders of ordered semihypergroups. Omidi et al. [8] discussed quasi-$\Gamma$-hyperideals and hyperfilters in ordered $\Gamma$-semihypergroups. Tang et al. [9] studied fuzzy quasi-$\Gamma$-hyperideals in ordered $\Gamma$-semihypergroups. In 2016, Omidi and Davvaz [10,11,12] studied some properties of hyperideals and $k$-hyperideals in ordered semihyperrigs and hyperrings. The study of weakly prime ideals of ordered $\Gamma$-semigroups was started by the pioneering work of Kwon and Lee [13]. In 2013, Changphas [14] defined right prime ideals and maximal right ideals in ordered semigroups. Weakly prime ideals in involution po-$\Gamma$-semigroups discussed by Abbasi and Basar [15].

Let $S$ be a non-empty set. A mapping $\bullet: S \times S \rightarrow P^*(S)$, where $P^*(S)$ denotes the family of all non-empty subsets of $S$, is called a hyperoperation on $S$. By a hypergroupoid we mean a non-empty set $S$ endowed with a hyperoperation $\bullet$. In the above definition, if $A$ and $B$ are two non-empty subsets of $S$ and $x \epsilon S$, then we denote $A \bullet B$ the union of $a \bullet b$, where $a \epsilon A$ and $b \epsilon B$. Moreover, for every $x \epsilon S$,

$$A \bullet x = A \bullet \{x\} \text{ and } x \bullet B = \{x\} \bullet B.$$

A hypergroupoid $(S,\bullet)$ is called a semihypergroup if for all $x,y,z$ of $S$, we have

**2010 Mathematics Subject Classification:** 16Y99, 20N20.
**Key words and Phrases:** Ordered Semihypergroup, Right Weakly Prime Hyperideal, Maximal Hyperideal.

$$x\bullet(y\bullet z)=(x\bullet y)\bullet z,$$

which means that the union of $x\bullet u$, where $u\epsilon y\bullet z$ is equal to the union of $v\bullet z$, where $v\epsilon x\bullet y$.

A non-empty subset $A$ of a semihypergroup $(S,\bullet)$ is called a subsemihypergroup of $S$ if $A\bullet A$ is a subset of $A$. Let $(S,\bullet)$ be a semihypergroup. Then, $S$ is called a hypergroup if it satisfies the reproduction axiom, for all $x\epsilon S$, $x\bullet S=S=S\bullet x$. A non-empty subset $K$ of $S$ is a subhypergroup of $S$ if $a\bullet K=K=K\bullet a$, for every $a\epsilon K$.

Let $S$ and $\Gamma$ be two non-empty sets. Then, $S$ is called a $\Gamma$-semihypergroup [16] if every $\gamma\epsilon\Gamma$ is a hyperoperation on $S$, i.e., $x\gamma y$ is a subset of $S$ for every $x,y\epsilon S$ and for every $\alpha,\beta\epsilon\Gamma$ and $x,y,z\epsilon S$, we have

$$x\alpha(y\beta z)=(x\alpha y)\beta z.$$

A $\Gamma$-semihypergroup $S$ is called commutative if for all $x,y\epsilon S$ and $\gamma\epsilon\Gamma$, we have $x\gamma y=y\gamma x$. For some properties of $\Gamma$-semihypergroups, readers can see [16]. The following concepts are adapted from [8,9].

An ordered semihypergroup $(S,\bullet,\leq)$ is a semihypergroup $(S,\bullet)$ together with a partial order $\leq$ that is compatible with the hyperoperation $\bullet$, meaning that for any $x,y,z\epsilon S$,

$$x\leq y \text{ implies that } z\bullet x\leq z\bullet y \text{ and } x\bullet z\leq y\bullet z.$$

Here, $z\bullet x\leq z\bullet y$ means for any $a\epsilon z\bullet x$ there exists $b\epsilon z\bullet y$ such that $a\leq b$. The case $x\bullet z\leq y\bullet z$ is defined similarly.

**Definition 1.1** An algebraic hyperstructure $(S,\Gamma,\leq)$ is called an ordered $\Gamma$-semihypergroup if $(S,\Gamma)$ is a $\Gamma$-semihypergroup and $(S,\leq)$ is a partially ordered set such that for any $x,y,z\epsilon S$ and $\gamma\epsilon\Gamma$, we have

$$x\leq y \text{ implies that } z\gamma x\leq z\gamma y \text{ and } x\gamma z\leq y\gamma z.$$

Here, $z\gamma x\leq z\gamma y$ means for any $a\epsilon z\gamma x$ there exists $b\epsilon z\gamma y$ such that $a\leq b$. The case $x\gamma z\leq y\gamma z$ is defined similarly.

See to [8,9] for the examples of the ordered $\Gamma$-semihypergroups. For a non-empty subset $A$ of an ordered $\Gamma$-semihypergroup $S$, we denote

$$(A]=\{x\epsilon S|\ x\leq a \text{ for some } a\epsilon A\}.$$

**Definition 1.2** A non-empty subset $I$ of an ordered $\Gamma$-semihypergroup $(S,\Gamma,\leq)$ is called a left (resp. right) $\Gamma$-hyperideal of $S$ if

(1) $S\Gamma I\subseteq I$ (resp. $I\Gamma S\subseteq I$);

(2) when $x\epsilon I$ and $y\epsilon S$ such that $y\leq x$, imply that $y\epsilon I$.

Note that the condition (2) in Definition 1.1 is equivalent to $(I] \subseteq I$. A non-empty subset $I$ of $S$ is called a $\Gamma$-hyperideal of $S$ if it is a right and left $\Gamma$-hyperideal of $S$. A $\Gamma$-hyperideal $T$ of $S$ is said to be proper if $T \neq S$.

**Theorem 1.3** [9] Let $(S,\Gamma,\leq)$ be an ordered $\Gamma$-semihypergroup. Then,

(1) $A \subseteq (A]$ for any $A \subseteq S$.

(2) If $A \subseteq B \subseteq S$, then $(A] \subseteq (B]$.

(3) $(A]\Gamma(B] \subseteq (A\Gamma B]$ and $((A]\Gamma B]] = (A\Gamma B]$ for any $A,B \subseteq S$.

Now, we present two examples of ordered Γ-semihypergroups. We refer the readers to see more examples of ordered Γ-semihypergroups in [9,17].

**Example 1.4** Let $S=[0,1]$ and $\Gamma=N$. For every $x,y \in S$ and $\gamma \in \Gamma$, we define $\gamma: S \times \Gamma \times S \rightarrow P^*(S)$ by $x\gamma y = [0, \frac{xy}{\gamma}]$. Then, γ is a hyperoperation. For every $x,y,z \in S$ and $\alpha,\beta \in \Gamma$, we have

$$(x\alpha y)\beta z = [0, \frac{xyz}{\alpha\beta}] = x\alpha(y\beta z).$$

This means that S is a $\Gamma$-semihypergroup [16]. Consider $S$ as a poset with the natural ordering.

Thus, $(S,\Gamma,\leq)$ is an ordered $\Gamma$-semihypergroup.

**Example 1.5** Let $S=\{a,b,c,d\}$ and $\Gamma=\{\gamma,\beta\}$ be the sets of binary hyperoperations defined as follows:

| $\gamma$ | $a$ | $b$ | $c$ | $d$ |
|---|---|---|---|---|
| $a$ | $a$ | $\{a,b\}$ | $\{c,d\}$ | $d$ |
| $b$ | $\{a,b\}$ | $b$ | $\{c,d\}$ | $d$ |
| $c$ | $\{c,d\}$ | $\{c,d\}$ | $c$ | $d$ |
| $d$ | $d$ | $d$ | $d$ | $d$ |

| $\beta$ | $a$ | $b$ | $c$ | $d$ |
|---|---|---|---|---|
| $a$ | $a$ | $\{a,b\}$ | $\{c,d\}$ | $d$ |
| $b$ | $\{a,b\}$ | $\{a,b\}$ | $\{c,d\}$ | $d$ |
| $c$ | $\{c,d\}$ | $\{c,d\}$ | $c$ | $d$ |
| $d$ | $d$ | $d$ | $d$ | $d$ |

Clearly, $S$ is a $\Gamma$-semihypergroup. We have $(S,\Gamma,\leq)$ is an ordered $\Gamma$-semihypergroup where the order relation ≤ is defined by:

$$\leq := \{(a,a), (a,b), (b,b), (c,b), (c,c), (c,d), (d,b), (d,d)\}.$$

## 2 MAIN RESULTS

For the sake of simplicity, throughout this paper, we denote $I^2=I\Gamma I$. Let $A$ be a non-empty subset of an ordered $\Gamma$-semihypergroup $(S,\Gamma,\leq)$. We denote by $I(A)$ the $\Gamma$-hyperideal of $S$ generated by $A$. One can easily prove that

$$I(A)=(A\bigcup S\Gamma A\bigcup A\Gamma S\bigcup S\Gamma A\Gamma S].$$

A non-empty subset $I$ of an ordered $\Gamma$-semihypergroup $(S,\Gamma,\leq)$ is called prime if for every $A,B\subseteq S$ such that $A\Gamma B\subseteq I$, we have $A\subseteq I$ or $B\subseteq I$.

**Definition 2.1** A non-empty subset $I$ of an ordered $\Gamma$-semihypergroup $(S,\Gamma,\leq)$ is called weakly prime if for all $\Gamma$-hyperideals $A,B$ of $S$ such that $A\Gamma B\subseteq I$ , we have $A\subseteq I$ or $B\subseteq I$. Also, $I$ is called a weally prime $\Gamma$-hyperideal if $I$ is a $\Gamma$-hyperideal which is weakly prime. A $\Gamma$-hyperideal $I$ of $S$ is said to be maximal if for any proper $\Gamma$-hyperideal $K$ of $S$, $I\subseteq K$ implies that $I=K$.

**Remark 2.2** It is easy to see that every prime $\Gamma$-hyperideal is weakly prime.

**Theorem 2.3** Let $(S,\Gamma,\leq)$ be a commutative ordered $\Gamma$-semihypergroup. If $P$ is a weakly prime $\Gamma$-hyperideal of $S$, then $P$ is prime.

**Proof.** Assume that $A,B$ are non-empty subsets of S such that $A\Gamma B\subseteq P$. We have

$$\begin{aligned}I(A)\Gamma I(B)&=(A\bigcup S\Gamma A\bigcup A\Gamma S\bigcup S\Gamma A\Gamma S]\Gamma(B\bigcup S\Gamma B\bigcup B\Gamma S\bigcup S\Gamma B\Gamma S]\\&\subseteq(A\Gamma S\bigcup S\Gamma A\Gamma B]\\&\subseteq I(A\Gamma B)\\&\subseteq I(P)\subseteq (P]=P.\end{aligned}$$

Since $P$ is a weakly prime $\Gamma$-hyperideal of $S$, we get $I(A)\subseteq P$ or $I(B)\subseteq P$. So, we have $A\subseteq P$ or $B\subseteq P$. Therefore, $P$ is prime.

**Lemma 2.4** Let $(S,\Gamma,\leq)$ be an ordered $\Gamma$-semihypergroup. If $A$ and $B$ are $\Gamma$-hyperideals of $S$, then $A\bigcup B$ and $A\bigcap B$ are $\Gamma$-hyperideals of $S$.

**Proof.** The proof is straightforward.

**Theorem 2.5** Let $P$ be a $\Gamma$-hyperideal of an ordered $\Gamma$-semihypergroup $(S,\Gamma,\leq)$. Then $P$ is weakly prime if and only if for all $\Gamma$-hyperideals $A$ and $B$ of $S$ such that $(A\Gamma B]\bigcap(B\Gamma A]\subseteq P$, we have $A\subseteq P$ or $B\subseteq P$.

**Proof.** Suppose that $P$ is a weakly prime $\Gamma$-hyperideal of $S$. Let $A$ and $B$ be $\Gamma$-hyperideals of $S$ such that $(A\Gamma B]\bigcap(B\Gamma A]\subseteq P$. First, we show that $(A\Gamma B]$ is a $\Gamma$-hyperideal of $S$. Let $y\epsilon S$ and $x\epsilon(A\Gamma B]$. Then there exist $x\epsilon(A\Gamma B]$, $a\epsilon A$, $b\epsilon B$ and $\alpha\epsilon\Gamma$ such that $x\leq c\leq a\alpha b$. Since $S$ is an ordered $\Gamma$-semihypergroup, we get

$$x\beta y \leq c\beta y \leq (a\alpha b)\beta y = a\alpha(b\beta y) \subseteq A\Gamma(B\Gamma S) \subseteq A\Gamma B,$$

where $\beta\epsilon\Gamma$. Hence, $x\beta y \subseteq (A\Gamma B]$. Similarly, we have $y\beta x \subseteq (A\Gamma B]$. If $y \leq x$, then $y \leq x \leq z\epsilon A\Gamma B$, and so $y\epsilon(A\Gamma B]$. Therefore $(A\Gamma B]$ is a $\Gamma$-hyperideal of $S$. Similarly, we can prove that $(B\Gamma A]$ is a $\Gamma$-hyperideal of $S$. Thus,

$$(A\Gamma B]\Gamma(B\Gamma A] \subseteq (A\Gamma B]\Gamma S \subseteq (A\Gamma B] \text{ and } (A\Gamma B]\Gamma(B\Gamma A] \subseteq S\Gamma(B\Gamma A] \subseteq (B\Gamma A].$$

So, we have

$$(A\Gamma B]\Gamma(B\Gamma A] \subseteq (A\Gamma B] \cap (B\Gamma A] \subseteq P.$$

Since $P$ is a weakly prime $\Gamma$-hyperideal of $S$, we get $(A\Gamma B] \subseteq P$ or $(B\Gamma A] \subseteq P$. By Theorem 1.3(1), we have $A\Gamma B \subseteq P$ or $B\Gamma A \subseteq P$. This implies that $A \subseteq P$ or $B \subseteq P$.

Conversely, assume that $A$ and $B$ are $\Gamma$-hyperideals of $S$ such that $A\Gamma B \subseteq P$. By Theorem 1.3(2), we have $(A\Gamma B] \cap (B\Gamma A] \subseteq (A\Gamma B] \subseteq (P] \subseteq P$. By hypothesis, we have $A \subseteq P$ or $B \subseteq P$. Therefore, $P$ is a weakly prime $\Gamma$-hyperideal of $S$.

In the following, we define right weakly prime $\Gamma$-hyperideals in ordered $\Gamma$-semihypergroups and investigate some of their related results.

**Definition 2.6** A right $\Gamma$-hyperideal $I$ of an ordered $\Gamma$-semihypergroup $(S,\Gamma,\leq)$ is said to be a right weakly prime $\Gamma$-hyperideal of $S$ if $(A\Gamma B] \cap (B\Gamma A] \subseteq I$ implies $A \subseteq I$ or $B \subseteq I$ for all right $\Gamma$-hyperideals $A,B$ of $S$.

**Theorem 2.7** Let $(S,\Gamma,\leq)$ be anordered $\Gamma$-semihypergroup. If $M$ is a maximal right $\Gamma$-hyperideal of $S$ such that $I \cap I^2 \neq \phi$, where $I=S\backslash M$, then $M$ is a right weakly prime $\Gamma$-hyperideal of $S$.

**Proof.** Suppose that $M$ is a maximal right $\Gamma$-hyperideal of $S$ such that $I \cap I^2 \neq \phi$, where $I=S\backslash M$. If $M$ is not a right weakly prime $\Gamma$-hyperideal of $S$, then there exist right $\Gamma$-hyperideals $A,B$ of $S$ such that $(A\Gamma B] \cap (B\Gamma A] \subseteq M$, $A \not\subset M$ and $B \not\subset M$. Since $A \not\subset M$, it follows that $M \subseteq A \cup M$. By Lemma 2.4, $A \cup M$ is a right $\Gamma$-hyperideal of $S$. So, we get $A \cup M=S$. Similarly, we have $B \cup M=S$. Hence,

$$I=S\backslash M=(A \cup M)\backslash M=A\backslash M \subseteq A \text{ and } I=S\backslash M=(B \cup M)\backslash M=B\backslash M \subseteq B,$$

which imply that

$$I^2 \subseteq A\Gamma B \cap B\Gamma A \subseteq (A\Gamma B] \cap (B\Gamma A] \subseteq M.$$

Since $I \cap I^2 \neq \phi$, it follows that $I \cap M \neq \phi$, which is a contradiction. Therefore, $M$ is a right weakly prime $\Gamma$-hyperideal of $S$.

An element $a$ of an ordered $\Gamma$-semihypergroup $(S,\Gamma,\leq)$ is called an idempotent of $S$ if $a\epsilon a\gamma a$ for every $\gamma\epsilon\Gamma$. In view of Theorem 2.7, we have the following corollaries.

**Corollary 2.8** Let $(S,\Gamma,\leq)$ be an ordered $\Gamma$-semihypergroup. If $M$ is a maximal right $\Gamma$-hyperideal of $S$ such that $S\backslash M$ contains an idempotent of $S$, then $M$ is a right weakly prime $\Gamma$-hyperideal of $S$.

**Proof.** Suppose that M is a maximal right Γ-hyperideal of S such that $I=S\backslash M$ contains an idempotent $a$ of $S$. Set $I=S\backslash M$. Since $a\epsilon a\gamma a\subseteq I\Gamma I=I^2$, it follows that $I\bigcap I^2\neq\phi$. By Theorem 2.7, $M$ is a right weakly prime $\Gamma$-hyperideal of $S$.

**Corollary 2.9** Let $(S,\Gamma,\leq)$ be an ordered $\Gamma$-semihypergroup. If $S=(a\gamma S]$ for some $a\epsilon S$ and $\gamma\epsilon\Gamma$, then every maximal right $\Gamma$-hyperideal of $S$ is a right weakly prime $\Gamma$-hyperideal of $S$.

**Proof.** Suppose that $S=(a\gamma S]$ for some $a\epsilon S$ and $\gamma\epsilon\Gamma$. Let $M$ be a maximal right $\Gamma$-hyperideal of $S$ and $I=S\backslash M$. If $a$ is not in $I$, then $a\epsilon M$. It follows that

$$S=(a\gamma S]\subseteq(M\Gamma S]\subseteq(M]=M,$$

which is a contradiction. This leads to $a\epsilon I$. So, we have $a\gamma a\subseteq I\Gamma I=I^2$. Now, let $a\gamma a\bigcap I=\phi$. Then $a\gamma a\subseteq M$. This implies that

$$S=(a\gamma S]=(a\gamma(a\gamma S]]\subseteq((a]\gamma(a\gamma S]]=(a\gamma a\gamma S]\subseteq(M\Gamma S]\subseteq(M]=M.$$

This is a contradiction. Hence, $a\gamma a\bigcap I\neq\phi$.Thus there exists $x\epsilon a\gamma a\subseteq I^2$ such that $x\epsilon I$. Therefore, $I\bigcap I^2\neq\phi$. Now, by Theorem 2.7, $M$ is a right weakly prime $\Gamma$-hyperideal of $S$.

## REFERENCES


[1] F. Marty, Sur une generalization de la notion de groupe, *Eight Congress Math. Scandinaves*, Stockholm, 45-49 (1934).

[2] P. Corsini, *Prolegomena of Hypergroup Theory*, Second edition, Aviani Editore, Italy, (1993).

[3] B. Davvaz, *Semihypergroup Theory, Elsevier*, (2016).

[4] D. Heidari and B. Davvaz, "On ordered hyperstructures", *U.P.B. Sci. Bull. Series A.*, **73(2)**, 85-96 (2011).

[5] B. Davvaz, P. Corsini and T. Changphas, "Relationship between ordered semihypergroups and ordered semigroups by using pseudoorder", *European J. Combinatorics*, **44**, 208-217 (2015).

[6] Z. Gu and X. Tang, "Ordered regular equivalence relations on ordered semihypergroups", *J. Algebra*, **450**, 384-397 (2016).

[7] S. Omidi and B. Davvaz, "A short note on the relation $N$ in ordered semihypergroups", *GU J. Sci.*, **29(3)**, 659-662 (2016).

[8] S. Omidi, B. Davvaz and C. Abdioglu, "Some properties of quasi-$\Gamma$-hyperideals and hyperfilters in ordered $\Gamma$-semihypergroups", *Southeast Asian Bull. Math.*, **42**, 223-242 (2018).

[9] J. Tang, B. Davvaz and X. Y. Xie, "A study on (fuzzy) quasi-$\Gamma$-hyperideals in ordered $\Gamma$-semihypergroups", *Journal of Intelligent & Fuzzy Systems* **32,** 3821-3838 (2017).

[10] B. Davvaz and S. Omidi, "Basic notions and properties of ordered semihyperrings", *Categ. General Alg. Structures Appl.* **4(1),** 43-62 (2016).
[11] S. Omidi and B. Davvaz, "Contribution to study special kinds of hyperideals in ordered Semihyperrings", *J. Taibah Univ. Sci.* **11**, 1083-1094 (2017).
[12] S. Omidi and B. Davvaz, "Ordered Krasner hyperrings", *Iranian Journal of Mathematical Sciences and Informatics*, **12(2)**, 35-49 (2017).
[13] Y. I. Kwon and S. K. Lee, "On weakly prime ideals of ordered $\Gamma$-semigroups", *Comm. Korean Math. Soc.,* **13(2)**, 251-256 (1998).
[14] T. Changphas, "Right prime ideals and maximal right ideals in ordered semigroups", *Far East Journal of Mathematical Sciences*, **73(1),** 65-72 (2013).
[15] M.Y. Abbasi and A. Basar, "Weakly prime ideals in involution po-$\Gamma$-semigroups", *Kyungpook Math. J.*, **54,** 629-638 (2014).
[16] S. M. Anvariyeh, S. Mirvakili and B. Davvaz, "On $\Gamma$-hyperideals in $\Gamma$-semihypergroups", *Carpathian J. Math*., **26(1)**, 11-23 (2010).
[17] J. Tang, B. Davvaz, X. Xie and N. Yaqoob, "On fuzzy interior $\Gamma$ -hyperideals in ordered $\Gamma$ – semihypergroups", *Journal of Intelligent & Fuzzy Systems* **32**, 2447-2460 (2017).

Received April 15, 2018

MATHEMATICA MONTISNIGRI
Vol XLII (2018)

# CONSTRUCTION OF EXACT SOLUTIONS OF SOME EQUATIONS OF HYPERBOLIC TYPE CONTAINING DISCONTINUITY MOVING ON A NON UNIFORM BACKGROUND

**YU.A. KRIKSIN, P.A. KUCHUGOV, M.E. LADONKINA, O.A. NEKLIUDOVA, V.F. TISHKIN AND V.P. VARIN**

Keldysh Institute of Applied Mathematics of RAS
Miusskaya Sq. 4, Moscow, Russia, 125047
e-mail: office@keldysh.ru, web page: http://keldysh.ru/

**Summary.** Exact solutions for the quasilinear transport equation and a system of shallow water equations that contain discontinuities propagating along an inhomogeneous background are constructed in this paper. These solutions can be used as test problems for verification of newly created software packages and numerical methods. The influence of the limiter on the order of approximation using the Galerkin discontinuous method was studied. To calculate the order of approximation, the exact solutions constructed in this paper were used.

## 1 INTRODUCTION

Equations and systems of equations such as conservation laws [1-4] arise in many practical applications, and therefore their numerical solution is of considerable interest [5-7]. For this purpose, more advanced numerical methods and algorithms are developed. The Galerkin method with discontinuous basis functions [8,9] is quite often used recently. This method has proved itself to solve a wide class of applied problems of mathematical physics with a complex geometry of the investigated object and a multiscale structure of the studied processes. This method has a number of advantages inherent in both finite-element and finite-difference approximations. As you know, there are two approaches to improve the accuracy of the solution. The first approach is to grind the grid in areas of existing solution features (hp-adaptation), the second - to increase the order of accuracy of the scheme. The application of the Galerkin discontinuous method makes it possible to use both approaches simultaneously [10,11]

An important component of the computational algorithm development process is the verification stage, with particular interest in the behavior of numerical solutions in regions containing strong and weak discontinuities. For this, it is necessary to have examples of exact solutions. The construction of which is described in numerous works.

The problems described by the system of shallow water equations are of great practical importance, such as the destruction of the hydroelectric dam, the emergence of large sea waves such as tsunami in shallow water, currents in the atmosphere, and others. Analytic solutions for these problems are constructed [12-22], however, either piecewise constant initial data [12-17] or solutions that exclude discontinuities [18,19] are considered. At the same time, the most important goal is to investigate the accuracy of computational techniques on model problems in which discontinuities propagate along a non-uniform background. The behavior of a numerical solution obtained using difference schemes of high order of accuracy in the flow behind the discontinuity region was studied [23], in which it was shown that the order of approximation in this region drops to the first. In order to eliminate this defect, a

**2010 Mathematics Subject Classification:** 58J45, 35L67, 76M25.
**Key words and Phrases:** Exact solutions, Hyperbolic Equations, Discontinuous Galerkin Method.

combined scheme is proposed in [24], which allows maintaining a high order of accuracy of the scheme. However, there is a very limited amount of test problems that have an exact solution with a discontinuity propagating along an inhomogeneous background. In this paper, the authors construct exact discontinuous solutions for the quasilinear transport equation and the system of shallow water equations, using the characteristic approach. A method for determining the time instant after which the characteristics intersect occurs is described in detail. This makes it possible to guarantee the correctness of the exact solution constructed before the specified time. In the second part of the paper, we describe the application of the discontinuous Galerkin method [9] and study the order of approximation of the exact solutions obtained in the first part of this article by numerical solutions.

## 2 QUASILINEAR TRANSPORT EQUATION

The simplest example of a quasilinear transport equation is the Hopf equation [25], by means of which the motion of a gas of noninteracting particles can be described. In the one-dimensional case, it has the following form:

$$\frac{\partial u}{\partial t} + u\frac{\partial u}{\partial x} = 0 \tag{1}$$

The general solution of equation (1) is the functional dependence $G(x-ut,u)=0$. In particular, we can consider a family of solutions of the

$$u(x,t) = \frac{x+A}{t+B} \tag{2}$$

Equation (1) admits the existence of discontinuous solutions. We construct this solution using two different solutions of the form (2):

$$u = \begin{cases} u_L = (x+A)/(t+B),\ x \le x_f, \\ u_R = (x+C)/(t+D),\ x > x_f, \end{cases} \tag{3}$$

where $x_f(t)$ is the position of the front of the shock wave, the expression for which must be found in order to obtain the final exact solution. According to [26-28], we obtain:

$$\frac{dx_f}{dt} = \frac{1}{2}\left(\frac{x_f+A}{t+B} + \frac{x_f+C}{t+D}\right) \tag{4}$$

or after integration

$$x_f(t) = C_1\sqrt{(t+B)(t+D)} + \frac{(A-C)t + AD - CB}{B-D} \tag{5}$$

where $C_1$ is the integration constant, which can be determined by specifying the initial condition $x_f(0) = x_0$.

We give an example of a constructed exact solution (5) containing a discontinuity propagating along an inhomogeneous background, concretizing the values of the constants.

Let's set $A=1$, $B=2$, $C=0$, $D=1$ and $x_0=1/2$. In this case $C_1=\sqrt{2}/4$. The corresponding profiles of $u$ at different times are given in Fig. 1.

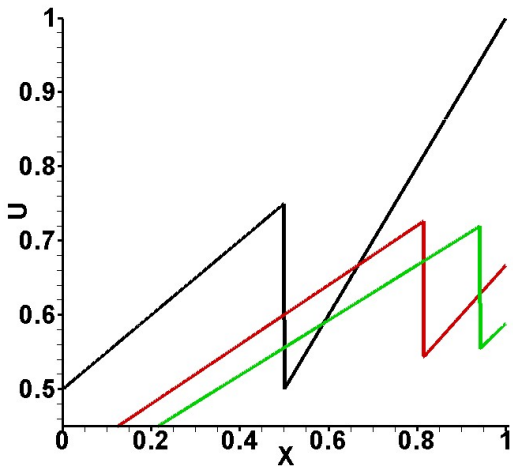


*Figure 1.* The exact solution of the Hopf equation at $t=0.0$ (black line), $0.5$ (red line) and $0.8$ (green line).

## 3 SHALLOW WATER EQUATIONS

Let us turn to the system of shallow water equations, for which it is possible to carry out a similar procedure of constructing an exact discontinuous solution. This system of equations can be obtained from the system of equations of hydrodynamics in the approximation, when the length of gravitational waves is large in comparison with the depth of the liquid [1]:

$$\begin{cases} \dfrac{\partial h}{\partial t}+\dfrac{\partial hu}{\partial x}=0, \\ \dfrac{\partial hu}{\partial t}+\dfrac{\partial}{\partial x}\left(hu^2+\dfrac{gh^2}{2}\right)=0, \end{cases} \tag{6}$$

where $h$ is the depth, $u$ is the flow velocity in the horizontal direction, the gravitational constant $g$ let's set equal to 1. The system of equations (6) can be rewritten in the following form:

$$\begin{cases} \dfrac{\partial R^+}{\partial t}+\left(u+\sqrt{h}\right)\dfrac{\partial R^+}{\partial x}=0, \\ \dfrac{\partial R^-}{\partial t}+\left(u-\sqrt{h}\right)\dfrac{\partial R^-}{\partial x}=0, \end{cases} \tag{7}$$

where $R^{\pm}=u\pm 2\sqrt{h}$ are Riemann invariants for the system (6).

Consider the domain $-\infty < x < \infty$. As a background solution in the region $x \geq x_0$ we set a solution in the form of a simple centered wave, for which the invariant $R^-$ remains constant. Let's set

$$R_r^- = \beta \tag{8}$$

In this case $h$ and $u$ are defined by:

$$u_r = \beta + 2\sqrt{h_r}, \sqrt{h_r} = \frac{1}{3}\left(\beta + \frac{x+A}{t+B}\right) \tag{9}$$

where $u_r = u(x \geq x_0, t)$, $h_r = h(x \geq x_0, t)$. We assume that in the region $x < x_0$ the other invariant $R^+$ remains constant. Let's set

$$R_l^+ = \alpha \tag{10}$$

The corresponding solution of the system (6) can also be given in the form of a simple centered wave:

$$u_l = \alpha - 2\sqrt{h_l}, \sqrt{h_l} = \frac{1}{3}\left(\alpha - \frac{x+C}{t+D}\right) \tag{11}$$

We require the fulfillment of the Hugoniot conditions on the discontinuity:

$$\begin{cases} h_l^* u_l^* - h_r^* u_r^* = W\left(h_l^* - h_r^*\right), \\ h_l^*\left(u_l^*\right)^2 + \dfrac{\left(h_l^*\right)^2}{2} - h_r^*\left(u_r^*\right)^2 - \dfrac{\left(h_r^*\right)^2}{2} = W\left(h_l^* u_l^* - h_r^* u_r^*\right) \end{cases} \tag{12}$$

where $W$ is the velocity of the discontinuity, $h_{l,r}^*$ and $u_{l,r}^*$ are the values of the corresponding functions to the right and left of the discontinuity. Eliminating $W$ from equations (12), you can get

$$\frac{h_l^* + h_r^*}{2}\left(h_l^* - h_r^*\right)^2 = h_l^* h_r^*\left(u_l^* - u_r^*\right)^2 \tag{13}$$

taking into account (8) and (10)

$$\frac{h_l^* + h_r^*}{2}\left(h_l^* - h_r^*\right)^2 = h_l^* h_r^*\left(\alpha - \beta - 2\sqrt{h_l^*} - 2\sqrt{h_r^*}\right)^2 \tag{14}$$

From (14) it is possible to determine the quantities $h_l^*$ and $u_l^*$ on the discontinuity.

To agree the solutions (9) and (11) to the left and right of the discontinuity, the constants in (11) must be determined with the following condition taken into account:

$$\frac{C+x_0}{D}=\alpha-3\sqrt{h_l^*} \tag{15}$$

obtained at the initial moment $t=0$.

On the basis of the following simple considerations, we can now draw some conclusions about the roots of equation (13). Thus, in the case of a discontinuity moving to the right, equation (13) with allowance for (10) can be rewritten in the form:

$$-2\sqrt{y}+(1-y)\sqrt{\frac{1}{2}(y^{-1}+1)}=\frac{u_r^*-\alpha}{\sqrt{h_r^*}} \tag{16}$$

relatively dimensionless variable $y=h_l^*/h_r^*$. The left-hand side of (16) is a monotonically decreasing function with respect to the variable $y>0$, which takes all values on the real line $(-\infty,+\infty)$,which follows from the negativity of the variable. This means that for any values of the right-hand side, equation (16) has a unique solution. We note that only solutions that satisfy the inequality $y>1$ are physicly correct, which is ensured if and only if $u_r^*+2\sqrt{h_r^*}<\alpha$. The investigation of the roots of the polynomial (14) is generally given in Appendix A.

The exact solution at any time $t$ in the region bounded from the left by the characteristic $x_0+\left(u_l^*-\sqrt{h_l^*}\right)t$ (see Fig. 2), will be determined by the functions (11), and the shock front bounded by the right $x_f(t)$ - functions (9).

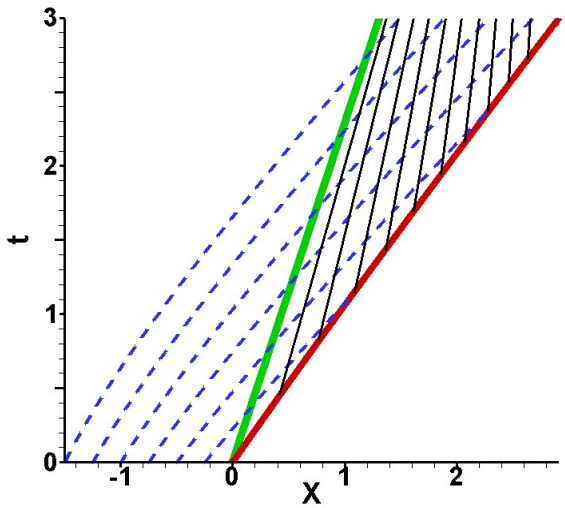


*Figure 2.* Trajectory of motion of the shock wave front (red line) and family of characteristics: a green line is a characteristic with a slope $u-\sqrt{h}$, which emerges from the point of the initial position of the discontinuity, continuous thin lines - a field of characteristics emerging from the shock wave trajectory, on which the value $R^-=u_l^*-2\sqrt{h_l^*}$, dashed thin lines - a field of characteristics on which the value of the invariant $R^+=u_l+2\sqrt{h_l}$, and by which this value is transferred to the front of the shock wave.

In the region between the indicated characteristic and the discontinuity, in which the value $R^+$ will remain constant, the solution will still be a simple wave, which, however, will no longer be centered. In this interval, the exact solution is determined using the method of characteristics. Let us describe this procedure in more detail.

Values before the rupture front $h_r^*$ and $u_r^*$ at each instant of time are determined by the formulas (9). Solving equation (14) we find the values $h_l^*$ and $u_l^*$ as functions of $x_f$ and $t$, where $x_f$ is a position of the rupture front. From (12) we determine the velocity of the discontinuity $W\left(x_f, t\right)$. Trajectory of the discontinuity motion $x_f\left(t\right)$ is defined as a solution of equation

$$\frac{dx_f}{dt} = W\left(x_f, t\right),\ x_f\left(0\right) = x_0 \tag{17}$$

From each point of this trajectory $x_f\left(t\right)$, $t$ release the characteristic on which the value is stored $R^- = u_l^* - 2\sqrt{h_l^*}$. In this case, these characteristics will have a constant slope, i.e. will be straight lines. Finally, we determine the point of intersection $x^*$ straight line $t = T$ and characteristics. Function values $u$ and $h$ to a given point are carried by characteristics in accordance with the values of the Riemann invariants.

We perform the above procedure for specific values of the constants. Let's set $\beta = 0$, $\alpha = 3/2$, $x_0 = 0$, $A = 1/2$, $B = 1$, $D = 1$, and $C$ is determined in accordance with (15). Equation (14) can be rewritten in the form

$$P\left(\xi\right) = 0 \tag{18}$$

where $P$ is polynomial with constant coefficients, $\xi = \sqrt{h}$. The graph of the dependence is given in Fig. 3.

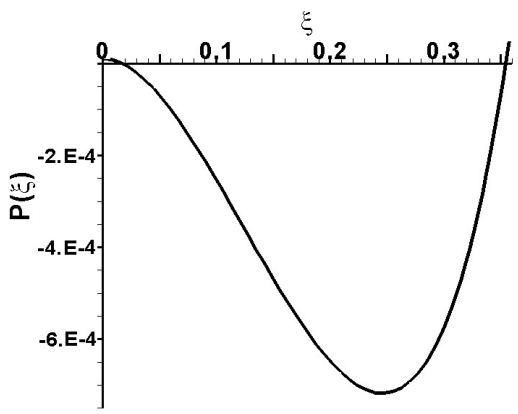


*Figure 3.* The function $P\left(\xi\right)$.

By building a series of Sturm for $P(\xi)$ and applying the Sturm theorem [29], we can determine that equation (17) has two roots on the positive semiaxis, one of which corresponds to a shock compression wave ($h_l^* > h_r^*$), another - a shock wave of rarefaction ($h_l^* < h_r^*$). From the physical considerations, we choose the first one. For this case, the system of characteristics is shown in Fig. 2, and the evolution of the exact solution is shown in Fig. 4.

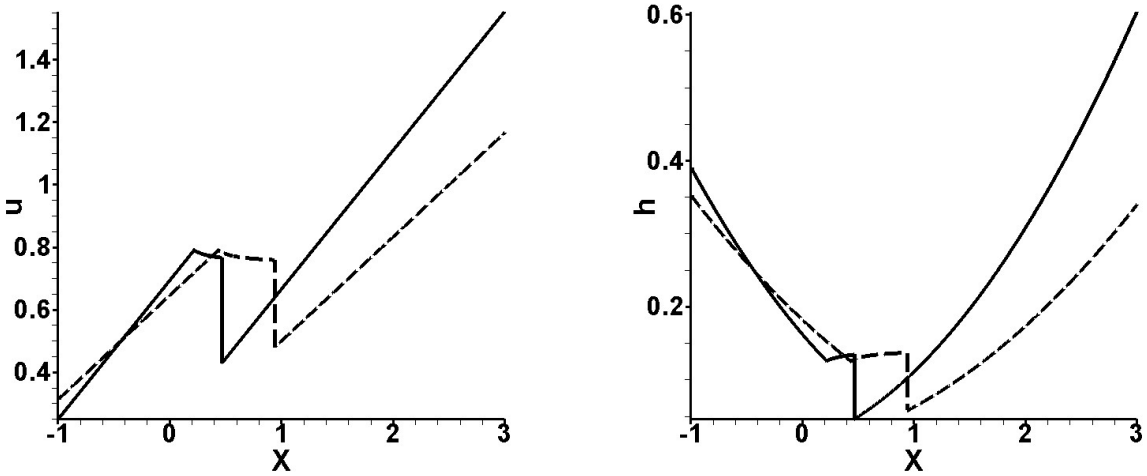


a) b)

*Figure 4.* The exact solution of the system of shallow water equations at times $0.5$ (solid line) and $1.0$ (dashed line).

It should be noted that the method of characteristics is applicable only when the characteristics do not intersect in the considered region. The condition for the intersection of two infinitely close characteristics at time T emerging from points $(x_f(t),t)$ and $(x_f(t+\Delta t),t+\Delta t)$ with different angular coefficients $a_1$ and $a_2$ respectively, is given by

$$a_1(t_c - t) + x_f(t) = a_2(t_c - t - \Delta t) + x_f(t + \Delta t) \tag{19}$$

allowing to find the moment of their intersection

$$t_c = t + (a_2 - a_1)^{-1}[a_2\Delta t - x_f(t+\Delta t) + x_f(t)] \tag{20}$$

The expression for the angular coefficient of an arbitrary characteristic with allowance for the constancy of the invariant $R^+ = \alpha$ is defined by

$$a = u_l^* - \sqrt{h_l^*} = \alpha - 3\sqrt{h_l^*} \tag{21}$$

In turn, the quantity $h_l^*$ is given by means of equation (16) as an implicit continuously differentiable function depending on the arguments $u_r^*$ and $h_r^*$, which in accordance with (9) are continuously differentiable functions of two variables x and t. Therefore, according to (19), the expression for the angular characteristic coefficient can be regarded as a

continuously differentiable function $a = a(x,t)$. In view of the latter circumstance $a_1 = a(x_f(t),t)$ and $a_2 = a(x_f(t+\Delta t), t+\Delta t)$. Passing to the limit as $\Delta t \to 0$ on the right-hand side of (20) and taking (16) into account, we obtain the instant of intersection of infinitely close characteristics emerging from the point $(x_f(t),t)$

$$t_c = t + \left( \frac{\partial a}{\partial t} + W(x_f(t),t)\frac{\partial a}{\partial x} \right)^{-1} [a(x_f(t),t) - W(x_f(t),t)] \tag{22}$$

Introducing the notation

$$X = \sqrt{\frac{1}{2}\left(\frac{1}{h_l^*} + \frac{1}{h_r^*}\right)},\ Y = 4X^2 + \frac{h_l^* - h_r^*}{(h_r^*)^2},\ Z = 4X^2\sqrt{h_l^*} + 4X - \frac{h_l^* - h_r^*}{h_l^*\sqrt{h_l^*}}, \tag{23}$$

expressions for the partial derivatives of the function $a = a(x,t)$ can be found

$$\frac{\partial a}{\partial x} = -\frac{3}{2}Z^{-1}\left( Y\frac{\partial h_r^*}{\partial x} - 4X\frac{\partial u_r^*}{\partial x} \right),\ \frac{\partial a}{\partial t} = -\frac{3}{2}Z^{-1}\left(Y\frac{\partial h_r^*}{\partial t} - 4X\frac{\partial u_r^*}{\partial t}\right). \tag{24}$$

Relations (22) - (24) for given values of the constants $A$, $B$, $C$ and $D$, which were defined above, allow us to numerically determine the minimum value of the right-hand side of (22) $t_c^* \approx 3.22$ on the set of all characteristics issuing from points $(x_f(t),t)$, that specifies the applicability boundary of the method of characteristics in the studied problem.

## 4 DISCONTINIOUS GALERKIN METHOD

We use the exact solutions obtained in the previous sections of the Hopf equation and the system of shallow water equations to determine the order of approximation when using the Galerkin discontinuous method for their numerical solution. In this section we briefly describe the essence of the approach using the example of a generalized hyperbolic system of quasilinear equations of the type of conservation laws:

$$\frac{\partial \mathbf{U}}{\partial t} + \frac{\partial \mathbf{F}(\mathbf{U})}{\partial x} = 0 \tag{25}$$

where $\mathbf{U}(x,t)$ is vector of variables, and $\mathbf{F}(\mathbf{U})$ are defined streaming vector functions containing $m$ components. For system (25) we set the Cauchy problem with initial data

$$\mathbf{U}(x,0) = \mathbf{U}_0(x), \tag{26}$$

Suppose that the Cauchy problem (25) - (26) has a unique generalized solution $\mathbf{U}(x,t)$, limited with $t > 0$. Let's set $\mathbf{U}^n(x) = \mathbf{U}(x,t_n)$ a numerical solution of this problem corresponding to the instant of time $t_n$.

To apply the Galerkin discontinuous method on a uniform grid, we define the following system of basis functions

$$\varphi_{i,k}(x)=\begin{cases}\phi_k(x), & x\in[x_i,x_{i+1}],\\ 0, & x\notin[x_i,x_{i+1}],\end{cases} \tag{27}$$

where $\phi_k(x)=\left((x-x_i^c)/\Delta\right)^k$, $x_i^c=(x_i+x_{i+1})/2$. Then on each time layer in each space cell $I_i=[x_i,x_{i+1}]$ an approximate solution of the system of equations (25) will be sought in the form of a polynomial of degree p

$$\mathbf{U}_i^n(x)=\mathbf{U}_i(x,t_n)=\sum_{k=0}^{p}\mathbf{U}_{ik}^n\phi_k(x) \tag{28}$$

with time-dependent coefficients $\mathbf{U}_{ik}^n=\mathbf{U}_{ik}(t_n)$.

Multiplying (25) by the basis function and performing integration over x on the interval $I_i$, we obtain the following expression

$$\int_{I_i}\frac{\partial}{\partial t}\mathbf{U}(x,t)\phi_l dx-\int_{I_i}\mathbf{F}(\mathbf{U})\phi_l' dx+\mathbf{F}(\mathbf{U})\phi_l\Big|_{x_i}^{x_{i+1}}=0 \tag{29}$$

on the basis of which Galerkin's discontinuous method is constructed. Replacing in the first two terms of equation (29) the function $\mathbf{U}(x,t)$ on function $\mathbf{U}_i^n(x)$, and in the third term - differential flows $\mathrm{F}(\mathbf{U}(x_j,t))$, where $j=i,i+1$, on numerical flows $\mathbf{F}_j^n=\mathbf{\Phi}\left(\mathbf{U}_{j-1}^n\left(x_j^-\right),\mathbf{U}_j^n\left(x_j^+\right)\right)$, in which $x_j^{\pm}=x_j\pm 0$, we get

$$\frac{\partial}{\partial t}\int_{I_i}\mathbf{U}_i^n\phi_l dx-\int_{I_i}\mathbf{F}\left(\mathbf{U}_i^n\right)\phi_l' dx+\mathbf{F}_{i+1}^n\phi_l\left(x_{i+1}^-\right)-\mathbf{F}_i^n\phi_l\left(x_i^+\right)=0 \tag{30}$$

In this paper we use the Rusanov-Lax-Friedrichs numerical flows [30,31], in which the function $\mathbf{\Phi}(\mathbf{x},\mathbf{y})$ is determined by the formula

$$\mathbf{\Phi}(\mathbf{x},\mathbf{y})=\frac{1}{2}\left(\mathbf{f}(\mathbf{x})+\mathbf{f}(\mathbf{y})-A(\mathbf{x},\mathbf{y})(\mathbf{y}-\mathbf{x})\right),\ A(\mathbf{x},\mathbf{y})=\max_m\left(\left|\lambda_m(\mathbf{x})\right|,\left|\lambda_m(\mathbf{y})\right|\right), \tag{31}$$

where $\lambda_m$ are eigenvalues of the Jacobi matrix $\dfrac{\partial\mathbf{F}(\mathbf{U})}{\partial\mathbf{U}}$ of set (25).

From (30), taking (28) into account, we obtain a system of ordinary differential equations

$$\frac{d\mathbf{U}_{ki}^n}{dt}=\mathbf{A}_i^{-1}\mathbf{R}_i,\qquad \mathbf{R}_i=\int_{I_i}\mathbf{F}\left(\mathbf{U}_i^n\right)\phi_l' dx-\mathbf{F}_{i+1}^n\phi_l\left(x_{i+1}^-\right)+\mathbf{F}_i^n\phi_l\left(x_i^+\right) \tag{32}$$

to calculate the coefficients $\mathbf{U}_{ki}^n$, where $\mathbf{A}_i^{-1}$ is an inverse matrix for matrix $\mathbf{A}_i=\left(a_{kl}^i\right)$,

whose coefficients are determined by the formula $a_{kl}^{i} = \int_{I_i} \phi_k(x)\phi_l(x)dx$. The system (32) is solved by the explicit Runge-Kutta method of the third order, in which the time step $\tau$ is chosen from the stability condition of Courant

$$\tau = \frac{z\Delta}{\max\limits_{m,j,n} |\lambda_m(\mathbf{U}_{j+1/2}^{n})|} \tag{33}$$

where $z \in (0,1)$ is safety factor.

The following calculations use polynomials (28) of the first order, i.e. $p = 1$.

To ensure the monotony of the numerical solution obtained by this method, it is necessary to introduce flow limiters, especially if the solution contains strong discontinuities. In this paper we apply the Cockburn limiter [9], which is widely used in applied multidimensional calculations conducted on grids of arbitrary structure. In the case when the solution (28) is sought in the form of linear $x$ functions

$$\mathbf{U}_i^n(x) = \mathbf{U}_{i0}^n + \mathbf{U}_{i1}^n \frac{x - x_i^c}{\Delta} \tag{34}$$

the action of this limiter leads to the fact that the vector coefficient $\mathbf{U}_{i1}^n$ in the formula (34) is replaced by the quantity

$$V_{i1}^n = M\left[U_{i1}^n, \alpha\left(U_{i+1,0}^n - U_{i0}^n\right), \alpha\left(U_{i0}^n - U_{i-1,0}^n\right)\right] \tag{35}$$

where $U_{j0}^n$ – the corresponding components of the vectors $\mathbf{U}_{j0}^n$, $\alpha \in [1,2]$– heuristic parameter, chosen as a result of test calculations, $M$ is a $\min\bmod$ operator, the action of which is determined by formula

$$M\left[u_1, u_2, u_3\right] = s\min\left(|u_1|, |u_2|, |u_3|\right), \tag{36}$$

where $s = sign(u_i)$ provided that all numbers $u_i$ have the same sign and $s = 0$ otherwise.

## 5 THE ORDER OF APPROXIMATION OF DISCONTINUOUS GALERKIN METHOD ON EXACT SOLUTIONS

We consider a sequence of difference solutions of the Cauchy problem (25) - (26) obtained using the numerical scheme based on the discontinuous Galerkin method on uniform grids with spatial steps $\Delta$ and $\Delta/2$. It is possible to calculate the approximation order achieved having the exact solution obtained in Sections 2 and 3:

$$r_{1i} = \log_2\left(\frac{\|u_\Delta - u_{ex}\|_{I_i}}{\|u_{\Delta/2} - u_{ex}\|_{I_i}}\right), \tag{37}$$

where $\|\varphi\|_{I_i} = \left( \int\limits_{x_i^c-\Delta/2}^{x_i^c+\Delta/2} \varphi^2(x)\,dx \right)^{1/2}$, $I_i = \left[x_i^c - \Delta/2, x_i^c + \Delta/2\right]$ is coarse grid, $x_i^c$ is cell center $I_i$.

Integral, included in the definition of the norm $\|\varphi\|_{I_i}$, is calculated analytically, as the exact solution of the Hopf equation is a fractional linear function (3), and the numerical solution obtained by the discontinuous Galerkin method is a linear polynomial (28). For the system of shallow water equations, it is impossible to write out an exact solution in the form of an analytic function in the region between the characteristics emerging from the discontinuity point at the initial time instant. Therefore, we shall consider local norm convergence:

$$r_{2i} = \log_3 \left( \frac{\left\| u_\Delta\left(x_i^c\right) - u_{ex}\left(x_i^c\right) \right\|}{\left\| u_{\Delta/3}\left(x_i^c\right) - u_{ex}\left(x_i^c\right) \right\|} \right), \tag{38}$$

where $\|\varphi(x)\| = |\varphi(x)|$.

Fig. 5-8 represent numerical solutions of the Hopf equation and the system of shallow water equations with and without the use of the limiting procedure in the discontinuous Galerkin method on grids of various dimension. In Fig. 5 and 7, the numerical solution practically coincides with the exact solution, with the exception of a narrow region, near the discontinuities. In more detail these areas are presented in Fig. 6 and 8. As the grid pitch decreases, the numerical solution converges to the exact one, which is clearly seen in Fig. 6 and 8. It can also be noted that without using the limiting procedure in a numerical solution near the discontinuity, strong enough oscillations are observed, suppression of which occurs when limiters are used to ensure the monotonicity of the solution.

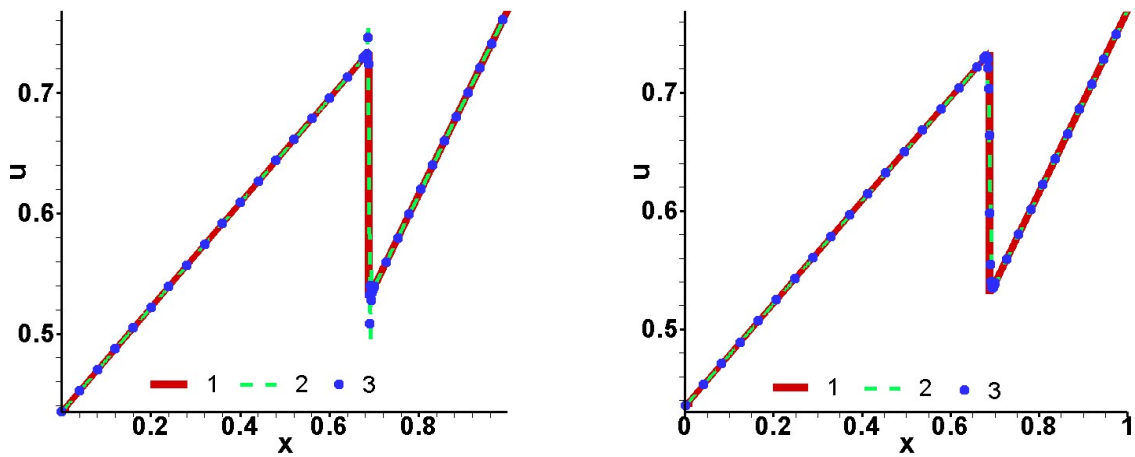


a) b)

*Figure* 5. Profiles of exact and numerical solutions of the Hopf equation at time moment $t = 0.5$. The exact solution on the graph corresponds to number 1. Numerical solutions were obtained using the discontinuous Galerkin method (a) without applying the restriction procedure on meshes containing 400 (2) and 800 (3) cells, (b) - the same with the application of the limiting procedure.

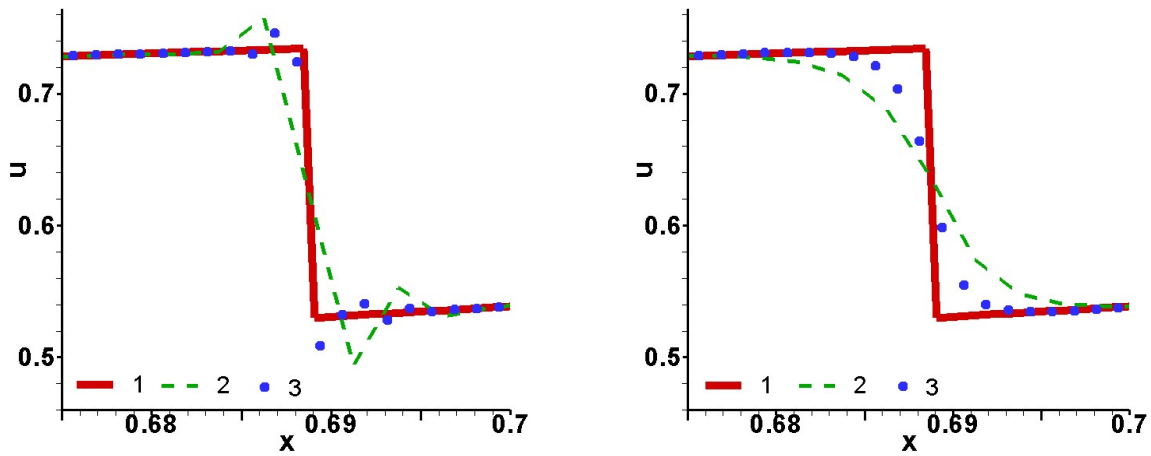


a) b)

*Figure* 6. Profiles of exact and numerical solutions of the Hopf equation at an instant $t = 0.5$ in the vicinity of the discontinuity. The exact solution on the graph corresponds to number 1. Numerical solutions were obtained using the Galerkin discontinuous method (a) without applying the restriction procedure on meshes containing 400 (2) and 800 (3) cells, (b) - the same with the application of the limiting procedure.

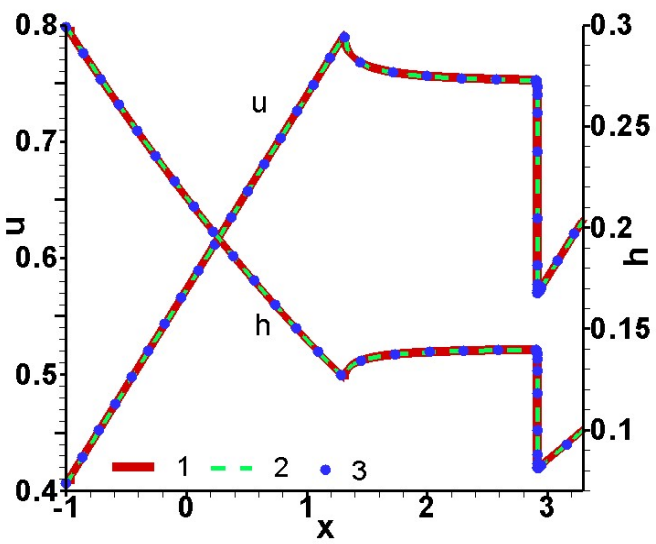


*Figure* 7. Profiles of exact and numerical solutions of the system of shallow water equations at a time moment $t = 3.0$. The exact solution on the graph corresponds to number 1. Numerical solutions were obtained using the discontinuous Galerkin method with the use of the limiting procedure on grids containing 3000 (2) and 9000 (3) cells.

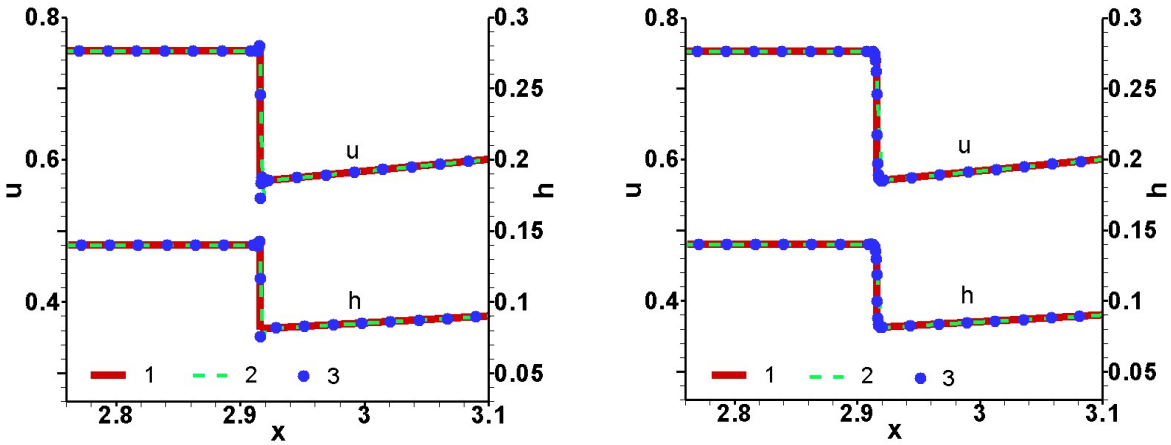


a) b)

*Figure* 8. The profiles of the exact and numerical solutions of the system of shallow water equations at the instant of time $t = 3.0$ in the vicinity of the discontinuity. The exact solution on the graph corresponds to number 1. Numerical solutions were obtained using the discontinuous Galerkin method (a) without applying the limiting procedure on grids containing 3000 (2) and 9000 (3) cells, (b) - the same with the use of the limiting procedure.

In Fig. 9 and 10 are the graphs of the discrepancy between the numerical solution of the Hopf equation and the approximation order calculated according to (37), respectively. In spite of the fact that, in the case of applying the limiting operator, the error in the numerical solution in the region beyond the gap increases by 3 orders of magnitude (see Fig. 9), the approximation order value remains equal to two, as in the case without the limiter [32,33].

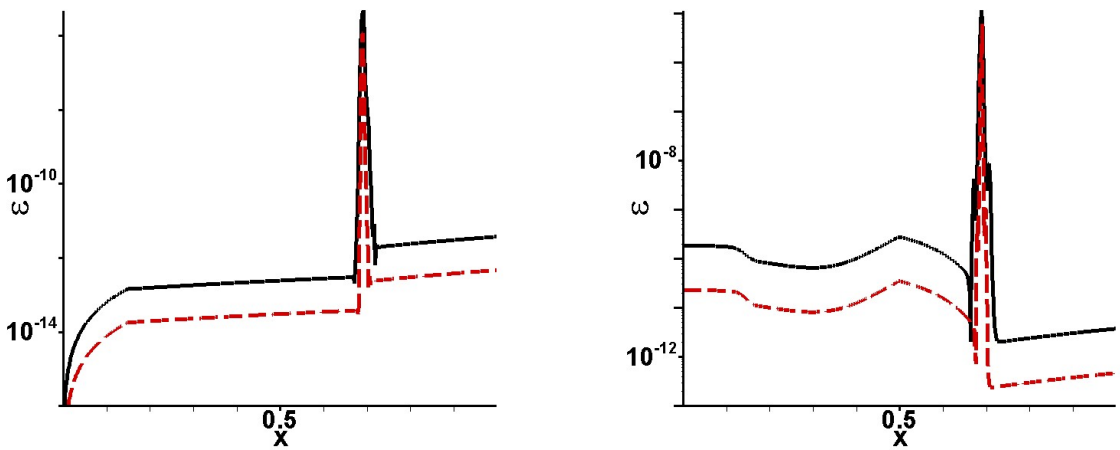


a) b)

*Figure* 9. The discrepancy between the numerical solution of the Hopf equation obtained using the discontinuous Galerkin method (a) without the use of the limiting procedure and (b) with it on meshes containing 400 (solid line) and 800 (dashed line) cells.

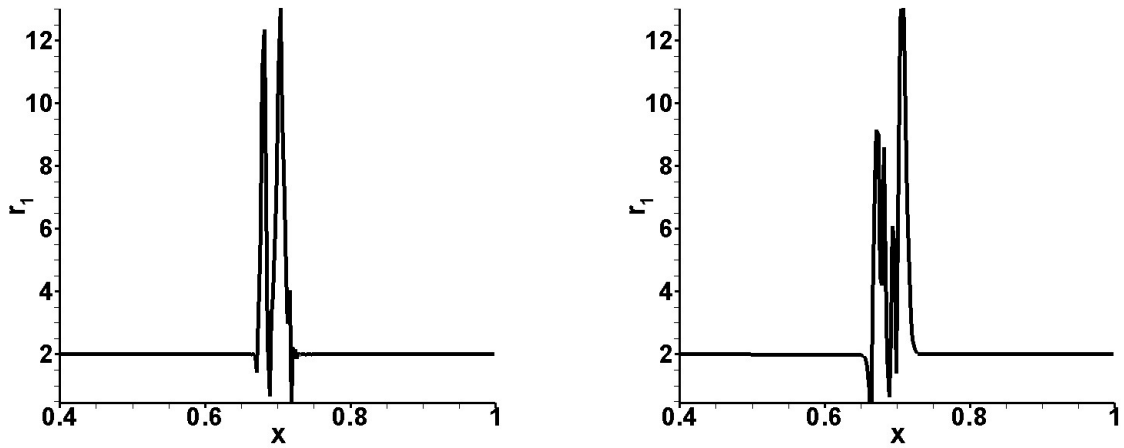


a) b)

*Figure* 10. The order of approximation of the exact solution of the Hopf equation using the Galerkin discontinuous method (a) without applying the limiting procedure and (b) with limiting.

The reason for this result is that in the nonlinear transport equation there is only one invariant that is transported by characteristics and is not affected by the shock wave. In contrast to the Hopf equation, the system of shallow water equations (6) contains two invariants and is more suitable for investigating the accuracy of the numerical method. In Fig. 11 shows the order of local convergence of the numerical solution to the exact one, calculated according to (38).

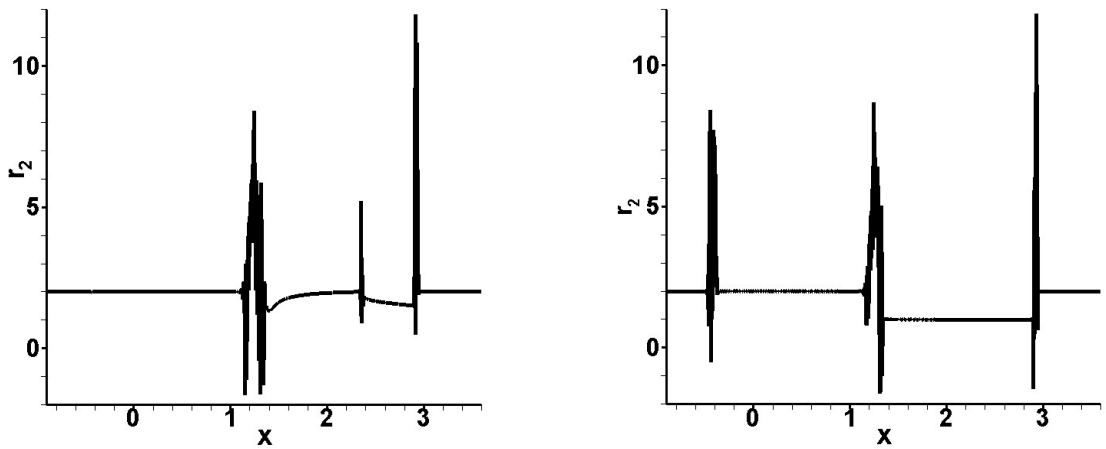


a) b)

*Figure* 11. The order of local convergence of numerical solutions obtained by using the discontinuous Galerkin method (a) without applying the limiting procedure and b) using a limiter on meshes containing 3000 cells and 9000 cells to an exact solution.

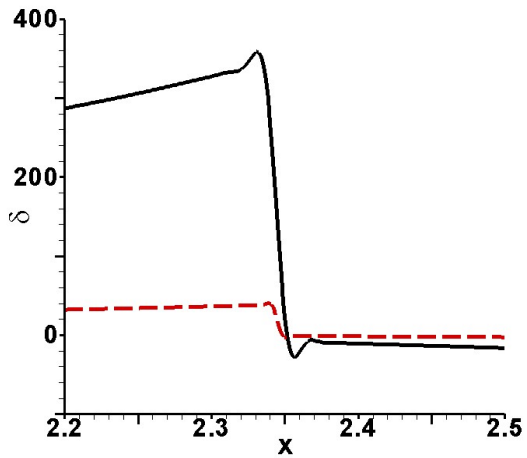


*Figure* 12. Deviations of the numerical solution from the exact one in the vicinity of the point $x \approx 2.3$ in the calculation without the use of a limiter; solid line corresponds to $A\cdot(h_{\Delta} - h_{ex})$, dashed line – $A\cdot(h_{\Delta/3} - h_{ex})$, where $A = 10^{10}$, $h_{\Delta}$ – the solution obtained on the grid of 3000 cells, $h_{\Delta/3}$ - the solution obtained on the grid of 9000 cells, $h_{ex}$ - the exact solution.

In calculations without using a limiter in the entire region, a second order of accuracy of the solution was obtained (see Fig. 11a). The jumps of orders at the point $x \approx 1.3$ correspond to the gluing of a solution of the type (9) and the solution between the characteristics emerging from the discontinuity point at the initial instant of time, and at the point $x \approx 3.0$ - to the position of the front of the shock wave. At the point $x \approx 2.3$, the intersection of numerical and exact solutions occurs. This can be clearly seen in Fig. 12, which shows the deviation of the numerical solution on different grids from the exact one. At the point $x \approx 2.3$ these functions change sign and, accordingly, in its vicinity the order of accuracy is not defined. The behavior of the order in the vicinity of the point $x \approx -0.44$ is shown on Fig. 11b when using the limiting operator can be explained in the similar way. However, the general behavior of the order is somewhat different. It can be seen from the calculations that the solution in the region of smoothness ahead of the front of the shock wave and in the solution region of type (9) has a second order of accuracy irrespective of the use of the limiting operator. In the solution region behind the front of the shock wave, but located between the characteristics emerging from the point of discontinuity at the initial instant of time, the accuracy of the solution drops to the first. An interesting fact is that in the region [0,1] a second order of accuracy is observed. In this region, both invariants are carried over the characteristics from the initial data, while in the region of reduced orders of accuracy the invariant is transferred from the front of the shock wave. Thus, it can be argued that the use of the limiting operator negatively affects the accuracy of the solution obtained only in the region of the impact of the shock wave [1.5, 3].

## 6 CONCLUSIONS

In this paper, exact discontinuous solutions are constructed for the quasilinear transport equation, and also for the system of shallow water equations using the method of characteristics. The results of calculations obtained by programs implementing the

discontinuous Galerkin method showed good agreement of the numerical solutions with the constructed exact solutions, confirming the possibility of using them as test tasks for verification of program complexes and numerical methods. Using the Hopf equation as an example, it was shown in the paper that the use of hyperbolic equations containing only one Riemann invariant is not sufficient to study the order of approximation of numerical methods. To this end, it is necessary to use more complex systems, for example, a system of shallow water equations. In this example, it was shown that the introduction of the limiter reduces the order of accuracy of the discontinuous Galerkin method in the regions of influence of strong discontinuities.

**Acknowledgements:** This work was supported by the Russian Science Foundation under the project No. 17-71-30014

## APPENDIX A

Let us introduce a new notation, namely, $\sqrt{h_l^*} = y$, $\sqrt{h_r^*} = x$, $\alpha - \beta = p$ In this case (14) is rewritten in the form:

$$P = x^2 y^2 \left(p - 2x - 2y\right)^2 - \frac{1}{2}\left(x^2 + y^2\right)\left(x^2 - y^2\right)^2, \tag{A1}$$

where $y$ is the chosen dependent variable, $x$ and $p$ are independent parameters.

As is known, the classical Sturm sequence [29] is defined only for polynomials with real coefficients. Degenerations and rearrangements of the solution set are possible in the case of the dependence of the coefficients on the parameters. However, for this problem it is possible to construct the Sturm sequence in general form. After an elaborate work we can get $S = \left[s_1, ..., s_7\right]$, where

$$s_1 = -x^6 + \left(2x^2p^2 - 8px^3 + 9x^4 + \left(16x^3 - 8px^2 + \left(9x^2 - y^2\right)y\right)y\right)y^2,$$

$$s_2 = \left(2x^2p^2 - 8px^3 + 9x^4 + \left(-12px^2 + 24x^3 + \left(18x^2 - 3y^2\right)y\right)y\right)y,$$

$$s_3 = 3x^4 + \left(-4p^2 + 16px - 18x^2 + \left(-24x + 12p - 9y\right)y\right)y^2,$$

$$s_4 = -12\left(2x - p\right)x^4 + \left(-18x^2\left(2x - p\right)^2 + \right.$$

$$\left. + \left(-4\left(2x - p\right)\left(2p + x\right)\left(-2p + 9x\right) + \left(-24x^2 + 36p^2 - 144px\right)y\right)y\right)y,$$

$$s_5 = -6x^4 p\left(-29px^2 + 180x^3 + p^3 - 8xp^2\right) + \left(-9x^2 p\left(-490px^3 + 312x^4\right.\right.$$

$$+295x^2p^2-80p^3x+8p^4\Big)-$$

$$-p\Big(-3456px^4-573x^2p^3+2024x^3p^2-8p^5+96xp^4+1728x^5\Big)y\Big)y, \tag{A2}$$

$$s_6=\Big(34992x^{10}+347760px^9+371556x^8p^2-2068672p^3x^7+3534048x^6p^4-$$

$$-3060540p^5x^5+1563205x^4p^6-501504x^3p^7+100464x^2p^8-11520xp^9+$$

$$+576p^{10}\Big)y+54\Big(648x^7+7196px^6+14616x^5p^2-28532p^3x^4+17850x^3p^4-$$

$$-5817x^2p^5+1008p^6x-72p^7\Big)x^4,$$

$$s_7=1.$$

Substituting the specific values of $x$ and $p$ in (A2), one can determine the number of nondegenerate roots on a given interval of variation $y$, as the difference between the number of sign changes in the Sturm sequences corresponding to the edges of the interval. Degenerate cases require particular consideration.

For the case considered in the text of the paper, namely, $\alpha=3/2$, $\beta=0$ ($p=3/2$), (A1) has the following graph of the dependence on the parameter $x$ – see Fig. 13.

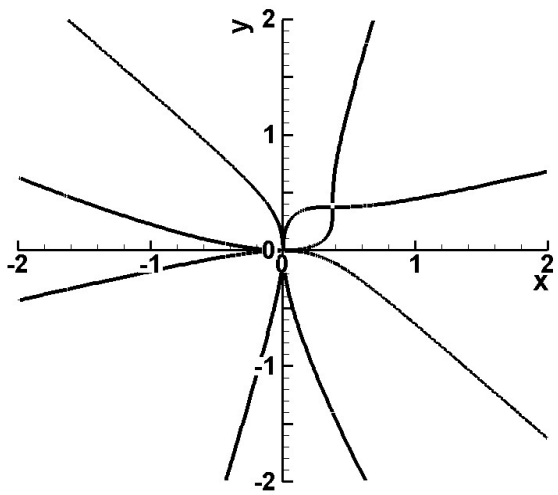


*Figure 13*. The dependency (A1) in the case of $p=3/2$.

From Fig. 13 is obvious that there is at least one degenerate case. Calculations show that this happens when value $x=p/4$. Asymptotic analysis shows that there are no other degenerate cases.

## REFERENCES


[1] L.D. Landau and E.M. Lifschitz, *Fluid Mechanics, Course of Theoretical Physics,* Pergamon, (1987).

[2] J.J. Stoker, *Water Waves The mathematical theory with applications*, Interscience Pub. Inc., (1957).

[3] A.G. Kulikovsky, N.V. Pogorelov, A.Y. Semenov, *Mathematical problems of numerical solution of hyperbolic systems of equation,* Physmathlit, (2001).

[4] V.V. Ostapenko, *Hyperbolic systems of conservation laws and their application to the theory of shallow water: A course of lectures,* Novosibirsk Univ., (2004).

[5] M.P. Galanin, V.T. Zhukov , N.V. Klushnev , V.V. Lukin, A.S. Rodin "On the solving of conjugate problems for definition of parameters of wrap and heat exchange between elements of constructions", *Mathematica Montisnigri*, **XXXIX**, 5-17 (2017).

[6] A.K. Alexeev, A.E. Bondarev, "On some features of Richardson extrapolation for compressible inviscid flows", *Mathematica Montisnigri*, **XL**, 42-54 (2017).

[7] Y. Karamzin, T. Kudryashova, S. Polyakov, "On one class of flow schemes for the convection-diffusion type equation", *Mathematica Montisnigri*, **XLI**, 21-32 (2018).

[8] *Proceedings of ECCOMAS Thematic Conference: European Conference on High Order Nonlinear Numerical Methods for Evolutionary PDEs: Theory and Applications*, 27-31 March, 2017, Stuttgart, Germany, 1-100 (2017).

[9] B. Cockburn, "An Introduction to the Discontinuous Galerkin Method for Convection - Dominated Problems, Advanced Numerical Approximation of Nonlinear Hyperbolic Equations", *Lecture Notes in Mathematics,* **1697**, 151-268 (1998).

[10] E. J. Kubatko, J. J. Westerinka, C. Dawson, "Discontinuous Galerkin methods for advection dominated problems in shallow water flow", *Clint Dawson Comput. Methods Appl. Mech. Engrg.* **196**, 437–451 (2006).

[11] A.V. Volkov, "Peculiarities of the application of the Galerkin method to the solution of the spatial Navier-Stokes equations on unstructured hexahedral meshes", *TSAGI,* **XL** (6), (2009).

[12] P.E. Karabut, V.V. Ostapenko, "Method of successive approximations for the Riemann problem with a small-amplitude discontinuity", *Doklady Mathematics*, **83** (2), 143-148 (2011).

[13] V.V. Ostapenko, E.V. Shinkarenko, "The currents arising after the passage of a discontinuous wave above the ledge of the bottom", *Mechanics of fluid and gas,* **1**, 106-122 (2009).

[14] V.V. Ostapenko, "The currents arising from the destruction of the dam above the bottom step", *Applied Mechanics and Technical Physics,* **44** (4), 51-63 (2003).

[15] O.A. Kovyrkina, V.V. Ostapenko, "Comparison between the theory and the numerical experiment in the problem of dam break on a jump of the cross-sectional area of a rectangular channel", *Fluid dynamics,* **48** (3), 291 (2013).

[16] P.E. Karabut, V.V. Ostapenko, "Problem of the decay of a small-amplitude discontinuity in two-layer shallow water: First approximation", *Journal of Applied Mechanics and Technical Physics*,. **52** (5), 698-708 (2011).

[17] G.S. Khakimzyanov, S.P. Bautin, S.L. Deryabin, A.F. Sommer, N.Y. Shokina, "Analytical and numerical investigation of solutions of shallow water equations in the vicinity of the line of cut", *International Conference "Modern Problems of Applied Mathematics and Mechanics: Theory, Experiment and Practice"*

[18] S.A. Beisel, N.Y. Shokina, G.S. Khakimzyanov, L.B. Chubarov, O.A. Kovyrkina, V.V. Ostapenko, "On some numerical algorithms for calculating the motion of the line of the edge in the framework of the shallow water model. I", *Computing technologies,* **19** (1), 1-25 (2014).

[19] V. Teshukov, G. Russo, A. Chesnokov, "Analytical and numerical solutions of the shallow water equations for 2d rotational flows", *Mathematical Models and Methods in Applied Sciences,* **14** (10), 1-29 (2004).

[20] N.M. Borisova, V.V. Ostapenko, "Numerical simulation of discontinuous waves propagating over a dry bed", *Computational Mathematics and Mathematical Physics*, **46** (7), 1254-1276 (2006).

[21] V.V. Ostapenko, A.A. Cherevko, A.P. Chupakhin, "Discontinuous solutions of the shallow water equations on a rotatable attracting sphere", *Fluid Dynamics*, **46** ( 2), 196-213 (2011).

[22] Y.A. Kriksin, P.A. Kuchugov, M.E. Ladonkina, O.A. Nekliudova, V.F. Tishkin, "Construction of exact solutions of certain equations of hyperbolic type containing a discontinuity propagating along a non-homogeneous background", *Keldysh Institute Preprints,* **17**, 1-14 (2018).

[23] Y.A. Bondarenko, "The order of approximation, the order of numerical convergence, and the economics of counting multidimensional gas dynamics in Euler variables, using the example of calculations for the convergence of the problem "BLAST WAVES"", *Questions of atomic science and technology. Mathematical modeling of physical processes,* **4**, 51-61 (2004).

[24] O.A. Kovyrkina, V.V. Ostapenko, "On the construction of combined difference schemes of increased accuracy", *Doklady Mathematics*, **478** (5), 517-522 (2018).

[25] E. Hopf, "The partial differential equation", *Communications on Pure and Applied Mathematics,* **3**, 201-230 (1950).

[26] O.A. Oleynik, "Discontinuous solutions of nonlinear differential equations", *Success of mathematical sciences,* **12**, 3-73 (1957).

[27] N.N. Kalitkin, *Numerical methods,* Nauka (1978).

[28] A.D. Polyanin, V.F. Zaitsev, A. Moussiaux, "Handbook of first order partial differential equations", *Differential and Integral Equations and Their Applications,* **1**, (2002).

[29] I.R. Shafarevich, *On the solution of higher-degree equations (the Sturm's method),* Gostechizdat, (1954).

[30] V.V. Rusanov, "Calculation of the interaction of non-stationary shock waves with obstacles", *Journal of Computational Mathematics and Mathematical Physics,* **1** (2), 267-279 (1961).

[31] P.D. Lax, "Weak solutions of nonlinear hyperbolic equations and their numerical computation", *Communications on Pure and Applied Mathematics,* **7** (1), 159-193 (1954).

[32] M.E. Ladonkina, O.A. Nekliudova, V.F. Tishkin, "Research of the impact of different limiting functions on the order of solution obtained by RKDG", *Keldysh Institute Preprints,* **34**, 1-31 (2012).

[33] M.E. Ladonkina, O.A. Nekliudova, V.F. Tishkin, "Research of the impact of different limiting functions on the order of solution obtained by RKDG", *Mathematical modeling,* **24** (12), 124-128 (2012).

*The results were presented at the 17-th International seminar "Mathematical models & modeling in laser-plasma processes & advanced science technologies" (May 26 – June 2, 2018, Budva, Montenegro).*

Received May 20, 2018.

# COMPARATIVE ANALYSIS OF THE QUALITY OF TWO-AND THREE-LAYER DIFFERENCE SCHEMES OF THE SECOND ORDER

**V.I.MAZHUKIN[1,2], A.V. SHAPRANOV[1,2], E.N. BYKOVSKAYA[1]**

[1] Keldysh Institute of Applied Mathematics of Russian Academy of Sciences (KIAM RAS)
4 Miusskaya square, 125047 Moscow, Russia
e-mail: vim@modhef.ru, web page: http://www.keldysh.ru

[2] National Research Nuclear University Moscow Engineering Physics Institute (NRNU MEPhi)
31 Kashirskoe shosse, 115409, Moscow, Russia

**Summary.** Using the example of a numerical solution of a model problem with a nonlinear Burgers equation, the quality of the approximation of the original equation by two and three-layer difference schemes written on grids with fixed and moving nodes is studied. Modeling with the subsequent analysis of its results has shown that in the Cartesian coordinate system the quality of the numerical solution essentially depends on the quality of the finite-difference approximation used for the initial equation. The application of the two-layer Crank-Nicholson scheme and the three-layer difference scheme of the Cabaret type with the second order of approximation formulated in the Cartesian coordinate system showed that the three-layer difference schemes have a distinct advantage and give a solution of higher quality, except for regions with large gradients. The application of an arbitrary non-stationary coordinate system made it possible to implement a dynamic adaptation of the grid in which the distribution of nodes is dependent and controlled by the sought solution, which makes it possible to automatically adjust the calculated grid in such a way that the approximation error turns out to be minimal practically regardless of the quality of the original difference scheme. The numerical solution of the nonlinear Burgers equation with the help of two and three-layer difference schemes on a dynamically adapting grid showed virtually complete coincidence of the calculations with each other, a good agreement with the exact solution with complete absence of oscillations in the solution. The calculation grid contained the number of nodes (n = 25) by two orders of magnitude smaller than the grid with fixed nodes.

## 1 INTRODUCTION

The numerical solution of the equations of continuum mechanics, which describe convection-diffusion processes with the predominance of the convective transport mechanism, is one of the fundamental problems of computational mathematics. The main difficulties of the computational process are due to the error that arises when differential equations are approximated by difference schemes. The approximation error is manifested in the form of dissipative and dispersive properties of finite-difference schemes. Depending on the relationship between these properties in the solution, not only quantitative, but also qualitative distortions can occur.

**2010 Mathematics Subject Classification:** 33F05, 68Q17, 01-08, 34K28
**Key words and Phrases:** difference schemes, dispersion, approximation, numerical solution, dynamic adaptation.

Such computational features are the most completely investigated and generalized in the systems of linear and nonlinear equations of hyperbolic type. These include the equations of gas dynamics [1], elasticity theory [2], shallow water [3,4], etc. For many years of research a large number of finite-difference schemes have been developed [5-9] for the solution of these equations, having their own advantages and disadvantages. It is known that classical finite-difference schemes with the first order of approximation for the equations of convective transport in Euler variables have too much dissipation, which leads to a strong smoothing of the solution in the regions of local extrema. The schemes of higher (2nd and higher) order according to the theorem of S.K. Godunov [10] are not monotonic due to a high approximation dispersion, which often causes the appearance of parasitic oscillations in the regions of large solution gradients. As a result, classical difference schemes can not always provide the necessary accuracy of numerical solutions.

The dissipative and dispersion properties of classical difference schemes are improved in various ways. A decrease in the scheme dissipation can be achieved by increasing the order of approximation [8], and for the monotonization of the solution, the methods of artificial viscosity [7] and nonlinear correction [11] are usually used. Recently, the methods for constructing nonlinear difference schemes (so-called high resolution algorithms) that improve the dissipative and dispersive properties of classical linear difference schemes with the help of nonlinear correction of fluxes have become most widely used. When constructing improved nonlinear schemes of high accuracy order, the dissipative difference schemes of Godunov [10] or Lax-Wendroff [12] are used as the initial ones.

In one of the first papers [13], the construction of a high-resolution scheme (the Flux Corrected Transport (FCT) method) was achieved by reducing the dissipation in the original low-dispersion scheme (the first-order Godunov scheme [10]), introducing antidiffusion fluxes while preserving the boundedness of the solution [14]. Another example of constructing high-resolution schemes is higher order approximation schemes based on the principle of non-increase of the total variation of the solution (TVD - Total Variation Diminishing) [11,15,16]. In this approach, to fight with numerical oscillations, an increase in the order of approximation is used, which is achieved by adding delimiters to the difference scheme in such a way that the scheme possesses a high order on smooth solutions and retains monotonicity in the regions of strong discontinuity. Methods for constructing difference schemes with low dispersion also include the ENO (essentially non-oscillatory) and WENO (weighted essentially non-oscillatory) methods [17-20]. These methods, like the TVD methods, are used to achieve a more subtle balance between dispersion and dissipation errors. Increasing the order of approximation in these schemes is achieved by increasing the computational template. Most highly accurate methods based on explicit wide-template difference schemes [21, 22] of an increased (up to the 12th [23]) approximation are found in shallow water problems [24] and aeroacoustics [25, 26]. However, the use of wide-scale schemes faces a number of difficulties associated with setting the boundary conditions, modifying the templates near the boundaries, and the sensitivity of the schemes used to the degree of homogeneity of the calculated grids.

The use of wide-template schemes is not the only way to obtain good dissipative and dispersion properties. Another direction for improving the properties of difference schemes was formulated in [27], [28]. On the example of the solution of the one-dimensional convection transfer equation, explicit linear 3-layer difference schemes with improved dispersive and dissipative properties were shown in these papers and are known as the

Upwind Leapfrog [27] and Cabaret (Compact Accurately Boundary-Adjusting High-REsolution Technique) schemes [28]. The Cabaret scheme is designed taking into account the results of the Upwind Leapfrog scheme. It was based on a new formulation of the compact Upwind Leapfrog scheme of the second order, which is achieved by introducing independent conservative and flux variables. The scheme proposed in the first papers [28], [29] was further developed in [30], [31]. The necessary monotonization of the solutions in the regions of large gradients was achieved with the help of a simple algorithm of nonlinear correction of fluxes based on the maximum principle [30].

A distinctive feature of the Cabaret scheme, in comparison with the most high-resolution schemes, is that it is completely discrete in space and time (x, t), has a second order in x and t ($O(\Delta x^2 + \Delta t^2)$) and, all improved properties are obtained on the least possible compact difference template. Later, the Cabaret scheme was generalized to the cases described by quasilinear hyperbolic equations [32], [33] and the equations of gas dynamics in the one-dimensional and two-dimensional approximation [34].

The brief overview shows that the problem of finding new ways to improve the dissipative and dispersive properties of the difference schemes used to solve the problems of fluid and gas mechanics remains open and is still relevant.

The purpose of this publication is to demonstrate a different approach to improving the dissipative-dispersion properties of difference schemes with a second order of approximation. The achievement of this goal is carried out using the method of dynamic adaptation [35], [36], in which the controlled distribution of nodes of the grid at each time is achieved by the sought solution. A complete matching of the motion of the grid nodes with the evolution of the solution leads to a decrease in the dissipation and to the complete zeroing of the dispersion of the difference scheme. Demonstration of the possibilities of the approach is carried out using the example of a numerical solution of the Burgers equation. The effectiveness of this approach is determined by comparing the results of the solution of the Burgers equation with the use of two-layer difference schemes of Crank-Nicolson and three-layered Cabaret type.

## 2 STATEMENT OF THE PROBLEM

A number of mathematical models that form the basis of the problems of fluid and gas mechanics are reduced to the convection-diffusion problems. These models describe two basic mechanisms of energy and substance transfer: diffusion and convection. Depending on the external conditions, each of the mechanisms may have a dominant influence. To estimate the predominance of a particular process, one usually uses dimensionless parameters, the so-called Peclet number ($Pe$) or Reynolds number ($Re$). At $Pe \ll 1$ ($Re \ll 1$) the diffusion process dominates in the system, and for $Pe \gg 1$ ($Re \gg 1$) the convective transfer predominates. In the case of strong dominance of the convective transport mechanism, a class of singularly perturbed nonlinear mathematical models with a small parameter $\mu = Pe^{-1}$ or $\mu = Re^{-1}$ with the highest derivative is obtained. Nonstationary singularly perturbed models on the basis of the Burgers-Buckley-Leverett equations allow the emergence of regions of strong change in the solution propagating in the form of various fronts and transition layers.

From a computational point of view, singularly perturbed problems are referred to as difficult problems to be solved. In particular, the difference schemes used to approximate the convection-diffusion equations, as a rule, have a strong dispersion, for the suppression of which special measures are applied. In computing practice, a wide application as a test

problem for the problems of the boundary layer, parabolized and complete Navier-Stokes equations has the Burgers equation with the corresponding boundary conditions. The complete non-linear Burgers equation contains a quadratic nonlinearity in the convective summand and a linear viscosity on the right-hand side. The solution of the Burgers equation, with a coefficient of viscosity tending to zero, can contain both strong (shock waves) and weak discontinuities, which allows one to analyze all the singularities of the solution for arbitrary initial data.

Taking into account the initial and boundary conditions, the Burgers problem is formulated as follows:

$$\frac{\partial u}{\partial t}+\frac{\partial}{\partial x}\left(\frac{u^2}{2}\right)=\mu\frac{\partial^2 u}{\partial x^2} \tag{1}$$

$$t>0,\quad x_0<x<x_R$$

$$t=0:\quad u(x,0)=u_0(x),\quad x_0<x<x_R \tag{2}$$

$$x=x_0:\quad g_0\left(x,t,u(x),\frac{\partial u}{\partial x}\right)=0,\quad x=x_R:\quad g_R\left(x,t,u(x),\frac{\partial u}{\partial x}\right)=0 \tag{3}$$

where the coefficient $\mu(x)$ has the meaning of viscosity, $u_0(x)$, $g_0\left(x,t,u(x),\frac{\partial u}{\partial x}\right)$, $g_R\left(x,t,u(x),\frac{\partial u}{\partial x}\right)$ are given functions.

## 3 ONE-PARAMETER FAMILIES OF TWO- AND THREE-LAYER DIFFERENCE SCHEMES OF THE SECOND, $O(\Delta t^2+h^2)$

Consider the calculation space $\Omega_{x,t}$, in which a Cartesian coordinate system is set with variables $(x,t)$. In the space $\Omega_{x,t}$ consider a computational grid $\omega_{\Delta x}^{\Delta t}$, in which for convenience we use nodes with integer and half-integer indices:

$$\omega_{\Delta x}^{\Delta t}=\left(x_m,t^k\right),\left(x_{m+\frac{1}{2}},t^{k+\frac{1}{2}}\right):x_{m+1}=x_m+\Delta x_m,\ x_{m+\frac{1}{2}}=x_m+\frac{\Delta x_m}{2},$$

$$t^{k+1}=t^k+\Delta t^k,\ t^{k+\frac{1}{2}}=t^k+\frac{\Delta t^k}{2},\quad m=\overline{0,N};\ k=\overline{0,J}$$

The one-parameter family of two-layer schemes for the Burgers equation, written out on a computational grid with fixed nodes, has the form:

$$\frac{u_{m-1/2}^{k+1}-u_{m-1/2}^{k}}{\Delta t^{j}}=\sigma\left[-\frac{1}{2\Delta x}\left(\frac{(u_{m+1/2}^{k+1})^2}{2}-\frac{(u_{m-3/2}^{k+1})^2}{2}\right)+\frac{\mu}{\Delta x}\left(\frac{u_{m+1/2}^{k+1}-u_{m-1/2}^{k+1}}{\Delta x}-\frac{u_{m-1/2}^{k+1}-u_{m-3/2}^{k+1}}{\Delta x}\right)\right]+$$

$$+(1-\sigma)\left[-\frac{1}{2\Delta x}\left(\frac{(u_{m+1/2}^{k})^2}{2}-\frac{(u_{m-3/2}^{k})^2}{2}\right)+\frac{\mu}{\Delta x}\left(\frac{u_{m+1/2}^{k}-u_{m-1/2}^{k}}{\Delta x}-\frac{u_{m-1/2}^{k}-u_{m-3/2}^{k}}{\Delta x}\right)\right] \quad (4)$$

where $\sigma$ is the weight factor, determining the degree of implicitness of the difference scheme, $0<\sigma<1$. For $\sigma$ = 0.5 we have a symmetric Crank-Nicolson scheme with the second order of approximation $O(\Delta t^2+\Delta x^2)$.

Using the approach to constructing an implicit three-layer difference scheme for the linear transport equation, presented in [34], we write out a family of three-layer implicit schemes of Cabaret type, consisting of 3 parts, for the Burgers equation (1).

Part one – time transition $u_{m-1/2}^{k}\to u_{m-1/2}^{k+1/2}$

$$\frac{u_{m-1/2}^{k+1/2}-u_{m-1/2}^{k}}{\Delta\tau/2}+\sigma_1\frac{1}{\Delta x}\left(\frac{\left(u_m^{k+1}\right)^2}{2}-\frac{\left(u_{m-1}^{k+1}\right)^2}{2}\right)+(1-\sigma_1)\frac{1}{\Delta x}\left(\frac{\left(u_m^{k}\right)^2}{2}-\frac{\left(u_{m-1}^{k}\right)^2}{2}\right)=$$

$$=(1-\sigma_2)\frac{\mu}{\Delta x}\left[\left(\frac{u_{m+1/2}^{k+1/2}-u_{m-1/2}^{k+1/2}}{\Delta x}\right)-\left(\frac{u_{m-1/2}^{k+1/2}-u_{m-3/2}^{k+1/2}}{\Delta x}\right)\right]+$$

$$+\sigma_2\frac{\mu}{\Delta x}\left[\left(\frac{u_{m+1/2}^{k}-u_{m-1/2}^{k}}{\Delta x}\right)-\left(\frac{u_{m-1/2}^{k}-u_{m-3/2}^{k}}{\Delta x}\right)\right]$$

Part two – extrapolation

$$u_m^{k+1}=\begin{cases}2u_{m-1/2}^{k+1/2}-u_{m-1}^{k}, & for \quad u_{m-1/2}^{k+1/2}>0;\\ u_{m-1/2}^{k+1/2}+u_{m+1/2}^{k+1/2}-u_m^{k}, & for \quad u_{m-1/2}^{k+1/2}=0;\\ 2u_{m+1/2}^{k+1/2}-u_{m+1}^{k}, & for \quad u_{m-1/2}^{k+1/2}<0;\end{cases} \quad (5)$$

Part three – time transition $u_{m-1/2}^{k+1/2}\to u_{m-1/2}^{k+1}$

$$\frac{u_{m-1/2}^{k+1}-u_{m-1/2}^{k+1/2}}{\Delta\tau/2}+(1-\sigma_1)\frac{1}{\Delta x}\left(\frac{\left(u_m^{k+1}\right)^2}{2}-\frac{\left(u_{m-1}^{k+1}\right)^2}{2}\right)+\sigma_1\frac{1}{\Delta x}\left(\frac{\left(u_m^{k}\right)^2}{2}-\frac{\left(u_{m-1}^{k}\right)^2}{2}\right)=$$

$$=\sigma_2\frac{\mu}{\Delta x}\left[\left(\frac{u_{m+1/2}^{k+1}-u_{m-1/2}^{k+1}}{\Delta x}\right)-\left(\frac{u_{m-1/2}^{k+1}-u_{m-3/2}^{k+1}}{\Delta x}\right)\right]+$$

$$+(1-\sigma_2)\frac{\mu}{\Delta x}\left[\left(\frac{u_{m+1/2}^{k+1/2}-u_{m-1/2}^{k+1/2}}{\Delta x}\right)-\left(\frac{u_{m-1/2}^{k+1/2}-u_{m-3/2}^{k+1/2}}{\Delta x}\right)\right]$$

For $\sigma_1 = \sigma_2 = 0.5$ we obtain a scheme with the second order of approximation $O(\Delta t^2+\Delta x^2)$.

## 4 ALGORITHM OF NUMERICAL SOLUTION

The system of difference equations (4) was solved by the Newton iterative method with the use of a three-diagonal sweep method at each iteration [37] to solve a system of linear algebraic equations. The step of integration $\Delta\tau^k$ was selected automatically based on the specified accuracy and the maximum number of iterations

Algorithm for the numerical solution of an implicit three-layer scheme (5) with $\sigma_1 = \sigma_2 = 0.5$ consists of three stages.

At the first stage, a system of nonlinear algebraic equations is solved (6), from where the conservative variables are found $u_{m-1/2}^{k+1/2}$ during the first half-timestep.

$$\begin{aligned}
&\frac{u_{m-1/2}^{k+1}-u_{m-1/2}^{k+1/2}}{\Delta\tau/2}+\frac{1}{2}\frac{1}{\Delta x}\left(\frac{\left(u_m^{k+1}\right)^2}{2}-\frac{\left(u_{m-1}^{k+1}\right)^2}{2}\right)+\frac{1}{2}\frac{1}{\Delta x}\left(\frac{\left(u_m^{k}\right)^2}{2}-\frac{\left(u_{m-1}^{k}\right)^2}{2}\right)= \\
&=\frac{1}{2}\frac{\mu}{\Delta x}\left[\left(\frac{u_{m+1/2}^{k+1}-u_{m-1/2}^{k+1}}{\Delta x}\right)-\left(\frac{u_{m-1/2}^{k+1}-u_{m-3/2}^{k+1}}{\Delta x}\right)\right]+ \\
&+\frac{1}{2}\frac{\mu}{\Delta x}\left[\left(\frac{u_{m+1/2}^{k+1/2}-u_{m-1/2}^{k+1/2}}{\Delta x}\right)-\left(\frac{u_{m-1/2}^{k+1/2}-u_{m-3/2}^{k+1/2}}{\Delta x}\right)\right]
\end{aligned} \tag{6}$$

At the second stage, extrapolation of the flux variables occurs within the space-time cells.

$$u_m^{k+1}=\begin{cases}2u_{m-1/2}^{k+1/2}-u_{m-1}^{k}, & \text{for} \quad u_{m-1/2}^{k+1/2}>0;\\ u_{m-1/2}^{k+1/2}+u_{m+1/2}^{k+1/2}-u_m^{k}, & \text{for} \quad u_{m-1/2}^{k+1/2}=0;\\ 2u_{m+1/2}^{k+1/2}-u_{m+1}^{k}, & \text{for} \quad u_{m-1/2}^{k+1/2}<0;\end{cases} \tag{7}$$

At the third stage, the system of the difference equations is solved, from which the conservative variables $u_{m-1/2}^{k+1}$ are found at the new time layer [29], [30]:

$$\begin{aligned}
&\frac{u_{m-1/2}^{k+1}-u_{m-1/2}^{k+1/2}}{\Delta\tau/2}+\frac{1}{2}\frac{1}{\Delta x}\left(\frac{\left(u_m^{k+1}\right)^2}{2}-\frac{\left(u_{m-1}^{k+1}\right)^2}{2}\right)+\frac{1}{2}\frac{1}{\Delta x}\left(\frac{\left(u_m^{k}\right)^2}{2}-\frac{\left(u_{m-1}^{k}\right)^2}{2}\right)= \\
&=\frac{1}{2}\frac{\mu}{\Delta x}\left[\left(\frac{u_{m+1/2}^{k+1}-u_{m-1/2}^{k+1}}{\Delta x}\right)-\left(\frac{u_{m-1/2}^{k+1}-u_{m-3/2}^{k+1}}{\Delta x}\right)\right]+\frac{1}{2}\frac{\mu}{\Delta x}\left[\left(\frac{u_{m+1/2}^{k+1/2}-u_{m-1/2}^{k+1/2}}{\Delta x}\right)-\left(\frac{u_{m-1/2}^{k+1/2}-u_{m-3/2}^{k+1/2}}{\Delta x}\right)\right]
\end{aligned} \tag{8}$$

Just as in the case of a two-layer scheme, the iterative Newton method was used to solve the difference schemes (6), (8) using sweeping at each iteration. The integration step $\Delta\tau^k$ was selected automatically based on the specified accuracy and the maximum number of iterations. To achieve monotonicity of the solution in the presence of large gradients, after each iteration, the solution was monotonized on the basis of the maximum principle:

$$u_m^{s+1} = \begin{cases} min(u_{m-1}^k, u_m^k), & for \quad u_{m-1/2}^{k+1/2} > 0, u_m^{s+1} \le min(u_{m-1}^k, u_m^k); \\ max(u_{m-1}^k, u_m^k), & for \quad u_{m-1/2}^{k+1/2} > 0, u_m^{s+1} \ge max(u_{m-1}^k, u_m^k); \\ u_m^{s+1}, & for \quad u_{m-1/2}^{k+1/2} > 0, min(u_{m-1}^k, u_m^k) \le u_m^{s+1} \le max(u_{m-1}^k, u_m^k); \\ min(u_{m+1}^k, u_m^k), & for \quad u_{m-1/2}^{k+1/2} < 0, u_m^{s+1} \le min(u_{m+1}^k, u_m^k); \\ max(u_{m+1}^k, u_m^k), & for \quad u_{m-1/2}^{k+1/2} < 0, u_m^{s+1} \ge max(u_{m+1}^k, u_m^k); \\ u_m^{s+1}, & for \quad u_{m-1/2}^{k+1/2} < 0, min(u_{m+1}^k, u_m^k) \le u_m^{s+1} \le max(u_{m+1}^k, u_m^k); \end{cases} \tag{9}$$

where $s$ - is the iteration number.

## 5 MODELING AND ANALYSIS OF THE QUALITY OF TWO- AND THREE-LAYER DIFFERENCE SCHEMES ON THE GRIDS WITH FIXED NODES

The developed difference schemes (4), (6-9) were used to perform a series of calculations with subsequent comparison and an analysis of the quality of the scheme properties. As a test problem, we considered a nonlinear equation (1) with an initial condition in the form of an asymmetric sinusoid

$$u_0(x) = u(x,0) = sin(2\pi x) + 0.5\, sin(\pi x) \tag{10}$$

and boundary conditions:

$$u(x_0, t) = u(x_R, t) = 0 \tag{11}$$

The calculations were carried out on a grid with the same number of nodes – $N = 2500$. The value of $\mu$ parameter was chosen from the range $\mu \in \{10^{-3} \div 10^{-6}\}$.

Modeling showed that two half-waves of the sinusoid moving towards each other form a steep front, the thickness of which is determined by the value of the parameter $\mu$. The use of the two-layer Crank-Nicolson scheme (5) showed that the first parasitic oscillations on the upper part of the front appear at $\mu=10^{-3}$ (Fig. 1a). The solution $u(x)$ obtained from the three-layer scheme with the flux correction (6) – (9) does not have any oscillations (Fig. 1b).

Further growth of the gradient of the solution, caused by a decrease in the parameter $\mu = 10^{-4}$ -$10^{-6}$ leads to an increase in parasitic oscillations in solutions obtained from a two-layer scheme (5), (Fig.2 – 4), which testifies to the deterioration of the dispersion properties of the scheme from which the three-layer scheme (6) - (9) is free, using the procedure for monotonization of the solution, over the whole range of the values of the parameter $\mu$ (Fig.5).

Thus, the three-layer difference schemes of the Cabaret type, written out on the computational grids with fixed nodes, have a distinct advantage in the dispersion properties over the two-layer Crank-Nicolson schemes.

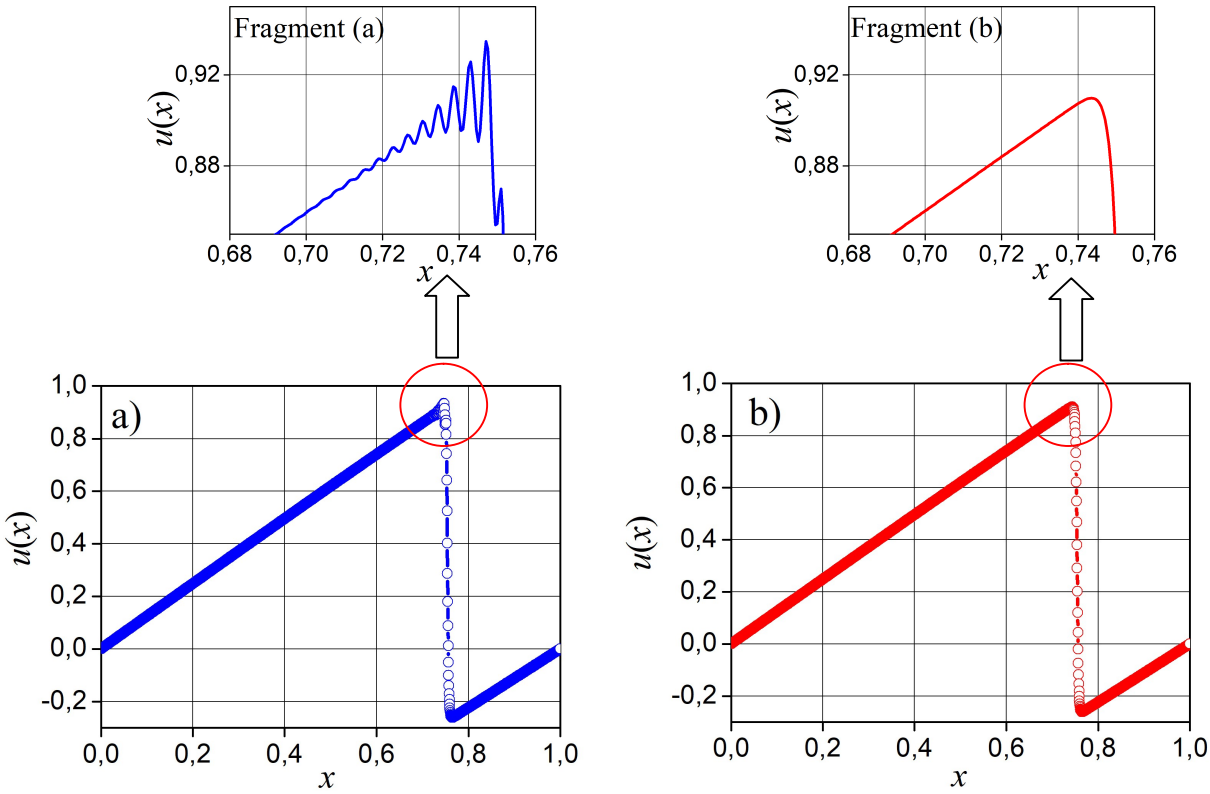


Fig. 1. Two-layer (a) and three-layer (b) schemes, $\mu=10^{-3}$

However, as noted in paper [34], the monotonization of the solution after each iteration in the region of large gradients leads to a deviation of the result from the exact solution of the original system of non-linear difference equations and can hinder the convergence of the iterative process.

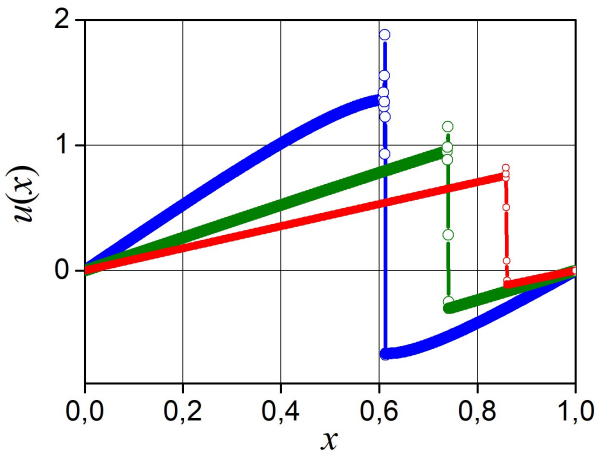


Fig. 2. Two-layer scheme, $\mu=10^{-4}$. Spatial profiles of the solution *u(x)* at the moments $t_{1\text{-}3}$ = 0.25, 0.63, 1.0

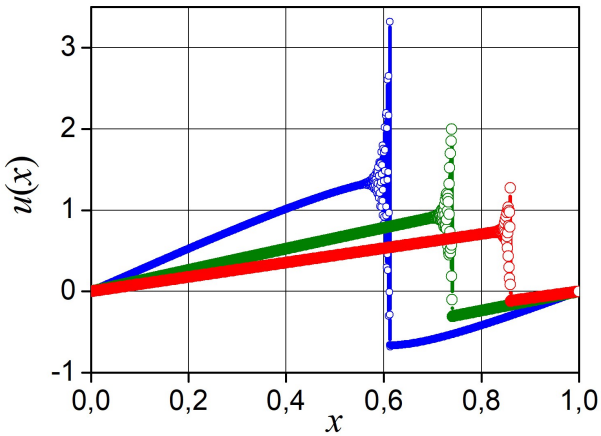


Fig. 3. Two-layer scheme, $\mu$=$10^{-5}$ . Spatial profiles of the solution *u(x)* at the moments $t_{1\text{-}3}$ = 0.25, 0.63, 1.0

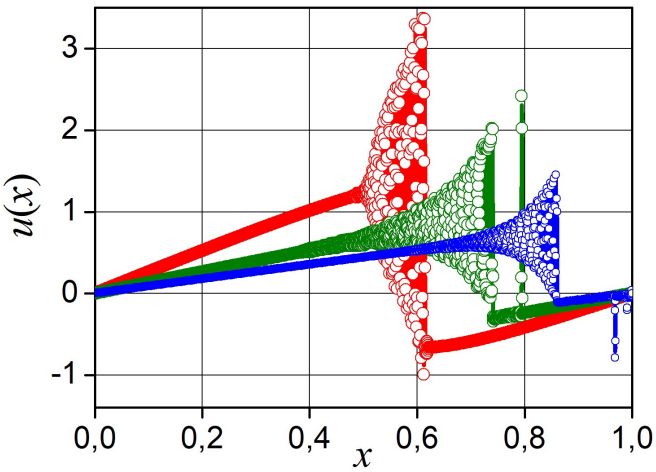


Fig. 4. Two-layer scheme, $\mu$=$10^{-6}$. Spatial profiles of the solution *u(x)* at the moments $t_{1\text{-}3}$ = 0.25, 0.63, 1.0

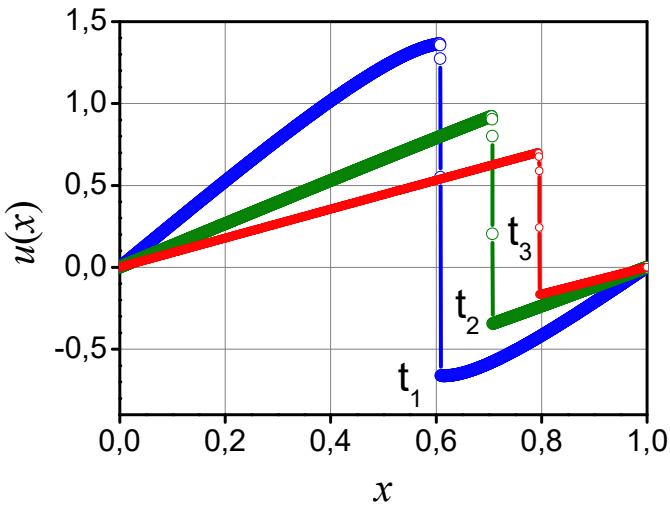


Fig. 5. Three-layer scheme, $\mu$=$10^{-4}$,. Spatial profiles of the solution *u(x)* at the moemnts $t_{1\text{-}3}$ = 0.25, 0.63, 1.0

In this model problem (1), (10), (11), this defect is most clearly manifested in the slowing down of the motion of the solution front in comparison with the front of the exact solution [1] (Fig. 6a, b). The deceleration depends on the value of the parameter $\mu$. The greatest lag is observed at $\mu = 10^{-3}$ and noticeably decreases at $\mu = 10^{-4}$, $\mu = 10^{-5}$.

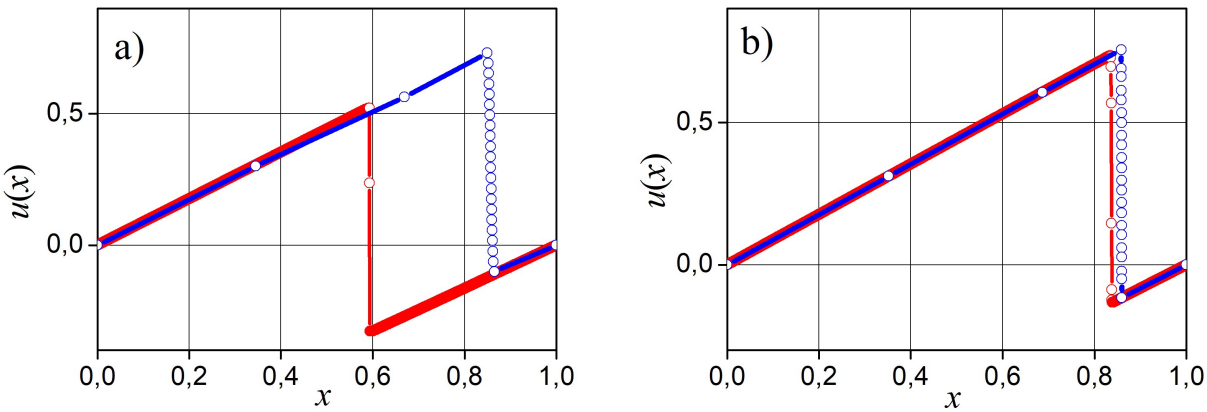


Fig. 6. Exact solution (blue line with symbols) and the solution obtained using the three-layer scheme (red line with symbols) for (a) -$\mu$=$10^{-3}$, (b) - $\mu$=$10^{-4}$.

The deviation from the exact solution in the region of large gradients is caused by the use of nonlinear correction of the fluxes, which is confirmed by comparing the results of calculations performed with monotonization of the solution and without it (Fig. 7 a, b). The front of the solution without the monotonization process is noticeably ahead of the front with monotonization. This indicates that the monotonization procedure used, despite the algorithmic simplicity, is not sufficiently flexible. Thus, the approach to improving the quality of the solution using difference schemes proposed in [28] - [34] is not free from certain shortcomings.

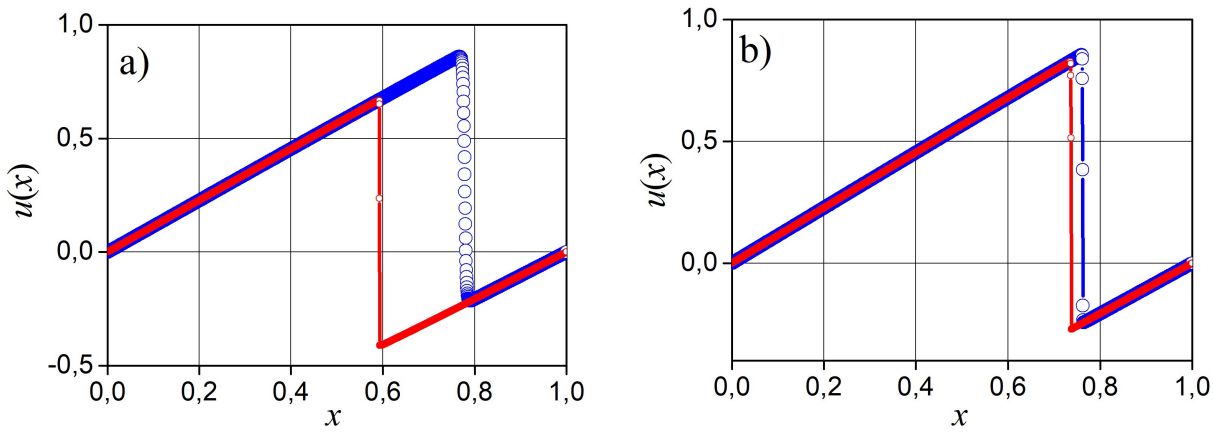


Fig. 7. The solution obtained using the three-layer scheme with monotonization (red line with symbols) and without monotonization (blue line with symbols) for (a) - $\mu$=$10^{-3}$, (b) - $\mu$=$10^{-4}$.

In the present paper, as an alternative, the reduction in the approximation error is proposed to be carried out using the method of dynamic adaptation of computational grids [35], [36], [38], [39]. The dynamic adaptation method was widely used to solve one-dimensional gasdynamic problems [40] - [45], one-dimensional and two-dimensional equations of parabolic type [46] - [49], one- and two-dimensional Stefan problems with moving phase boundaries [50] - [56] and a number of problems of laser action on matter [57] - [61].

## 6 MODELING AND ANALYSIS OF THE QUALITY OF THE TWO- AND THREE-LAYER DIFFERENCE SCHEMES ON THE GRIDS WITH MOVING NODES

The dynamic adaptation method is based on the procedure for transition from physical space $\Omega_{x,t}$ with a Cartesian coordinate system and variables $(x,t)$ to some calculation space $\Omega_{q,\tau}$ with an arbitrary non-stationary coordinate system and variables $(q,\tau)$. The arbitrariness of a non-stationary coordinate system means that the speed of this coordinate system is unknown beforehand and must be determined in the course of the solution. The transition to an arbitrary nonstationary coordinate system makes it possible to formulate the problem of constructing and adapting computational grids at a differential level, because of this, in the resulting mathematical model, part of the differential equations describes physical processes, and the other describes the behavior of grid nodes [35], [40]. This allows adapting grids to various features of the solution, such as: large gradients [35], [36], [39] moving boundaries [48] - [52] and discontinuous solutions [40], [43] - [ 45].

The transition to an arbitrary non-stationary coordinate system is carried out by means of automatic transformation of coordinates with the help of the sought solution. The partial derivatives of the independent variables in the transition from one system to another are related by the following expressions:

$$\frac{\partial \cdot}{\partial t}=\frac{\partial \cdot}{\partial \tau}+\frac{Q}{\psi}\frac{\partial \cdot}{\partial q}\ ; \qquad \frac{\partial \cdot}{\partial x}=\frac{1}{\psi}\frac{\partial \cdot}{\partial q}; \qquad \frac{\partial^2 \cdot}{\partial x^2}=\frac{1}{\psi}\frac{\partial \cdot}{\partial q}\frac{1}{\psi}\frac{\partial}{\partial q} \tag{12}$$

where $\psi=\partial x/\partial q$ is the Jacobian of inverse transformation, the function $Q$ characterizes the speed of motion of an unsteady coordinate system, is unknown in advance and is to be determined.

Using the relations (12) we represent the differential model (1) in the variables $(q,\tau)$:

$$\frac{\partial u}{\partial \tau}+\frac{Q}{\psi}\frac{\partial u}{\partial q}+\frac{1}{\psi}\frac{\partial}{\partial q}\left(\frac{u^2}{2}\right)=\frac{\mu}{\psi}\frac{\partial}{\partial q}\frac{1}{\psi}\frac{\partial u}{\partial q} \tag{13}$$

$$\frac{\partial x}{\partial \tau}=-Q \tag{14}$$

where (14) is the equation of inverse transformation with transformation function $Q$. The equation (14) is used to construct the grid that adapts to the solution. Its difference analog describes the dynamics of grid nodes, while the function $Q$ realizes controlled movement of grid nodes, coordinated with the dynamics of the sought solution. The coordination is achieved by introducing a dependence of the function $Q$ on the sought solution. Optimal transformation function $Q$, which ensures the complete coherence of the adaptation

mechanism with the desired solution, is determined from the quasi-stationary principle [36], [39], [48].

The meaning of the principle of quasi-stationarity lies in the requirement of transition to a non-stationary coordinate system in which the time derivatives of the solution are close to or equal to zero: $\partial u/\partial\tau = 0$ . When this condition is satisfied, the equation (13) takes the form

$$\frac{Q}{\psi}\frac{\partial u}{\partial q}+\frac{1}{\psi}\frac{\partial}{\partial q}\left(\frac{u^2}{2}\right)=\frac{\mu}{\psi}\frac{\partial}{\partial q}\frac{1}{\psi}\frac{\partial u}{\partial q} \tag{15}$$

and serves to determine the function $Q$:

$$Q=-\left(u-\frac{\partial}{\partial q}\left(\frac{\mu}{\psi}\right)-\frac{\mu}{\psi}\left(\frac{\partial^2 u}{\partial q^2}\right)\left(\frac{\partial u}{\partial q}+re\right)^{-1}\right) \tag{16}$$

where $re << 1$ is the regularizer that prevents the first derivative from going to zero. The third term in (16) does not play any important role and can be ignored.

### 6.1 Differential approximation of difference schemes

By analyzing the differential approximation of the three-layer difference scheme, we show that the function found is optimal in the sense of the quality of the solution with a minimal number of grid nodes.

We introduce in the computational space $\overline{\Omega}_{q,\tau}$ a computational grid $\omega_{\Delta q}^{\Delta\tau}$ :

$$\omega_{\Delta q}^{\Delta\tau}=\left(\begin{array}{l}\left(q_m,\tau^k\right);\quad q_{m+1}=q_m+\Delta q,\quad \tau^{k+1}=\tau^k+\Delta\tau^k, q_{m+\frac{1}{2}}=q_m+\dfrac{\Delta q}{2},\quad t^{k+\frac{1}{2}}=t^k+\dfrac{\Delta t^k}{2}\\ m=0,1,\ldots N\text{-}1,\quad k=0,1,\ldots,J\end{array}\right).$$

and consider the first part of the three-layer difference scheme for equation (15)

$$\begin{aligned}&\frac{1}{\Delta q}\left(\frac{(u_m^{k+1})^2}{2}-\frac{(u_{m-1}^{k+1})^2}{2}+Q_m^{k+1}u_m^{k+1}-Q_{m-1}^{k+1}u_{m-1}^{k+1}\right)+\frac{1}{\Delta q}\left(\frac{(u_m^{k})^2}{2}-\frac{(u_{m-1}^{k})^2}{2}+Q_m^{k}u_m^{k}-Q_{m-1}^{k}u_{m-1}^{k}\right)=\\
&=\frac{\mu}{2\Delta q}\left[\left(\frac{2}{\psi_{m+1/2}^{k+1}+\psi_{m-1/2}^{k+1}}\frac{u_{m+1/2}^{k+1}-u_{m-1/2}^{k+1}}{\Delta q}\right)-\left(\frac{2}{\psi_{m-1/2}^{k+1}+\psi_{m-3/2}^{k+1}}\frac{u_{m-1/2}^{k+1}-u_{m-3/2}^{k+1}}{\Delta q}\right)\right]+\\
&+\frac{\mu}{2\Delta q}\left[\left(\frac{2}{\psi_{m+1/2}^{k}+\psi_{m-1/2}^{k}}\frac{u_{m+1/2}^{k}-u_{m-1/2}^{k}}{\Delta q}\right)-\left(\frac{2}{\psi_{m-1/2}^{k}+\psi_{m-3/2}^{k}}\frac{u_{m-1/2}^{k}-u_{m-3/2}^{k}}{\Delta q}\right)\right]+\\
&+\frac{\mu}{\Delta q}\left[\left(\frac{2}{\psi_{m+1/2}^{k+1/2}+\psi_{m-1/2}^{k+1/2}}\frac{u_{m+1/2}^{k+1/2}-u_{m-1/2}^{k+1/2}}{\Delta q}\right)-\left(\frac{2}{\psi_{m-1/2}^{k+1/2}+\psi_{m-3/2}^{k+1/2}}\frac{u_{m-1/2}^{k+1/2}-u_{m-3/2}^{k+1/2}}{\Delta q}\right)\right]\end{aligned} \tag{17}$$

When using the finite difference method, not the initial partial differential equation is solved numerically, but some modified equation, called differential approximation of the

difference scheme [62,63]. The right-hand side of this approximation is the approximation error and is equal to the difference between the original partial differential equation and its finite-difference analogue. An analysis of the right-hand sides of differential approximations makes it possible to establish the predominant contribution to the error in approximating the higher derivatives and associated properties of difference schemes such as dissipation and dispersion. It is known that if the principal term in the expression for the approximation error contains derivatives of even order, then the predominant properties of the difference schemes will be dissipative, and if the derivatives of odd order – then will be dispersive.

Let us write down the differential approximation for the difference scheme (17). To obtain differential approximations, we use the standard procedure for expanding the grid functions in a neighborhood of the point $(m,m_{+1/2})$ in a Taylor series. Omitting simple but cumbersome transformations, we write the differential approximation in the final form.

$$\frac{Q}{\psi}\frac{\partial u}{\partial q}+\frac{1}{\psi}\frac{\partial}{\partial q}\left(\frac{u^2}{2}\right)-\frac{1}{\psi}\frac{\partial}{\partial q}\left(\frac{\mu}{\psi}\frac{\partial u}{\partial q}\right)=\frac{1}{\psi}\left(\alpha\frac{\partial^2 u}{\partial q^2}+\beta\frac{\partial^3 u}{\partial q^3}+\gamma\frac{\partial^4 u}{\partial q^4}+\delta\frac{\partial^3}{\partial q^3}\left(\frac{1}{\psi}\right)\right) \tag{18}$$

The coefficients of the derivatives on the right-hand side of Eq. (18) α, β, γ, δ are expressed as follows

$$\alpha=-\frac{\Delta q^2}{32}\left(4\frac{\partial u}{\partial q}-\mu\frac{\partial^2}{\partial q^2}\left(\frac{1}{\psi}\right)\right),\quad \beta=\frac{\Delta q^2}{24}\left(\mu\frac{\partial}{\partial q}\left(\frac{1}{\psi}\right)-u+Q\right),\quad \gamma=\frac{\Delta q^2}{48}\frac{\mu}{\psi},\quad \delta=\mu\frac{\Delta q^2}{96}\frac{\partial u}{\partial q}$$

In the differential approximation (18), the most important role is played by the terms on the right-hand side of the second and third derivative equations, characterizing the dissipation and dispersion of the difference scheme, respectively. The coefficients $\alpha$ and $\beta$, standing respectively before the second and third derivatives, depend on the adaptation parameters. This means that the dissipation and dispersion of the difference schemes depend on the method of adaptation and can be changed in the necessary direction. The coefficient $\beta$ explicitly depends on the fucntion $Q$, which allows, using the appropriate choice of $Q$ to convert the coefficient $\beta$ to zero. Thus, one can almost completely get rid of the internal dispersion of the difference scheme. The coefficient $\beta$ vanishes if the function $Q$ is set equal to:

$$Q=-\left(u-\frac{\partial}{\partial q}\left(\frac{\mu}{\psi}\right)\right) \tag{19}$$

A similar analysis for a two-layer scheme was carried out in Refs. [35-36].

### 6.2 Modeling results

We consider the possibilities of reducing the error in the approximation of two and three-layer difference schemes by considering the numerical solution of the Burgers problem (1), (11), (12) using the dynamic adaptation method. For this, in the computational space $\Omega_{q,\tau}$ with variables $(q,\tau)$ we represent the Burgers equation (14) in a divergence form, and write the equation of the inverse transformation (15) in a modified, more convenient form

$$\frac{\partial(\psi u)}{\partial \tau} = -\frac{\partial(Q\cdot u)}{\partial q} - \frac{\partial}{\partial q}\left(\frac{u^2}{2}\right) + \frac{\partial}{\partial q}\frac{\mu}{\psi}\frac{\partial u}{\partial q}, \tag{20}$$

$$\frac{\partial \psi}{\partial \tau} = -\frac{\partial Q}{\partial q}, \qquad q_0 < q < q_R, \quad \tau > 0 \tag{21}$$

The equations (20), (21) are supplemented by the initial

$$u(q,0) = sin(2\pi q) + 0.5\,sin(\pi q) \qquad \psi(q,0) = 1$$

and boundary conditions:

$$u(q_0,\tau) = u(q_R,\tau) = 0 \qquad Q(q_0,\tau) = Q(q_R,\tau) = 0$$

The function $Q$ was set in the form (19) $\quad Q = -\left(u - \frac{\partial}{\partial q}\left(\frac{\mu}{\psi}\right)\right)$

### 6.3 Algorithm of numerical solution on a dynamic grid

Using a computational grid with integer and half-integer nodes, we write out a family of two-layer conservative difference schemes for the system of equations (20), (21). The functions $x_m^k$, $u_m^k$, $Q_m^k$ are written in the integer nodes and the grid fucntions $\psi_{m+1/2}^k$ are written in the half-integer nodes $\left(q_{m+1/2}, \tau^k\right)$. The family of the two-layer difference schemes has the form:

$$(\psi u)_m^{k+1} = (\psi u)_m^k - \frac{\Delta\tau^k}{\Delta q}\left\{ \begin{array}{l} (1-\sigma)\left[\begin{array}{l} \frac{1}{2}\left(\frac{u_{m+1}^2}{2} - \frac{u_{m-1}^2}{2}\right) - \frac{\mu}{\psi_{m+1/2}}\frac{u_{m+1}-u_m}{\Delta q} + \frac{\mu}{\psi_{m-1/2}}\frac{u_m - u_{m-1}}{\Delta q} + \\ + \frac{(uQ)_{m+1} - (uQ)_{m-1}}{2} \end{array}\right]^k + \\ + \sigma\left[\begin{array}{l} \frac{1}{2}\left(\frac{u_{m+1}^2}{2} - \frac{u_{m-1}^2}{2}\right) - \frac{\mu}{\psi_{m+1/2}}\frac{u_{m+1}-u_m}{\Delta q} + \frac{\mu}{\psi_{m-1/2}}\frac{u_m - u_{m-1}}{\Delta q} + \\ + \frac{(uQ)_{m+1} - (uQ)_{m-1}}{2} \end{array}\right]^{k+1} \end{array}\right\} \tag{22}$$

$$\psi_{m+1/2}^{k+1} = \psi_{m+1/2}^k - \frac{\Delta\tau^k}{\Delta q}\left((1-\sigma)\left[Q_{m+1} - Q_m\right]^k + \sigma\left[Q_{m+1} - Q_m\right]^{k+1}\right) \tag{23}$$

$$Q_m = -\left[u_m - \frac{\mu}{\Delta x}\left(\frac{1}{\psi_{m+1/2}} - \frac{1}{\psi_{m-1/2}}\right)\right]$$

In the calculations, the Crank-Nicolson scheme (σ = 0.5) was used with the second order of approximation O($\Delta\tau^2 + \Delta q^2$). Since the dynamic adaptation mechanism is formulated at the differential level, the main differences between the computational algorithm in the variables

$(q,\tau)$ are associated with the appearance of an additional equation (21). A system of two-layer difference schemes (22), (23) was solved by separate sweeps with internal and external iterations.

The algorithm for the numerical solution of an implicit three-layer scheme, as in variables $(x,t)$, consists of three stages. First, a system of nonlinear algebraic equations is solved in the first half-step in time, from which the conservative variables $u_{m-1/2}^{j+1/2}$ are found.

$$\begin{aligned}
&\frac{\psi_{m-1/2}^{k+1/2}u_{m-1/2}^{k+1/2}-\psi_{m-1/2}^{k}u_{m-1/2}^{k}}{\Delta\tau/2}+\frac{1}{2}\frac{1}{\Delta q}\left(\frac{(u_m^{k+1})^2}{2}-\frac{(u_{m-1}^{k+1})^2}{2}+Q_m^{k+1}u_m^{k+1}-Q_{m-1}^{k+1}u_{m-1}^{k+1}\right)+\\
&+\frac{1}{2}\frac{1}{\Delta q}\left(\frac{(u_m^{k})^2}{2}-\frac{(u_{m-1}^{k})^2}{2}+Q_m^{k}u_m^{k}-Q_{m-1}^{k}u_{m-1}^{k}\right)=\\
&=\frac{1}{2}\frac{\mu}{\Delta q}\left[\left(\frac{2}{\psi_{m+1/2}^{k+1/2}+\psi_{m-1/2}^{k+1/2}}\frac{u_{m+1/2}^{k+1/2}-u_{m-1/2}^{k+1/2}}{\Delta q}\right)-\left(\frac{2}{\psi_{m-1/2}^{k+1/2}+\psi_{m-3/2}^{k+1/2}}\frac{u_{m-1/2}^{k+1/2}-u_{m-3/2}^{k+1/2}}{\Delta q}\right)\right]+\\
&+\frac{1}{2}\frac{\mu}{\Delta q}\left[\left(\frac{2}{\psi_{m+1/2}^{k}+\psi_{m-1/2}^{k}}\frac{u_{m+1/2}^{k}-u_{m-1/2}^{k}}{\Delta q}\right)-\left(\frac{2}{\psi_{m-1/2}^{k}+\psi_{m-3/2}^{k}}\frac{u_{m-1/2}^{k}-u_{m-3/2}^{k}}{\Delta q}\right)\right]
\end{aligned} \tag{24}$$

At the secodn stage – extrapolation of stream variables within space-time cells is performed

$$u_m^{k+1}=\begin{cases}2u_{m-1/2}^{k+1/2}-u_{m-1}^{k}, & for\ \left(u_{m-1/2}^{k+1/2}-Q_{m-1/2}^{k+1/2}\right)>0;\\ u_{m-1/2}^{k+1/2}+u_{m+1/2}^{k+1/2}-u_m^{k}, & for\ \left(u_{m-1/2}^{k+1/2}-Q_{m-1/2}^{k+1/2}\right)=0;\\ 2u_{m+1/2}^{k+1/2}-u_{m+1}^{k}, & for\ \left(u_{m-1/2}^{k+1/2}-Q_{m-1/2}^{k+1/2}\right)<0;\end{cases} \tag{25}$$

At the third stage, the system of difference equations is solved at the second half-step so the conservative variables $u_{m-1/2}^{k+1}$ are found at the new time layer

$$\begin{aligned}
&\frac{\psi_{m-1/2}^{k+1}u_{m-1/2}^{k+1}-\psi_{m-1/2}^{k+1/2}u_{m-1/2}^{k+1/2}}{\Delta\tau/2}+\frac{1}{2}\frac{1}{\Delta q}\left(\frac{(u_m^{k+1})^2}{2}-\frac{(u_{m-1}^{k+1})^2}{2}+Q_m^{k+1}u_m^{k+1}-Q_{m-1}^{k+1}u_{m-1}^{k+1}\right)+\\
&+\frac{1}{2}\frac{1}{\Delta q}\left(\frac{(u_m^{k})^2}{2}-\frac{(u_{m-1}^{k})^2}{2}+Q_m^{k}u_m^{k}-Q_{m-1}^{k}u_{m-1}^{k}\right)=\\
&=\frac{1}{2}\frac{\mu}{\Delta q}\left[\left(\frac{2}{\psi_{m+1/2}^{k+1}+\psi_{m-1/2}^{k+1}}\frac{u_{m+1/2}^{k+1}-u_{m-1/2}^{k+1}}{\Delta q}\right)-\left(\frac{2}{\psi_{m-1/2}^{k+1}+\psi_{m-3/2}^{k+1}}\frac{u_{m-1/2}^{k+1}-u_{m-3/2}^{k+1}}{\Delta q}\right)\right]+\\
&+\frac{1}{2}\frac{\mu}{\Delta q}\left[\left(\frac{2}{\psi_{m+1/2}^{k+1/2}+\psi_{m-1/2}^{k+1/2}}\frac{u_{m+1/2}^{k+1/2}-u_{m-1/2}^{k+1/2}}{\Delta q}\right)-\left(\frac{2}{\psi_{m-1/2}^{k+1/2}+\psi_{m-3/2}^{k+1/2}}\frac{u_{m-1/2}^{k+1/2}-u_{m-3/2}^{k+1/2}}{\Delta q}\right)\right]
\end{aligned} \tag{26}$$

The difference schemes of the first (24) and third (26) stages were solved together with the scheme (21). The principal point of the computational algorithm is the elimination from the solution of the procedure of non-linear flux correction (monotonization), since it turns out to be excessive.

### 6.4 Analysis of the computaion results

The numerical solution of problem (20) - (21) in the perameter range $\mu \in \left(10^{-3} \div 10^{-6}\right)$ was carried out by means of two and three-layer difference schemes (22), (23) and (24) - (26). All calculations were carried out on adaptive grids with the same number of nodes. To achive the same precision as with the grids with fixed nodes, the number of nodes for the adaptive grid N = 25 turned out to be by 2 orders lower. Fig. 8,9 show the spatial profiles of the grid functions $u(x)$ and $\psi(x)$ at 4 moments of time for $\mu = 10^{-4}$. The results of calculations using the two-layer (22), (23) and three-layer (24)-(26) schemes showed a good match between each other and the exact solution. The profiles of the function $u(x)$ are completely free from the parasitic oscillations. In this case, the three-layer scheme (24) - (26) does not contain a flux correction procedure. As in the case of using the two-layer scheme, the improvement of the quality of the solution in the three-layer scheme is achieved due to the controlled distribution of the grid nodes, the motion of which is completely coordinated with the sought solution.

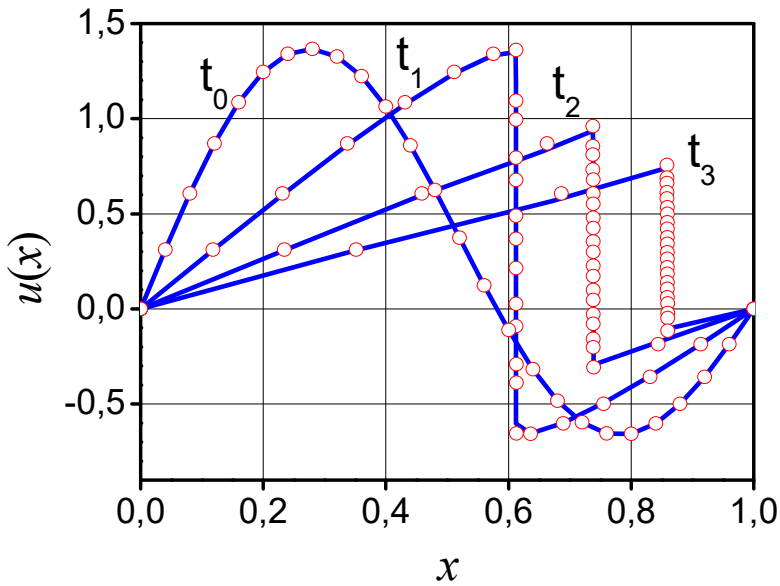


Fig. 8. Spatial profile of the function *u(x)* at different moments.

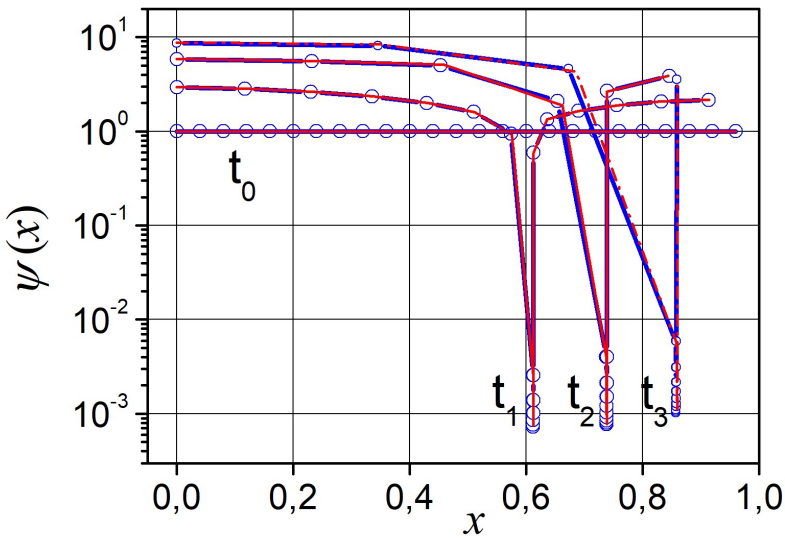


Fig. 9. Spatial profiles of the function *ψ(x)* at different moments.

The dynamics of distribution of the grid nodes in the physical space $\Omega_{x,t}$ with variables $(x,t)$ is characterized by the function $\psi(x)$, Fig. 9. The function $\psi(x)$ representing the ratio $\psi(x) \approx \Delta x / \Delta q$ characterizes the dimensionless spatial step of the grid in the space $\Omega_{x,t}$ since $\Delta q$ does not change with time. The function $\psi(x)$ shows how much the spatial grid step $\Delta x(t)$ changes at each moment of time.

The spatial profiles of $u(x)$ and $\psi(x)$ indicate a smooth concentration of the grid nodes in the region of the front of the function, which corresponds to a decrease in the grid spacing by 3 orders of magnitude, Fig. 9, with a simultaneous increase in the grid spacing by 2-9 times in the region of a slow change in the solution.

Thus, due to full conformity with the sought solution, dynamic adaptation turned out to be a more subtle and flexible mechanism for reducing the error of approximation of difference schemes in comparison with the method of nonlinear correction of fluxes.

## 7 CONCLUSION

- The families of two-layer and three-layer difference schemes of the second order for the complete burgers equation in fixed cartesian and arbitrary non-stationary coordinate systems were constructed.
- Modeling with the subsequent analysis of its results has shown that in the cartesian coordinate system the quality of the numerical solution essentially depends on the quality of the finite-difference approximation used for the initial equation.
- The main drawback of three-layer difference schemes is the presence in the region of large gradients of a difficultly removable deviation of the numerical solution from the exact one, which is caused by the process of forced monotonization of the solution. This circumstance stimulates the search for other ways of reducing the error of approximation.

- The use of non-stationary coordinate systems makes it possible to change the approximation error in the course of the solution by controlling the motion of the grid nodes, in contrast to stationary coordinate systems in which the approximation error is determined by the original structure of the difference scheme. The application of an arbitrary non-stationary coordinate system made it possible to create a universal dynamic adaptation method for a wide class of problems in mathematical physics in which the distribution of nodes is dependent and controlled by the sought solution. This makes it possible to automatically adjust the calculated grid in such a way that the approximation error is minimal practically regardless of the quality of the original difference scheme. The numerical solution of the nonlinear burgers equation with the help of two and three-layer difference schemes on a dynamically adapting grid showed virtually complete coincidence of the calculations among themselves, good agreement with the exact solution with complete absence of oscillations in the solution. The computational grid contained the number of nodes (N = 25) by two orders of magnitude smaller than the grid with fixed nodes.
- Dynamic adaptation of grids is an independent, flexible and the most accurate way of reducing the approximation error, in particular in the problems of convection-diffusion with the dominant convection mechanism.

**Acknowledgements**: The work was funded by Russian Science Foundation, grant No. 18-11-00318 and the Competitiveness Enhancement Program of the MEPhI.

## REFERENCES

[1] B.L. Rozhdestvenskij, N.N. Yanenko, *Sistemy` kvazilinejny`x uravnenij i ix prilozheniya k gazovoj dinamike*, M.: Nauka (1978)
[2] C. Truesdell, *A First Course in Rational Continuum Mechanics*, The Johns Hopkins University, Baltimore, Maryland, 1972
[3] L. D. Landau, E.M. Lifshicz, *Gidrodinamika. Izdanie 4*, M.: Nauka (1988).
[4] A.S. Petrosyan*, Dopolnitel`ny`e glavy` teorii melkoj vody`, Seriya «Mexanika, upravlenie i informatika»*, Moskva, Nauchno - obrazovatel`ny`j Centr Institutf kosmicheskix issledovanij Rossijskoj Akademii nauk (IKI RAN) (2014)
[5] C.K. Godunov, B.C. Ryaben`kij, *Raznostny`e sxemy`*, M.: Nauka, 1980.
[6] P.J. Roache, *Computational Fluid Dynamics, Hermosa*, Albuquerque, 1982
[7] A.A. Samarskij, Yu.P.Popov*, Raznostny`e metody` resheniya zadach gazovoj dinamiki*, Moskva, Izd-vo: URSS (2004)
[8] A. A. Samarskii, *The theory of difference schemes*, New York – Basel. Marcel Dekker (2001)
[9] D. Anderson, J. C. Tannehill, R. H. Pletcher, *Computational Fluid Mechanics and Heat Transfer*, CRC Press; 3 Edition (2012)
[10] S.K. Godunov, "Raznostnaya sxema dlya chislennogo vy`chisleniya razry`vny`x reshenij uravnenij gidrodinamiki", *Matem. Sbornik,* **47**, 271-306 (1959).
[11] A. Harten*, "*High Resolution Schemes for Hyperbolic Conservation Laws", *J. Comput. Phys*, **49** (3), 357–393 (1983)
[12] P.D. Lax, V. Wendroff, "Systems of conservation laws", *Comm. Pure. Appl. Math*., **13**, 217-237 (1960).
[13] J.P.Boris , D.L.Book, K. Hain, "Flux-corrected transport: Generalization of the method", *J. Comput. Physics*, **31**, 335-350 (1975)
[14] B. Van Leer, "Towards the ultimate conservative difference scheme V. A second-order sequel to Godunov's method", *J. Comput. Phys.,* **32**, 101–136 (1979).

[15] A. Harten, "On a class of high resolution total-variation-stable finite-difference schemes", *SIAM Journal on Numerical Ana lysis*, **21**(1), 1-23 (1984)
[16] K. V. Vyaznikov, V. F.Tishkin, A. P. Favorskij, "Postroenie monotonny`x raznostny`x sxem povy`shennogo poryadka approksimacii dlya sistem uravnenij giperbolicheskogo tipa", *Matematicheskoe modelirovanie*, **1**(5), 95-120 (1989)
[17] A. Harten, S. Osher, *Uniformly high-order accurate non-oscillatory schemes*, I. Springer Berlin Heidelberg, 187-217(1997)
[18] C. W.Shu, S. Osher, "Efficient Implementation of Essentially Non-Oscillatory Shock Capturing Schemes", *Journal of Computational Physics*, **77**(2), 439-471(1988)
[19] S. Osher, C. Shu, "Efficient implementation of essentially non-oscillatory shock-capturing schemes, II", *J. Comput. Phys*, **83**(1), 32-78(1989)
[20] X.D. Liu, S. Osher, T. Chan, "Weighted essentially non-oscillatory schemes", *J. Comp. Phys*, **115**, 200-212 (1994).
[21] S.K. Lele, "Compact finite-difference scheme with spectral-like resolution", *J. Comput. Phys*, 103, 16-42 (1992)
[22] C.K.W. Tam, J. C, Webb, "Dispersion-relation-preserving finite difference schemes for computational acoustics", *J. Comput Phys*, **107**, 262-281 (1993)
[23] C. Bogey, C. Bailly, "A family of low dispersive and low dissipative explicit schemes for flow and noise computations", *J. Comput. Phys*, **194**, 194-214 (2004)
[24] Yu.A. Kriksin, P.A. Kuchugov, M.E. Ladonkina, O.A. Nekliudova, V.F. Tishkin and V.P. Varin, "Construction of exact solutions of some equations of hyperbolic type containing discontinuity moving on a non uniform background", *Mathematica Montisnigri*, 42 (2018)
[25] T. Colonius, S.K. Lele, "Computational aeroacoustics: progress on nonlinear problems of sound generation", *Progress in Aerospace Sei*, **40**, 345-416 (2004)
[26] V. M. Goloviznin, S. A. Karabasov, T. K. Kozubskaya, N. V. Maksimov, "Sxema "Kabare" dlya chislennogo resheniya zadach ae`roakustiki: obobshhenie na linearizirovanny`e uravneniya E`jlera v odnomernom sluchae", *Zh. vy`ch. mat. matem. fiz*., **49** (12), 2265–2280 (2009)
[27] A. Iserles, "Generalized Leapfrog Methods", *IMA J. Numer. Analys*., **6**, 381-392 (1986)
[28] V.M. Goloviznin, A.A. Samarskij, "Raznostnaya approksimaciya konvektivnogo perenosa s prostranstvenny`m rasshhepleniem vremennoj proizvodnoj", *Matem. modelirovanie*, **10**(1), 86 (1998)
[29] V.M Goloviznin, A.A. Samarskij, "Nekotory`e svojstva raznostnoj sxemy` Kabare", *Mat. mod*, **10** (1), 101–116 (1998)
[30] V.M Goloviznin, S.A. Karabasov, "Nelinejnaya korrekciya sxemy` Kabare", *Matem. modelirovanie*, **10** (12), 107–123 (1998)
[31] V.M. Goloviznin, S.A. Karabasov, I.M. Kobrinskij, "Balansno-xarakteristicheskie sxemy` s razdelenny`mi konservativny`mi i potokovy`mi peremenny`mi", *Matem. modelirovanie*, **15** (9), 29–48 (2003)
[32] A. Chintagunta, S.E. Naghibi, S.A. Karabasov, "Flux-corrected dispersion-improved CABARET schemes for linear and nonlinear wave propagation problems", Computers and Fluids, **169**, 111–128 (2018)
[33] S.A. Karabasov, V.M., Goloviznin, "Compact accurately boundary adjusting high-REsolution technique for fluid dynamics", *J. Comput. Phys*, **228**, 7426-7451 (2009)
[34] V.M. Goloviznin, D.Yu. Gorbachev, A.M. Kolokol`nikov, P.A. Majorov, P.A. Majorov, B.A. Tlepsuk, "Neyavny`e obratimy`e po vremeni sxemy` "kabare" dlya kvazilinejny`x uravnenij melkoj vody", *Vy`ch. met. programmirovanie*, **17**(4), 402–414 (2016)
[35] V. I. Mazhukin, A. A. Samarskij, A. V. Shapranov, "Metod dinamicheskoj adaptacii v probleme Burgers", *Dokl. Akad. Nauka*, **333** (2), 165-169 (1993)
[36] A.V. Mazhukin and V.I. Mazhukin, "Dynamic Adaptation for Parabolic Equations", *Computational Mathematics and Mathematical Physics*, **47** (11), 1833–1855 (2007)

[37] A. A. Samarskij, *Vvedenie v chislennye metody*, Izdatel`stvo Nauka, (1982)
[38] N.A. Dar'in, V.I. Mazhukin, "Ob odnom podxode k postroeniyu adaptivny`x raznostny`x setok", *Akademiia Nauk SSSR, Doklady*, 298 (1), 64-68 (1988)
[39] V.I.Mazhukin, O.Kastel`yanos, A.A.Samarskiy, A.V.Shapranov," Metod dinamicheskoy adaptacii dlya nestacionarnyh zadach s bol`shimi gradientami", *Matematicheskoe modelirovanie*, **5**(4), 32-56 (1993)
[40] N.A.Dar`in, V.I.Mazhukin, A.A.Samarskiy, "Konechno-raznostnyy metod resheniya odnomernyh uravneniy gazovoy dinamiki na adaptivnyh setkah", *Doklady AN SSSR*, **302**(5), 1078-1081 (1988)
[41] P. V. Breslavskiy, V. I. Mazhukin, "Algoritm chislennogo resheniya gidrodinamicheskogo varianta zadachi Stefana pri pomoshhi dinamicheski adaptiruyushhihsya setok", *Matematicheskoe modelirovanie*, **3**(10), 104–115 (1991)
[42] P.V.Breslavskiy, V.I.Mazhukin, "Metod dinamicheskoy adaptacii v zadachah gazovoy dinamiki", *Matematicheskoe modelirovanie* , **7**(12), 48-78 (1995)
[43] P. V. Breslavskii, V. I. Mazhukin, "Dynamically Adapted Grids for Interacting Discontinuous Solutions", *Computational Mathematics and Mathematical Physics*, **47**(4), 687–706 (2007)
[44] P.V. Breslavskiy, V.I. Mazhukin, "Metod dinamicheskoy adaptacii v zadachah gazovoy dinamiki s nelineynoy teploprovodnost`yu", *Zhurnal vychislitel`noy matematiki i matematicheskoy fiziki*, **48**(11), 2067–2080 (2008)
P. V. Breslavskii and V. I. Mazhukin, "Dynamic Adaptation Method in Gasdynamic Simulations with Nonlinear Heat Conduction", *Computational Mathematics and Mathematical Physics*, **48**(11), 2102–2115 (2008)
[45] V.I. Mazhukin, P.V. Breslsavskii, A.V.Shapranov, "Dinamicheskaya adaptaciya v differencial`nyh uravneniyah v chastnyh proizvodnyh giperbolicheskogo tipa", *Enciklopediya nizkotemperaturnoy plazmy, Matematicheskoe modelirovanie v nizkotemperaturnoy plazme, Chast 1, Moskva, Yanus-K*, Seriya B, Vol. YII, pp. 217 - 247, (2008)
[46] N.A.Dar`in, V.I.Mazhukin, "Matematicheskoe modelirovanie nestacionarnyh dvumernyh kraevyh zadach na setkah s dinamicheskoy adaptaciey", *Matematicheskoe modelirovanie*, **1**(3), 29-43 (1989)
[47] V.I.Mazhukin, L.Yu.Takoeva, "Principy postroeniya dinamicheski adaptiruyushhihsya k resheniyu setok", *Matematicheskoe modelirovanie*, **2**(3), 101-118 (1990)
[48] V.I.Mazhukin, M.M.Demin, A.V.Shapranov, I.Smurov, "The method of construction dynamically adapting grids for problems of unstable laminar combustion", *Numerical Heat Transfer, Part B: Fundamentals*, **44**(4), 387 – 415 (2003)
[49] V.I. Mazhukin, A.V. Mazhukin, A.V.Shapranov, "Dinamicheskaya adaptaciya v differencial`nyh uravneniyah v chastnyh proizvodnyh parabolicheskogo tipa", *Enciklopediya nizkotemperaturnoy plazmy, Matematicheskoe modelirovanie v nizkotemperaturnoy plazme, Chast 1, Moskva, Yanus-K*, Seriya B, Vol. YII, 190 – 216 (2008)
[50] V.I.Mazhukin, A.A.Samarskiy, M.M.Chuyko, "Metod dinamicheskoy adaptacii dlya chislennogo resheniya nestacionarnyh mnogomernyh zadach Stefana", *Doklady RAN*, **368**(3), 307 – 310 (1999)
[51] V.I.Mazhukin, M.M. Chuiko, "Solution of two-dimensional multi-interface Stefan problem by the method of dynamic adaptation", *Mathematical Modeling and Analysis*, **6**(1), 129 – 137 (2001)
[52] V.I.Mazhukin, O.N.Koroleva, M.M.Chuiko, "Modeling of formation of deep 2D channels in metal targets via laser irradiation", *SPIE "Laser Processing of Advanced Materials and Laser Microtechnologies"*, **5121**, 87 – 97 (2002)
[53] V.I.Mazhukin, M.M.Chuiko, "Solution of multi-interface Stefan problem by the method of dynamic adaptation", *Computation Methods in Applied Mathematics*, **2**(3), 283-294 (2002)
[54] V.I.Mazhukin, M.M.Chuiko A.M.Lapanik, "Dynamic adaptation method for numerical solution of axisymmetric Stefan problems", *Mathematical Modeling and Analysis*, **8**(4)303 -314 (2003)

[55] V.I.Mazhukin, M.M. Chuiko, A.M.Lapanik, "Dynamic adaptation method for modeling of melting and evaporation processes with convection", *Mathematical Modeling and Analysis*, **10**, 473 – 478 (2005)
[56] V.I. Mazhukin, A.V. Shapranov, A.V. Mazhukin, O.N. Koroleva, "Mathematical formulation of a kinetic version of Stefan problem for heterogeneous melting/ crystallization of metals", *Mathematica Montisnigri*, **36**, 58-77 (2016)
[57] V.I.Mazhukin, I. Smurov, C. Dupuy, D. Jeandel, "Simulation of Laser Induced Melting and Evaporation Processes in Superconducting", *J. Numerical Heat Transfer Part A*, **26**, 587-600 (1994)
[58] V.I.Mazhukin, A.A. Samarskii, "Mathematical Modeling in the Technology of Laser Treatments of Materials", *Review. Surveys on Mathematics for Industry*, **4**(2), 85-149 (1994)
[59] O.N.Korolyova, V.I.Mazhukin, "Matematicheskoe modelirovanie lazernogo plavleniya i ispareniya mnogosloynyh materialov", *Zhurnal vychislitel`noy matematiki i matematicheskoy fiziki*, **46**(5), 910 – 925 (2006)
O.N.Koroleva, V.I.Mazhukin, "Mathematical Simulation of Laser Induced Melting and Evaporation of Multilayer Materials", *Computational Mathematics and Mathematical Physics*, **46**(5), 848 – 862 (2006)
[60] V.I. Mazhukin, M.M. Demin, A.V. Shapranov, "High-speed laser ablation of metal with pico- and subpicosecond pulses", *Applied Surface Science*, 302, 6–10 (2014)
[61] V.I. Mazhukin, A.V. Mazhukin, M.M. Demin, A.V. Shapranov, "Nanosecond laser ablation of target Al in a gaseous medium: explosive boiling", *Applied Physics A*, **124** (3), 237(1-10) (2018)
[62] R.E. Warming, B.J. Hyett, "The Modified Equation Approach to the Stability and Accuracy Analysis of Finite difference Nethods", *J. Comput. Phys.*, **14**, 159 -179, (1974)
[63] Yu.I. Shokin, *Pervoe differenzial`noe priblizhenie*, - Izdatel`stvo Nauka, (1979)

*The results were presented at the 17-th International seminar "Mathematical models & modeling in laser-plasma processes & advanced science technologies" (May 26 – June 2, 2018, Budva, Montenegro).*

Received April 10, 2018.

MATHEMATICA MONTISNIGRI
Vol XLII (2018)

# ON THE CONSTRUCTION OF THE GENERALIZED NUMERICAL EXPERIMENT IN FLUID DYNAMICS

**A.E. BONDAREV**[1]

[1] Keldysh Institute of Applied Mathematics Russian Academy of Sciences
Miusskaya sq. 4, 125047 Moscow, Russia
e-mail: bond@keldysh.ru

**Summary.** The paper considers the construction of a generalized numerical experiment for problems of computational fluid dynamics (CFD). Generalized numerical experiment allows to obtain a solution not for one specific mathematical modeling problem, but for a class of problems defined in the multidimensional space of defining parameters. The basis of this approach is the use of parallel computing for the organization of multitasking. We consider the construction of interfaces for the organization of calculations, processing and analysis of the results. Some examples are given illustrating the application of the approach for constructing such an experiment for various classes of CFD problems in computational gas dynamics. Also examples of such experiment application to problems of analyzing the accuracy of numerical methods and the effectiveness of parallelization tools are considered.

## 1 INTRODUCTION

Long before the advent of the computer age, the main source of information in the problems of gas dynamics was a physical experiment. It was the experiment that made it possible to obtain the necessary information about flows and their properties, to obtain a visual representation of the flow pattern, and to obtain the relationships between gas-dynamic quantities characteristic of this picture. The results of such experiments are extensively presented in papers [1, 2]. However, in practical applications it was always not enough simply to obtain in the experiment the flow field for some single case. The main goal of a physical experiment has always been not the modeling of the physical phenomenon itself, but the elucidation of the circumstances under which it occurs, i.e. obtaining the dependence of the appearance of the phenomenon on the defining parameters of the problem, such as Mach numbers, Reynolds, Prandtl numbers, etc., and geometric parameters of the problem. In fact, the establishment of such physical laws for shock waves, separated flows, characteristic configurations of streamlined bodies was the main task of fluid and gas mechanics. Accordingly, it was necessary to carry out a series of physical experiments where the determining parameters of the flow varied, such as the velocity, viscosity, properties of the medium, etc. Such large-scale experimental work made it possible to obtain key relationships for the dependence of the gasdynamic functions of interest or the conditions for the appearance of a physical effect on the key determining parameters.

As a striking example of such a dependence, one can cite the famous formula of G.I. Petrov, representing the fundamental law on the ultimate pressure drop in the shock, which the turbulent boundary layer is able to withstand without detachment from the wall [3]:

**2010 Mathematics Subject Classification:** 49Q99, 76M27.
**Key words and Phrases:** generalized numerical experiment, parallel computations, parametric studies

$$P_2 / P_1 = 0.713M_e + 0.213$$

Here $P_2 / P_1$ is the pressure drop, $M_e$ is the Mach number before the separation point, varying from 1.5 to 4.

Another example is the famous Kozlov formula [4], which represents the dependence of surface friction on Mach numbers, Reynolds numbers and the temperature factor:

$$c_{fw} = 0{,}085 Re_w^{-0{,}29+0{,}01\lg Re_w} \bar{T}_{we}^{0{,}39} \bar{T}_e^{0{,}2}$$

Here $c_{fw}$, $Re_w$ is the coefficient of surface friction and the Reynolds number calculated with reference to the wall temperature, $T_e$ is the temperature at the outer boundary of the boundary layer, and is the temperature factor.

The advent of computer technology allowed solving the problems of mathematical modeling of currents, which sharply reduced the need for large-scale physical experiments. However, in the problems of mathematical modeling, the main tendency of carrying out series of calculations with the variation of the defining parameters of the problem also remained. The main goal was the same - to determine the conditions for the appearance of a physical phenomenon when the external conditions of the problem are varied. The determination of such conditions and their approximation with the aid of an analytical expression was the main goal of practical computational fluid dynamics. There are many examples of such studies. Here we give an author's example [5], which presents a series of numerical experiments on the flow of a backward ledge by a viscous gas flow. As a result of the experiments, a generalized formula is obtained that represents the characteristic time of the establishment of the flow as a function of the Mach and Reynolds numbers of the external flow:

$$\tau^* = 10{,}7[1 - 0{,}14(M_\infty - 2)]\left[1 + 19{,}45\left(\frac{1}{\sqrt{Re}} - \frac{1}{\sqrt{10^3}}\right)\right]$$

Here $\tau^*$ is the characteristic settling time, $M_\infty$ , $Re$ are the Mach and Reynolds numbers. The generalized formula is given for the range $2 \le M_\infty \le 3$, $1000 \le Re \le 5000$.

Nevertheless, obtaining such dependencies required a huge number of computational experiments and was very laborious.

The emergence of high-performance computing that allows for parallel computations has ensured the possibility of parallel calculation of the same problem with different input data in multitask mode. This makes it possible at the present time to construct and carry out *a generalized computational experiment*.

## 2 FORMULATION OF THE PROBLEM

A generalized computing experiment involves splitting each of the defining parameters of a problem within a certain range. Thus, a grid decomposition is formed for some multidimensional parallelepiped composed of the defining parameters of the considered

problem of gas dynamics. For each point of this grid, the problem is calculated in the space of the determining parameters. Formally, this can be written as follows.

Suppose that there is a reliable numerical method for solving two-dimensional and three-dimensional nonstationary problems of computational gas dynamics. Then we can obtain a numerical solution $F(x, y, z, t, A_1, \dots, A_N)$ for any point in the space of a computational domain, where *x, y, z* are the spatial coordinates, $t$ is the time, $A_1, \dots, A_N$ are the defining parameters of the problem. As defining parameters of the problem, we will keep in mind the characteristic numbers describing the properties of the flow under consideration, such as the Mach numbers, Reynolds, Prandtl, Strouhal, etc., and the characteristic geometric parameters. Each of the characteristic parameters is limited in a certain range:

$$A_i^{min} \leq A_i \leq A_i^{max}, \quad i = 1, \dots, N$$

We divide each of the parameters $A_i$ into $k$-1 parts, so we obtain for each parameter a partition consisting of $k$ points. The volume of an $N$-dimensional space formed by a set of defining parameters $A_i$ is filled with a set of $k^N$ points.

Denoting the point from the given set, as $(A_1^*, \dots, A_N^*)$, we arrive at the fact that for each point of the collection it is necessary to obtain a numerical solution of the gas-dynamic problem $F(, x, y, z, t, A_1^*, \dots, A_N^*)$.

It is easy to see that this will require solving $k^N$ gasdynamic problems, which is impossible without the use of parallel calculations in a multitask mode. In practice, the number $N$ usually does not exceed 5, which corresponds to the computing capabilities at the current time.

It should also be noted that we formulated the classical problem of parametric study. Parametric numerical studies allow one to obtain a solution not for one particular mathematical modeling problem, but for a class of problems defined in a multidimensional space of defining parameters. Also, such a formal formulation allows numerical study of optimization analysis problems, when the inverse problem is solved at each point of the grid partition of the multidimensional space of the determining parameters. Both types of similar problems are considered in a series of papers [6 - 9].

## 3 PARALLEL SOLUTIONS

The only way to effectively carry out a generalized numerical experiment is applying of parallel computations. The problem of the optimal and effective way of parallelization was thoroughly discussed in the papers [7,8 ]. There were considered parts of the whole algorithm for parameter optimization and analysis. For these parts the main criterion of applicability for parallelizing is independence of specific numerical method. From this point of view the most perspective way for parallelizing is applying the approach of multitask parallelism using the principle “one task – one process”. Due to minimal quantity of internal exchanges between the processes we are able to create an effective practical tool for generalized numerical experiment.

The general parallel computing scheme used for such experiment is shown in Figure 1.

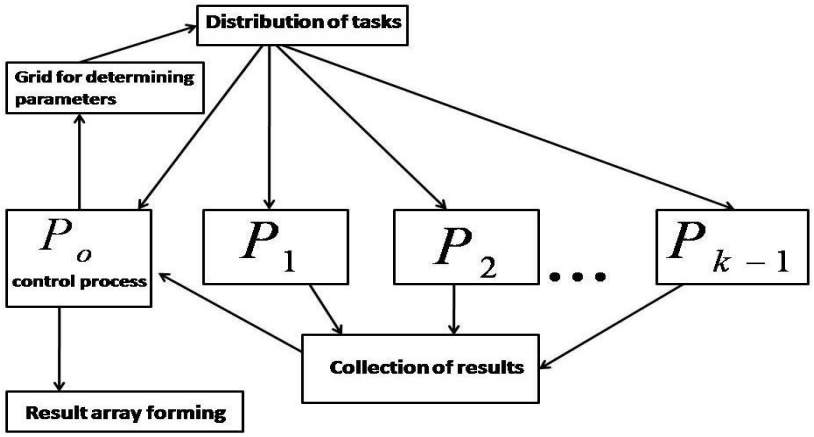


Figure 1: Parallel computing scheme for generalized numerical experiment.

We assume that $k$ processes are provided for parallel computation. The control process $P_0$ creates the grid in the multidimensional space of determining parameters, then $P_0$ forms tasks and sends the tasks to others processes and to itself also. After task completion $P_0$ collects the results and implements all procedures defined by user, such as data processing and transformation.

Due to the absence of internal exchanges between the processes the procedure of parallelizing amounts to creation of control interface for tasks distribution and data collecting in one multidimensional array.

There are two effective and easy ways to create such interface for parallel computations. The first way is to apply MPI (Message Passing Interface) [10]. This variant of parallelizing allows implementing a program tool for generalized numerical experiment. The computation can be carried out $k$ times faster according to the number of provided processes.

The other way of parallelization is application of DVM technology [11, 12], elaborated in Keldysh Institute of Applied Mathematics RAS. DVM-system provides unified toolkit to develop parallel programs of scientific-technical calculations in C and Fortran. DVM parallel model is based on data parallel model. The DVM name reflects two names of the model - Distributed Virtual Memory and Distributed Virtual Machine. These two names show that DVM model is adopted both for shared memory systems and for distributed memory systems. DVM high level model allows not only to decrease cost of parallel program development but provides unified formalized base for supporting Run-Time System, debugging, performance analyzing and prediction. Unified parallel model is built in C and Fortran languages on the base of the constructions, that are "transparent" for standard compilers, that allows to have single version of the program for sequential and parallel execution. C-DVM and Fortran DVM compilers translate DVM-program in C or Fortran program correspondingly, including parallel execution Run-Time Support system calls. So only requirement to a parallel system is availability of C and Fortran compilers. This way of code parallelizing allows one to save a lot of human resources for coding and debugging. At the same time DVM parallelization provides less speed of computations in comparison with MPI.

For both types of parallel technologies special control interfaces for parameter optimization and analysis were designed [8]. Both control interfaces were applied to jet

interaction problem for testing. Testing computations were carried out for 20 processors. According to test results the time of computations for DVM method is 205 seconds. The same test for MPI case requires 144 seconds. At the same time DVM application allowed to decrease human expenses for coding and debugging up to ten times as against MPI. So both types of parallel technologies are quite applicable for problems in question. The calculations were performed using a hybrid supercomputer K-100 [13] in Keldysh Institute of Applied Mathematics RAS.

With the help of the constructed interfaces, a series of calculations were carried out, realizing the concept of a generalized numerical experiment for various classes of problems. The results of the calculations will be shown in the following sections. Both developed interfaces are very versatile. They can be applied to almost any software code for solving the CFD problem chosen as the base one.

It should be noted that modern version of Aiwlib library [14] has some similar properties which make this library applicable for construction of generalized numerical experiment. Aiwlib library is a library for C++11 and Python languages, which is aimed for the development of high-performance computing numerical simulation applications running under GNU/Linus OS. It also provides means for batch calculations.

## 4 PROCESSING AND ANALYSIS OF THE RESULTS

As a result of implementing the construction of a generalized numerical experiment and performing parallel calculations, we obtain a large data set representing a set of numerical solutions $F(x, y, z, t, A_1, \dots, A_N)$ for each point $(A_1^*, \dots, A_N^*)$ of the partition of the multidimensional volume of the defining parameters $(A_1, \dots, A_N)$ of the problem under consideration. This volume in its original form is rather difficult to use, although its availability for further purposes is necessary. As a rule, when studying the conditions for the appearance of a physical effect (for example, the emergence of a space-time structure), the object of primary interest is not gas-dynamic fields, but certain markers or objective functions determined with the help of these fields. The creation of such markers and goal functions is an extensive topic that deserves a separate discussion and is beyond the scope of this article. Suppose that some function $P$ that plays the role of a marker is defined and can be calculated for each solution $F(x, y, z, t, A_1, \dots, A_N)$ obtained from the calculated fields of gas-dynamic quantities. Then the main task is to analyze the multidimensional array $P(A_1, \dots, A_N)$. This problem is considerably covered by the fact that, as indicated above, in practice the number $N$ usually does not exceed 5. Practical approaches to solving problems of this kind are described in [8, 9, 15]. As the basic method of solution, the following is indicated: decreasing the dimensionality of the investigated array to 3, visual representation of the new array, approximation of the dependence using geometric primitives of the first or second order.

There are some ways to decrease the array dimensionality. These ways are well known from the group of methods for multidimensional data processing and analysis. Being frank we should note the fact that most of these methods were used for a long time before computers appearance. This field of science was known as “experimental data processing”.

The first way is the analysis of variances for each characteristic parameter. Characteristic parameter is considered as coordinate direction. Data variances $D_1$, $D_2$, ... $D_N$ are computed

along the each direction. Then the variances should be arranged. The direction with minimal variance $D_{\min} = \min\{D_i\}$ is rejected. This procedure sometimes is called as compactification.

More radical kind of compactification can be implemented as follows. After variances computing and arranging one chooses three directions with maximal variances. If other variances are much less than this triplet one changes the data for directions corresponding to other variances by means. After such decreasing of dimensionality one can operate in standard 3D space. This approach has one disadvantage - it does not work if multidimensional data are close to hypersphere. Nevertheless for many practical cases with small dimensionality (4 or 5) the approach works well enough.

Another way is the construction of different 3D data projections for various triplets of determining parameters. If the data on projections for some direction are close to constant then this direction can be rejected.

Also, to reduce the dimension of a multidimensional array, methods of mapping into embedded manifolds of smaller dimension are very effective [16, 17]. Among them, the most common method is the principal component method (PCA). The essence of the method consists in the transition from the initial coordinate system to the new orthogonal basis in the multidimensional space under consideration, whose axes are oriented along the directions of maximum dispersion. The possible scheme of working with an array in this case is the approximation by primitives of the data array in the space of the first three main components and the subsequent transition to the initial space of the determining parameters.

Among the modern methods of reducing the dimension that are common in solving the problems of computational gas dynamics, it is necessary to mention the POD-method (Proper Orthogonal Decomposition) [18]. It involves the creation of a functional orthogonal basis of a smaller dimension, to which the multidimensional dynamic volume under investigation is "pulled on". In this formulation, the eigenvectors of the covariance matrix serve as the vectors of the desired basis. Also, in recent years, dynamical mode decomposition (DMD) has become increasingly popular in the analysis of flows [19, 20]. The dynamic mode decomposition method (DMD) is an algorithm for searching for an evolution operator (inverse operator problem solutions) in a finite-dimensional space of solution of a problem (numerical or experimentally obtained) in a set of solutions (slices, "snapshots") at some successive instants.

## 5 EXAMPLES OF THE GENERALIZED NUMERICAL EXPERIMENT

This section contains the examples of the proposed above approach applied to some practical problems. It is applied in some variations due to different aims for each class of problems.

The first example is the problem of unsteady interaction of the supersonic viscous flow with jet obstacle [7]. Figure 2 illustrates the example. The obstacle appears due to co-current underexpanded jet exhausting from the nozzle. The nozzle is placed to external supersonic viscous flow. Expanding jet propagates on the external surface of the nozzle creating obstacle in external flowfield. Typical flow structure is shown in Figure 2 (a) by streamlines. Time-dependent control action (the velocity of pressure ratio growth in underexpanded jet) allows to change time-space structure of flowfield (Figure 2 (b)). New space-time structure presents

specific flow regime where jet propagates upwind on the external wall of the nozzle. We consider crucial velocity of jet pressure ratio growth as control parameter. The main target of research is estimating and defining the control parameter dependence on four characteristic parameters of the problem – Mach, Reynolds, Prandtl and Strouhal numbers. These parameters are varied in definite ranges creating four-dimensional space. We want to find for each point in this space the crucial velocity corresponding to a new time-space structure appearance. According to the scheme presented in the previous chapters parallel algorithm is implemented for computations. For the space of determining parameters two types of grids are chosen: 5 and 10 points for each determining parameter. It requires computing 625 and 10000 problems. Both MPI and DVM technologies were applied to control parallel computations.

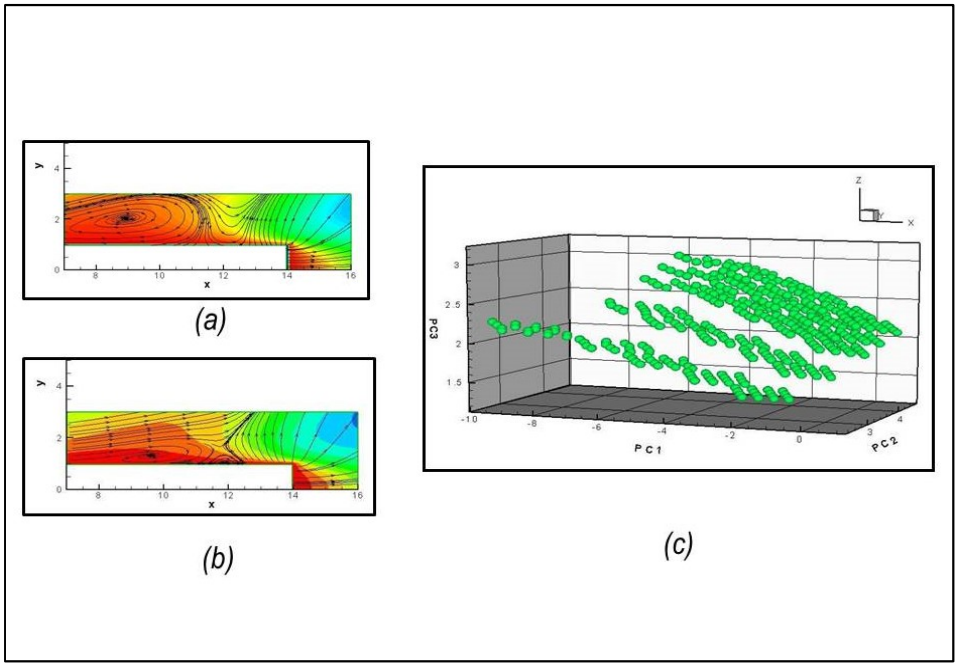


Figure 2: Parameter optimization and analysis applied to jets interaction

As a result of approach application five-dimensional data array is obtained, where variables are four characteristic parameters $M_\infty$, $Re_\infty$, $Pr$, $Sh_\infty$ and crucial velocity $V^*$. For obtained data three principal components are defined and we construct data visual presentation in principal components (Figure 2 (c)). The presentation allows us to suppose that the points of data volume can be roughly approximated by parametric plane. After defining the coefficients for plane and inverse transformation to the original variables we obtain the sought-for dependence $V^*= F(M_\infty, Re_\infty, Pr, Sh_\infty)$ in analytical form. The dimensionality of four-dimensional array under consideration can be decreased up to three, because characteristic parameter $Re_\infty$ has a very small influence on the solution. So the final form for $V^*$ cam be written as follows:

$$V^*= - 0.1\, M_\infty + 0.115\, Pr + 0.24\, Sh_\infty$$

Obtained results present a result of generalized numerical experiment for the class of problems, where the class is defined by multidimensional volume of characteristic parameters.

The second example of application of general numerical experiment is devoted to optimization problem. The example presents a search the optimal shape of a power plant three-dimensional blade assembly [21]. This experiment is based on developed computational technology for the computation of power loads on the 3D blade assembly of a power plant in a wind flow. The calculation for various combinations of the key geometric parameters of the assembly using parallel computations makes it possible to find the optimal shape of the assembly with respect to its power characteristics. A virtual experimental facility for simulating the flow around the power plant based on the solution of the Navier–Stokes equations was created. Computations aimed at determining the optimal shape of the blade assembly taking into account constraints on its design were carried out, and the results were thoroughly analyzed using the proposed optimization procedure. The solution of the optimization problem is based on the parameterization of the design using three key parameters. On the discrete set of values of these parameters, the maximums of two objective functions—the magnitude of the total aerodynamic force and the magnitude of the rotation torque—determining the lift-to-drag ratio of the power plant are found. Figure 3 presents the shape of 3D blade assembly and pressure distribution on its surface.

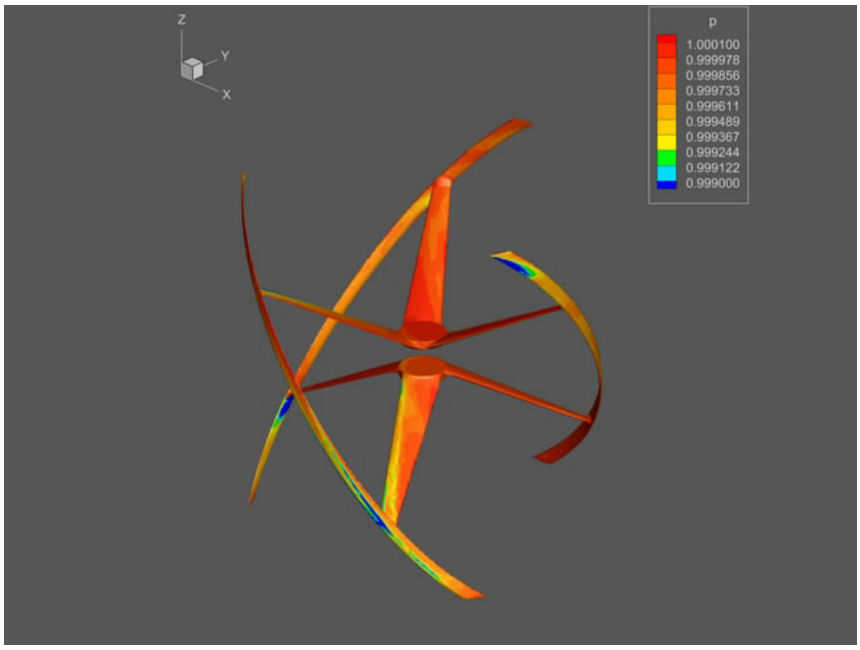


Figure 3: Pressure distribution on the surface of 3D blade assembly.

The next example is addressed to the problem of the evaluation of the accuracy for different numerical methods. The problem of inviscid compressible flow around a cone at zero angle of attack is used as a base one. The results obtained with the help of various OpenFOAM solvers are compared with the known numerical solution of the problem with the variation of cone angle and flow velocity [22]. Cone angle β changes from 10° to 35° in steps

of 5°. Mach number varies from 2 to 7. The scheme of a flow around a cone is presented in Fig. 4. Here angle β is a half of cone angle as shown in Fig. 4. For comparison, four solvers were selected from the OpenFOAM software package: *RhoCentralFoam, SonicFoam, RhoPimpleFoam, RhoPimpleFoam.* The results of such kind of numericsl experiment were presented as errors in the form of an analog of the L2 norm for all solvers. Fig.5 illustrates the results in a form of a change in deviation from the exact solution for pressure depending on the cone angle and the velocity for the solver *rhoCentralFoam*. Such changes were obtained for all solvers.

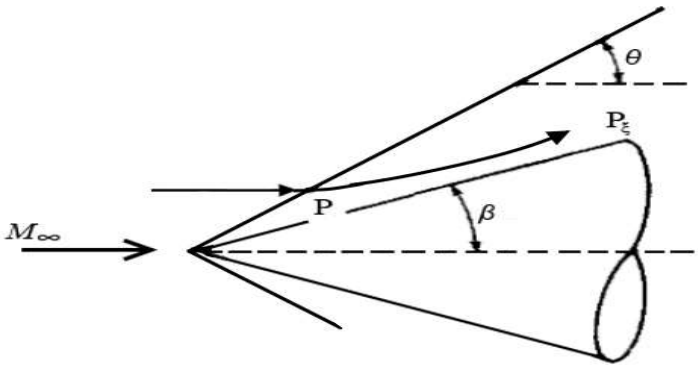


Figure 4: Scheme of a flow around a cone.

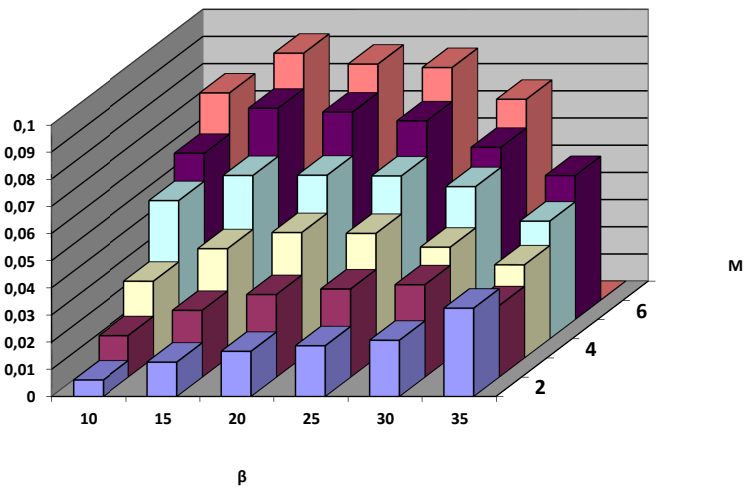


Figure 5: Change in deviation from the exact solution for pressure depending on the cone angle and the velocity for the solver *rhoCentralFoam*.

This methodical research can serve as a basis for selecting the OpenFoam solver for calculating the inviscid supersonic flow around the elongated bodies of rotation. The results of solvers comparison can also be useful for developers of OpenFoam software content. The results obtained made it possible to get a general idea of the calculation errors for all solvers.

Another one example of generalized numerical experiment is devoted to the problem of tuning the properties of hybrid finite-difference schemes [23]. The paper [23] contains the description of developed program tool Burgers2. This program tool is intended for tuning and optimization of computational properties for hybrid finite-difference schemes applied to Burgers equation. One-dimensional model Burgers equation describes propagation of disturbances for dissipative medium. The equation has exact solution, so it is widely used for tuning-up of computational tools. Described program tool is based on combining of optimization problem solution and visual data presentation. Visual presentations of maximal error surface and error function are implemented as program tool features. User is able to visualize error function distribution for any chosen moment of time. These visual presentations allow analyzing and control computational properties of hybrid finite-difference schemes under consideration. Users have possibility of creating hybrid finite-difference schemes and analyzing computational properties for chosen grid template provided by program tool. Visual presentation of optimization problem solution allows finding of suitable weight coefficients for hybrid finite-difference scheme under consideration. The user can make the calculations simultaneously different sets of weight coefficients in accordance with the concept of generalized numerical experiment. Figure 6 presents the surface of absolute error for one of the hybrid scheme variants. The negative data area indicates where the oscillations occur.

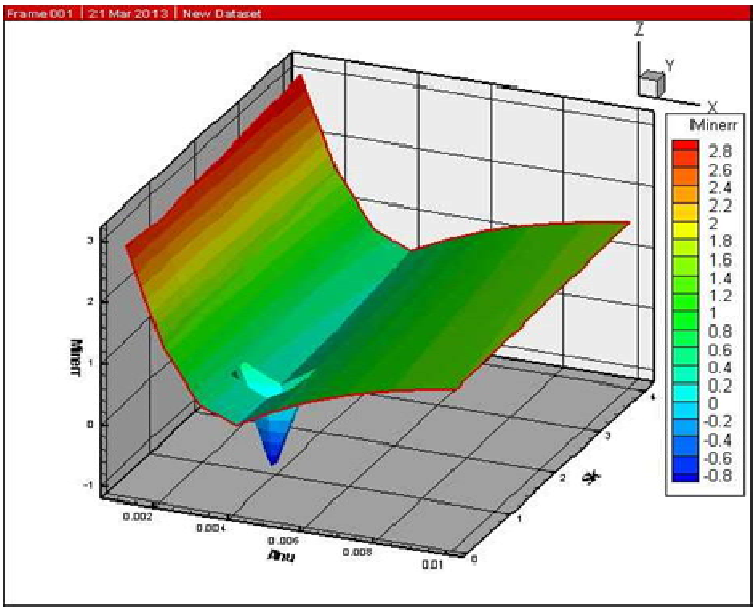


Figure 6: Surface of absolute error.

The next example is aimed to evaluation of parallelization effectiveness. Here the problem of Burgers equation from previous example is used as a base one. To solve this problem, we used an implicit finite difference scheme, described in detail in [23]. When solving the parametric problem, the viscosity coefficient and weight coefficient of the difference scheme split in certain ranges, and for each pair of values the problem described above was solved. During the experiments on parallelization of this program code with DVM, the following

parameters varied: N is the number of MPI processes, PPN is the number of MPI processes per compute node. In the conducted experiments, the number of MPI processes N varied from 1 to 32, and the number of MPI processes per one PPN computing node ranged from 1 to 8. The results are presented in Table 1 below. In the table, the following notation is used: N is the number of MPI processes, PPN is the number of MPI processes running on one node, T is the time in seconds, S is the acceleration T/Tserial, E is the efficiency of parallelization.

| N | PPN | T | S | E |
|---|---|---|---|---|
| serial | ------ | 51,4 | 1 | 1 |
| 1 | 1 | 51,4 | 1,001 | 1,001 |
| 2 | 1 | 25,7 | 1,997 | 0,998 |
| 2 | 2 | 25,7 | 1,998 | 0,999 |
| 4 | 1 | 12,9 | 3,988 | 0,997 |
| 4 | 2 | 12,9 | 3,987 | 0,997 |
| 4 | 4 | 12,9 | 3,991 | 0,998 |
| 8 | 1 | 7,61 | 6,753 | 0,844 |
| 8 | 2 | 6,71 | 7,662 | 0,958 |
| 8 | 4 | 6,73 | 7,641 | 0,955 |
| 8 | 8 | 6,98 | 7,363 | 0,920 |
| 16 | 2 | 4,09 | 12,580 | 0,786 |
| 16 | 4 | 3,64 | 14,129 | 0,883 |
| 16 | 8 | 3,76 | 13,652 | 0,853 |
| 32 | 2 | 2,08 | 24,684 | 0,769 |
| 32 | 4 | 2,09 | 24,613 | 0,769 |
| 32 | 8 | 2,16 | 23,782 | 0,743 |

Table 1 : Burgers equation, implicit scheme.

The obtained results of calculations allow to estimate the effectiveness of the implemented solution for multi-tasking parallelization.

The examples show applicability of presented approach for a wide range of practical applications, so the approach can be considered as quite universal one.

## 6 CONCLUSIONS

The concept of generalized computing experiment presented in the article has a wide range of possible applications. First of all, for the problems of computational fluid dynamics such an approach makes it possible to obtain a solution not only for one, separately taken, problem, but for a whole class of problems defined in a certain range of the complex of determining parameters. A generalized computing experiment involves splitting each of the defining parameters of a problem within a certain range. Thus, a grid decomposition is formed for some multidimensional parallelepiped composed of the defining parameters of the considered problem of gas dynamics. For each point of this grid, the problem is calculated in the space of

the determining parameters. Practical implementation of the approach becomes possible with the use of parallel calculations in multitask mode. The results of calculations are multidimensional volumes of data that can be processed using data analysis tools and visual analytics It should be noted that the application of the approach makes it possible to conduct exploratory calculations on coarse grids for a class of problems with subsequent refinement for sets of determining parameters of special interest.

**Acknowledgements:** Author acknowledges the support by grants of RFBR № 16-01-00553A and 17-01-444A.

## REFERENCES

[1] M. D. Van Dyke, *Album of Fluid Motion* (Parabolic, California, 1982; Mir, Moscow, 1986).
[2] T. J. Mueller, "Flow Visualization by Direct Injection," in *Fluid Mechanics Measurements* (Hemisphere, 1983), pp. 307–375.
[3] E.N. Bondarev, V.T. Dubasov, Y.A. Ryzhov et al., *Aerigidromeckanika.* M.: Mashinostroenie, (1993).
[4] L.V. Kozlov, "Experimental investigation of surface friction on a flat plate in a supersonic flow in the presence of heat transfer". *Izvestiya AN SSSR, OTN, Mekhanika i mashinostroenie*, 2, (1963).
[5] A.E. Bondarev, "Effect of supersonic stream parameters on the characteristic time of transient step flow". *Izvestiya AN SSSR, Mekhanika zhidkosti I gaza*, 4, 137-140 (1989).
[6] A.E. Bondarev, "Analysis of Space-Time Flow Structures by Optimization and Visualization Methods", *Transactions on Computational Science XIX, LNCS* 7870, 158-168 (2013).
[7] A.E. Bondarev and V.A. Galaktionov, "Parametric Optimizing Analysis of Unsteady Structures and Visualization of Multidimensional Data", *International Journal of Modeling, Simulation and Scientific Computing*, V.04, supp01, (2013) DOI 10.1142/S1793962313410043.
[8] A.E. Bondarev and V.A. Galaktionov, "Analysis of Space-Time Structures Appearance for Non-Stationary CFD Problems", *Procedia Computer Science*, 51, 1801–1810 (2015).
[9] A.E. Bondarev, "Design and analysis of multidimensional parametrical solutions for time-dependent CFD problems", *Mathematica Montisnigri*, XXXIII, 58-68 (2015).
[10] P. Pacheco, *Programming Parallel with MPI.* San Francisco, CA: Morgan Kaufmann, 1997.
[11] DVM-system. [Online]. Available: http://dvm-system.org/
[12] V.A. Bakhtin, B.N. Chetverushkin, V.A. Kryukov, E.V. Shil'nikov, "Extension of the DVM parallel programming model for clusters with heterogeneous nodes", *Doklady Mathematics*, 84 (3), 879-881 (2013).
[13] Hybrid supercomputer K-100. [Online]. Available: http://www.kiam.ru/MVS/resourses/k100.html
[14] A. V. Ivanov and S. A. Khilkov, "Aiwlib library as the instrument for creating numerical modeling applications", *Scientific Visualization*, 10(1), 110 - 127 (2018). DOI: 10.26583/sv.10.1.09
[15] A. Bondarev, "Multidimensional Data Analysis in CFD Problems", *Scientific Visualization*, 6(5), 61-68 (2014).
[16] A. Gorban, B. Kegl, D. Wunsch, A. Zinovyev (Eds.), *Principal Manifolds for Data Visualisation and Dimension Reduction* (LNCSE 58 ed.). Berlin – Heidelberg – New York: Springer, (2007).
[17] A. Zinovyev, *Vizualization of multidimensional data,* Krasnoyarsk: Krasnoyarsk Univ., (2000).
[18] G. Kerschen, J.-C. Golinval, A. F. Vakakis, L. A. Bergman, "The Method of Proper Orthogonal Decomposition for Dynamica Characterization and Order Reduction of Mechanical Systems: An Overview", *Nonlinear Dynamics* 41, 147–169 (2005).

[19] P.J. Schmid, "Dynamic mode decomposition of numerical and experimental data", *Journal of Fluid Mechanics* 656(1), 5-28 (2010).
[20] A. K. Alekseev, D. A Bistrian, A. E. Bondarev, I. M. Navon, "On Linear and Nonlinear Aspects of Dynamic Mode Decomposition", *International Journal for Numerical Methods in Fluids*, 82(6), 348–371 (2016). DOI: 10.1002/fld.4221.
[21] Andreev S.V. et al., "A Computational Technology for Constructing the Optimal Shape of a Power Plant Blade Assembly Taking into Account Structural Constraints", *Programming and Computer Software*, 43(6), 345-352 (2017). DOI: 10.1134/S0361768817060020
[22] Alexander E. Bondarev and Artem E. Kuvshinnikov, "Analysis of the Accuracy of OpenFOAM Solvers for the Problem of Supersonic Flow Around a Cone", *Lecture Notes in Computer Science (LNCS)*, 10862, 221–230, (2018). DOI: 10.1007/978-3-319-93713-7_18
[23] A. E. Bondarev et al., "Design of program tool BURGERS2 for hybrid finite-difference schemes optimization and visualization", *Scientific Visualization*, 5(1), 26-37 (2013).

Received May 15, 2018

MATHEMATICA MONTISNIGRI
Vol XLII (2018)

# HYBRID MOLECULAR DYNAMICS AND MONTE CARLO MODELING TO STUDY PHYSICAL-MECHANICAL PROPERTIES OF HIGH-ENTROPY ALLOY CoCrFeMnNi

**A. V. KORCHUGANOV**

Institute of Strength Physics and Material Science of the Siberian Branch of the Russian Academy of Sciences
Akademicheskii 2/4, 634021 Tomsk, Russia
e-mail: avkor@ispms.ru

**Summary.** Structural and physical-mechanical properties of CoCrFeMnNi high-entropy alloys of different stoichiometric composition are investigated on the base of computer modeling. An approach based on the combined use of molecular dynamics and Monte Carlo methods was applied. This made it possible to obtain the thermodynamically equilibrium configurations of CoCrFeMnNi alloys at given fractions of chemical elements, temperature and pressure. Based on the obtained data set, the influence of the stoichiometric composition of CoCrFeMnNi high-entropy alloy on its structural characteristics (lattice parameter, radial distribution functions), phase stability (energy of different phases, configuration entropy) and physical-mechanical properties (Young's modulus and elastic limit) was investigated.

## 1 INTRODUCTION

The study of the structure, physical properties and behavior of high-entropy alloys (HEAs) under thermal and mechanical loading is one of the most actual topics of modern materials science [1]. This is due to the unique complex of HEA properties, which is largely determined by their multicomponent composition. Typically, these alloys consist of five or more elements. According to the thermodynamic considerations, in spite of the complex chemical composition, HEA can be a single-phase solid solution if the alloy elements are in equal ratios. This is also important for the formation of excellent properties of alloy. At the same time, many studies show that HEAs with non-equiatomic composition also remain stable and often have better properties [2]. Therefore, the search for new stoichiometric compositions of HEAs is an actual material science task [3]. The great success in high-throughput combinatorial materials research is achieved for wide variety of applications [4]. For example, making only one sample with compositional gradient allowed to study how the properties of a material change with a chemical composition. However, such approaches allow one to study a limited range of properties, and they are not yet well developed for HEAs. It should be noted that, along with laborious and costly experimental studies, computer modeling is an effective tool that allows one to quickly process large amounts of information and determine the optimal chemical composition of the material that meets the required properties. For example, on the basis of the computer algorithm

**2010 Mathematics Subject Classification:** 65C05, 74N15, 82D35, 93A30.
**Key words and phrases:** computational modeling, molecular dynamics, Monte Carlo method, crystalline structure, mechanical properties, high-entropy alloys.

developed in [5] automated tuning of chemical composition of $Al_xCrCoFeNi$ multicomponent alloys allowed increasing their ultimate tensile strength in molecular dynamics calculations. In the framework of Monte Carlo method and ab-initio modeling, the stability of different phases in the HfNbTaZr HEA was determined [6]. A theoretical approach on the base of phase diagram calculation allowed finding more than 150 single-phase compositions of HEAs with potentially high mechanical properties [7].

To date, CoCrFeMnNi is one of the most promising systems among HEAs, which is characterized by high physical and mechanical properties and has a great potential for their improvement [8,9]. However, the atomic level insights into its high properties and the influence of stoichiometric composition on them are still not clear. In this connection, for better understanding of CoCrFeMnNi HEA properties, the application of theoretical and computational methods is required. It should be noted, that molecular dynamics method has significant advantages in the study of the atomic structure of metallic materials [10,11]. It explicitly takes into account the discrete structure of a material and allows to track the evolution of atomic system under various kinds of external loading even in substantially non-equilibrium conditions [12–16]. Therefore, the objective of our work is to investigate the effect of stoichiometric composition on atomic structure, phase stability, physical and mechanical properties of CoCrFeMnNi high-entropy alloys by means of computer modeling.

## 2 COMPUTATIONAL MODEL

In order to investigate the properties of CoCrFeMnNi HEA we first prepared the samples with different stoichiometric compositions. They were the single crystals with fcc and bcc lattice having cubic shape and dimensions of $10 \times 10 \times 10$ lattice parameters. Axes of the samples were the [100], [010] and [001] directions in which periodic boundary conditions were applied. Initially atoms of different chemical elements were placed randomly into lattice sites according to specified fractions $C_i$ which were 0.1, 0.2, or 0.3. Additional requirement, coming from the definition of HEA [17], was that combination of these fractions would give value of configuration entropy $\Delta S_{\text{conf}} = -R\sum_{i=1}^{5} C_i \ln C_i$ higher than $1.5R$, where $R$ is gas constant. As a result, 43 stoichiometric compositions with different fractions of elements were chosen.

Computer calculations were carried out in LAMMPS software [18]. Dynamics was described for $N$ atoms by the system of $2N$ ordinary differential equations of motion:

$$\begin{cases} \dfrac{\mathrm{d}\mathbf{r}_i}{\mathrm{d}t} = \mathbf{v}_i, \\ m_i \dfrac{\mathrm{d}\mathbf{v}_i}{\mathrm{d}t} = -\dfrac{\partial U(\mathbf{r}_i, \ldots, \mathbf{r}_N)}{\partial \mathbf{r}_i}, \end{cases} \quad i = 1, \ldots, N, \quad i \neq j, \tag{1}$$

where $i$, $\mathbf{r}_i$, $\mathbf{v}_i$, $m_i$ are the number, radius vector, velocity vector, and mass of atom $i$, correspond-

ingly. Function $U(r_i,\ldots,r_N)$ is the interatomic interaction potential. The numerical solution of the equations of motion was carried out using the velocity Verlet scheme with an integration step of $10^{-16}$ s. The interatomic potential was constructed in the works [19, 20] in the approximation of the second nearest neighbor modified embedded atom method [21]. According to this method the total energy of system is:

$$E=\sum_{i=1}^{N}\left[F_i(\overline{\rho_i})+\frac{1}{2}\sum_{j=1}^{N}S_{ij}\phi_{ij}(r_{ij})\right],\quad r_{ij}=|\mathbf{r}_i-\mathbf{r}_j|,\quad i\neq j, \tag{2}$$

where $F_i$ is the embedding function for the atom $i$, $\overline{\rho_i}$ is corresponding background electron density, $\phi_{ij}(r_{ij})$ is the $i$–$j$ pair interaction potential and $S_{ij}$ is the screening function.

To obtain the thermodynamically equilibrium configurations of modelled alloys hybrid molecular dynamics and Monte Carlo calculations were performed. According to this scheme, two random atoms of different chemical elements swap with the probability

$$p=\begin{cases}1, & \text{if } \Delta E\leqslant 0,\\ \exp\left(\dfrac{-\Delta E}{k_{\mathrm{B}}T}\right), & \text{if } \Delta E>0,\end{cases} \tag{3}$$

where $k_{\mathrm{B}}$ is Boltzmann constant, $T$ is temperature, $\Delta E$ is the change of sample total energy after swap. After every Monte Carlo swap the system was relaxed for 250 integration steps in molecular dynamics calculations with $NPT$ ensemble (constant number of particles $N$, pressure $P$ and temperature $T$). In our calculations $T=300$ K and $P=0$. If $\Delta E<0.1\%$ of system total energy, that structural configuration of the sample was assumed to be equilibrium. Its further relaxation was done for $10^5$ steps in $NVE$ ensemble (constant number of particles $N$, volume $V$ and total energy $E$). The obtained samples were used to calculate the structural characteristics and physical-mechanical properties of the alloys.

Radial distribution function (RDF) is calculated by binning all distances between atoms of type I and J in a histogram. Count of atoms with type $J$ in spherical bin with radius from $r$ to $r+\mathrm{d}r$ is divided to its volume and then normalized to average density of atoms of type J:

$$g_{\mathrm{IJ}}(r,r+\mathrm{d}r)=\frac{N_{\mathrm{J}}(r,r+\mathrm{d}r)}{4\pi r^2\mathrm{d}r}\frac{V}{N_{\mathrm{J}}}. \tag{4}$$

To calculate mechanical properties of alloys, samples were subjected to uniform tension along the [100] direction with rate $10^8$ s$^{-1}$, while in other two directions samples were allowed to change dimensions to keep zero stress component along them. Periodic boundary conditions were applied in all directions. Young's modulus of alloy was calculated as the slope of the linear region of tensile stress vs. strain curve.

Determination of local type of crystal lattice was performed in the OVITO software [22] which used an algorithm called Common Neighbor Analysis (CNA) [23]. It analyzes topology of bonds between nearest neighbors of a given atom and can identify to which structure it corresponds: fcc, bcc or hcp lattice.

## 3 RESULTS AND DISCUSSION

Calculations of the system total energy have shown that the bcc lattice is less energetically favorable and structurally stable than fcc. After complete relaxation of the samples with an initially ideal bcc lattice, the CNA algorithm in some cases determined that more than half of the atoms have a local environment that does not correspond to any of the crystal lattices. The structure of the alloys with 30% of iron (the maximum atom fraction in chosen compositions) was least disordered, apparently because bulk Fe has bcc lattice. Moreover, undistorted regions with bcc lattice in samples with lower Fe fraction contain more Fe than distorted ones, which points to the fact that iron may be considered as a local bcc stabilizer in a modeled system. For all 43 compositions, samples with an fcc lattice retained a stable crystal structure without significant distortion, which agrees with experimental studies of the phase stability and structure of CoCrFeMnNi alloys with near-equiatomic composition [24]. In addition, our calculations show that alloy retains the fcc structure as being more energetically favorable even with a significant deviation in the fraction of any element from the equiatomic value, which agrees with the experimental results on the stability of non-equiatomic CoCrFeMnNi alloys [25]. The dependence of the system total energy per atom on the lattice parameter of fcc alloys with different compositions is shown in figure 1. It is seen that the alloys with low energy have lower lattice parameters. The computer modeling has shown that for all the compositions considered there is no correlation of the configuration entropy with the calculated properties of the alloys. Based on the analysis of phase stability, we will next consider the properties of alloys with fcc lattice.

As calculations have shown, not all types of atoms are mixed absolutely randomly in the alloy studied. But at the same time, no microscopic segregation has been observed. To illustrate the features of alloy atomic structure let us consider radial distribution functions (RDFs) for two characteristic stoichiometric compositions: all contain 20% Ni, in figure 2(*a*) the alloy contains both 10% of Co and Cr, in figure 2(*b*) the alloy contains both 30% of Co and Cr. For the first composition the first Cr peak is higher and larger in area compared to peaks for other elements. For the second composition, the first Cr peak has the same height with others but it is broader. The second and third Fe peaks are larger in area than others by 50 and 20% correspondingly, but remaining peaks have the same area as others. In both cases, RDFs for Cr are shifted to the right, which means larger interatomic distance for this pair. RDFs for pairs of different elements are shown in figure 3. Their common feature is the higher first peaks for Co–Fe and Ni–Mn pairs,

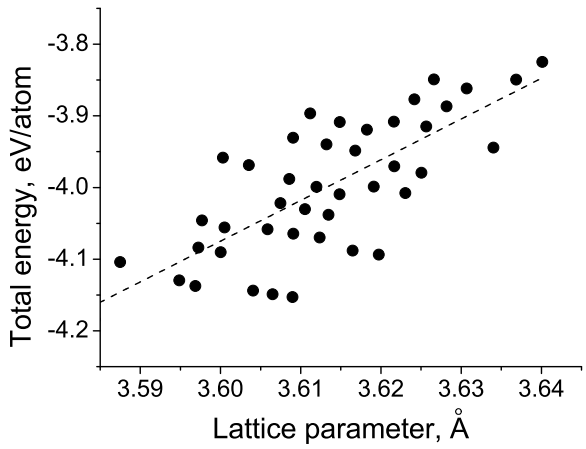


Figure 1. Total energy of fcc alloys per atom as a function of their lattice parameter.

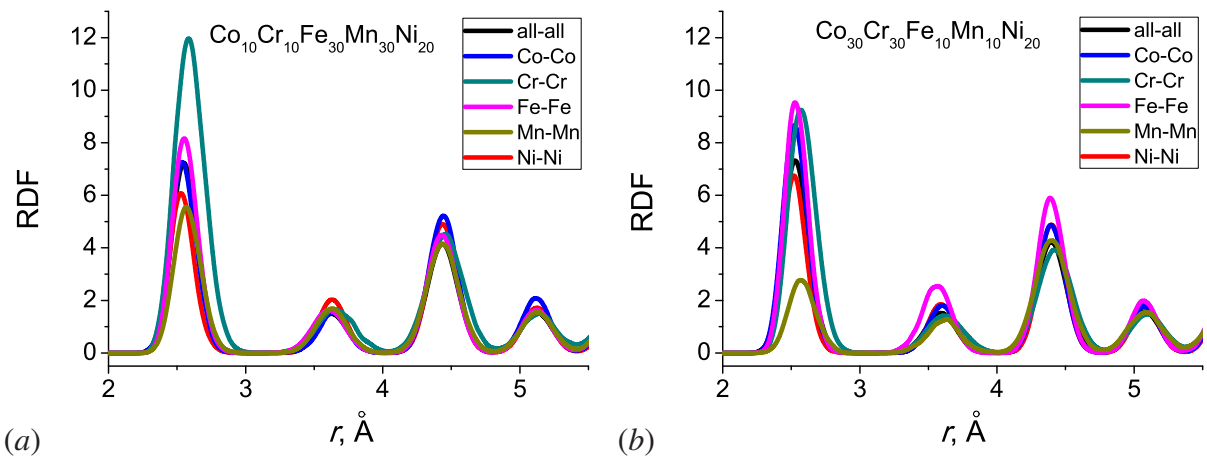


Figure 2. Radial distribution functions for single elements in alloys with different compositions: $Co_{10}Cr_{10}Fe_{30}$–$Mn_{30}Ni_{20}$ (*a*), $Co_{30}Cr_{30}Fe_{10}Mn_{10}Ni_{20}$ (*b*).

which means strong short-range interaction between these elements. First peaks for Cr–Mn and Ni–Fe are also high for the first and second composition, respectively. But this strong interaction is restricted by the first coordination sphere: the second and further peaks are almost the same as peaks for other pairs of elements, which means no segregation—there are no clusters which consist entirely of these atoms and exceed an elementary fcc cell in size. Moreover, if we plot the distribution of the number of atoms along the length of the sample, it will be a straight line.

We have investigated the effect of the stoichiometric composition on the lattice parameter of 43 alloys. For alloys whose lattice parameter lies in a certain range of values, we have calculated the average fraction of each element in them. The results of the calculations are shown in figure 4(*a, b*). It is clearly seen, that increasing of Cr, Fe and Mn or decreasing Ni and Co fraction

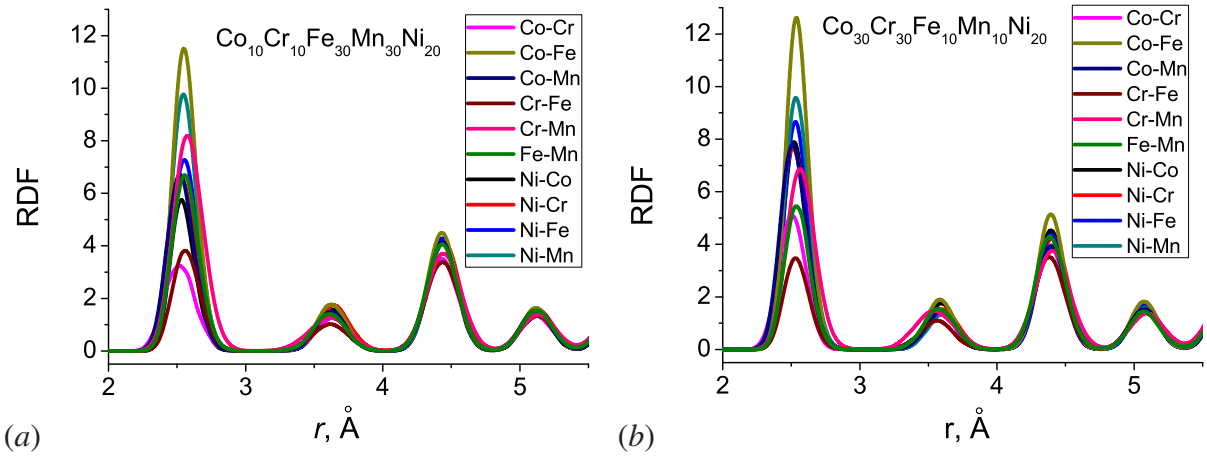


Figure 3. Radial distribution functions for pairs of different elements in alloys with different compositions: $Co_{10}$–$Cr_{10}Fe_{30}Mn_{30}Ni_{20}$ (*a*), $Co_{30}Cr_{30}Fe_{10}Mn_{10}Ni_{20}$ (*b*).

lead to increase of lattice parameter. It is interesting that these simple dependences exist even in spite of the fact that in each range of lattice parameters there are alloys with completely different stoichiometric composition. For example, the equiatomic alloy $Co_{20}Cr_{20}Fe_{20}Mn_{20}Ni_{20}$ and such alloys as $Co_{10}Cr_{20}Fe_{30}Mn_{10}Ni_{30}$ and $Co_{30}Cr_{20}Fe_{10}Mn_{30}Ni_{10}$ all correspond to the interval 3.609–3.611 Å. In our opinion, this is due to the stronger long-range interaction of Cr–Cr, Co–Fe and Ni–Mn pairs in comparison with other interactions which is expressed in the high first peaks of corresponding RDFs, as shown in figures 2 and 3. Now if back to figure 1, it will be seen that the lowest total energy is typical for alloys with small lattice parameter, i.e. with a high fraction of Fe, Mn and Cr and low fraction of Co and Ni.

Calculations show that, fraction of Ni, Co, Fe, and Cr have the opposite effect on Young's modulus compared to lattice parameter. Increasing of Ni and Co fraction or decreasing of Fe and Cr fraction lead to increase of Young's modulus, figure 4(*c, d*). Mn has little effect on the modulus value. It should be noted that the elements Co and Fe, which have a different effect on the modulus, are characterized by the strongest interaction between each other. As a consequence, for example, two alloys with 40% total fraction of Co and Fe and the same fractions of other elements, $Co_{30}Cr_{20}Fe_{10}Mn_{10}Ni_{30}$ and $Co_{10}Cr_{20}Fe_{30}Mn_{10}Ni_{30}$, have close moduli 83.5 and 84.2 GPa, correspondingly. This allows one to change the fractions of individual elements, keeping the constant value of the module and changing other properties of the alloy at the same time. Calculations show that the elastic limit of alloys is almost linearly dependent on Young's modulus, and therefore general conclusions on the effect of the stoichiometric composition on the modulus can also be applied to the elastic limit.

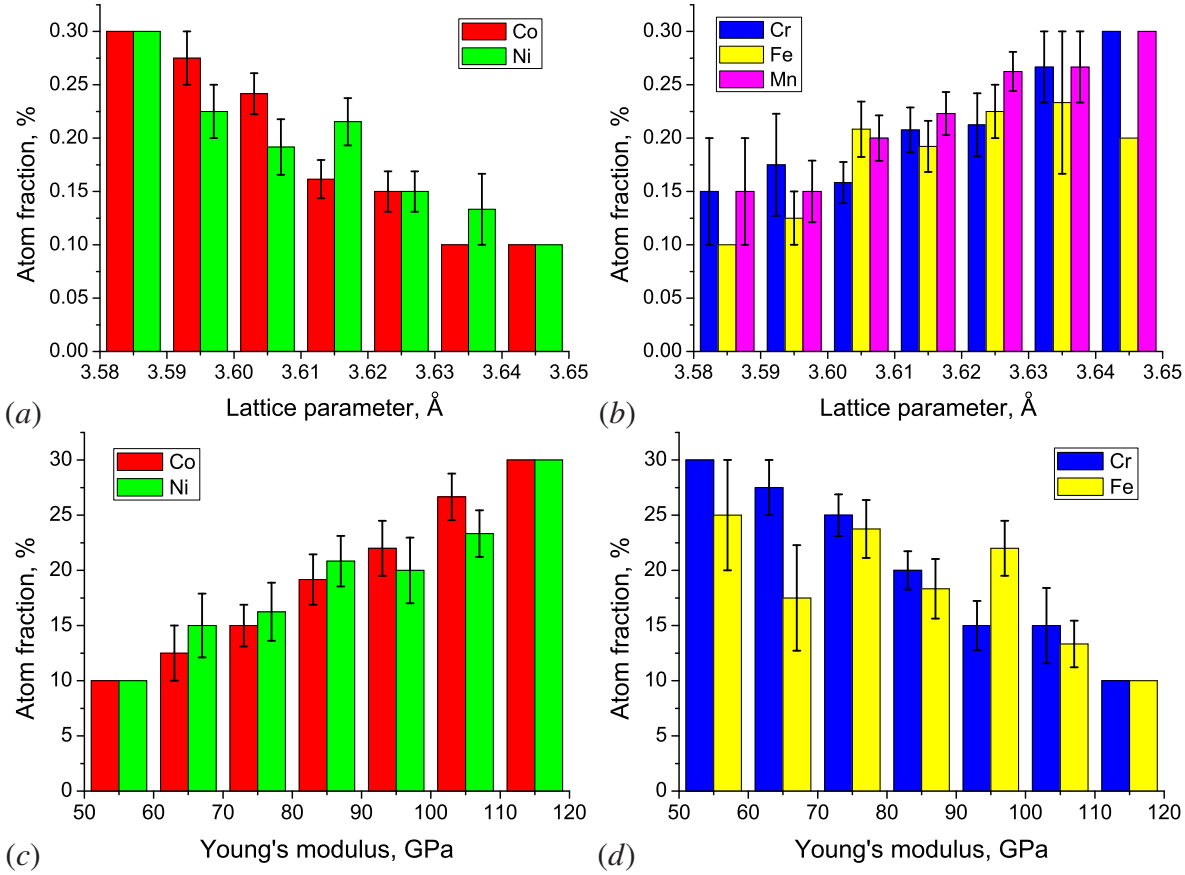


Figure 4. Average fractions of Co and Ni (*a*), Cr, Fe and Mn (*b*) as a function of lattice parameter; the same for Co and Ni (*c*), Cr and Fe (*d*) as a function of Young's modulus of alloys. Error bars show standard deviation.

## 4 CONCLUSIONS

Influence of stoichiometric composition on structure, phase stability, physical and mechanical properties of CoCrFeMnNi high-entropy alloy was studied by computer modeling based on combination of molecular-dynamics and Monte-Carlo methods. It was shown that fcc alloys more stable than bcc for all 43 considered stoichiometric compositions with fractions of each element varying in range 10–30%. RDFs are characterized by high first peaks for Cr–Cr, Co–Fe and Ni–Mn pairs, which mean a high degree of interaction between these elements in the CoCrFeMnNi alloy. It was shown that these structural features cause strong influence of stoichiometric composition on physical and mechanical properties of alloys. Namely, increasing of Cr, Fe and Mn fraction or decreasing Ni and Co fraction lead to increase of lattice parameter and increase of alloy cohesive energy. Opposite to lattice parameter, increasing of Ni and Co fraction or decreasing of Fe and Cr fraction lead to increase of Young's modulus and elastic limit. But in this case fraction of Mn has little effect on the modulus and the limit.

**Acknowledgments:** The work was carried out with the financial support of the Russian Science Foundation (project No. 17-79-10108).

The paper is based on the proceedings of the XXXIII International Conference on Equations of State for Matter, which was held in Elbrus and Tegenekli settlements, in the Kabardino-Balkar Republic of the Russian Federation, from March 1 to 6, 2018.

## REFERENCES

[1] D. B. Miracle and O. N. Senkov, "A critical review of high entropy alloys and related concepts", *Acta Mat.* **122**, 448–511 (2017).

[2] K. G. Pradeep, C. C. Tasan, M. J. Yao, Y. Deng, H. Springer, and D. Raabe, "Non-equiatomic high entropy alloys: Approach towards rapid alloy screening and property-oriented design", *Mater. Sci. Eng. A* **648**, 183–192 (2015).

[3] D. Miracle, B. Majumdar, K. Wertz, and S. Gorsse, "New strategies and tests to accelerate discovery and development of multi-principal element structural alloys", *Scripta Mat.* **127**, 195–200 (2017).

[4] M. L. Green, I. Takeuchi, and J. R. Hattrick-Simpers, "Applications of high throughput (combinatorial) methodologies to electronic, magnetic, optical, and energy-related materials", *J. Appl. Phys.* **113**(23), 231101 (2013).

[5] A. Sharma, R. Singh, P. K. Liaw, and G. Balasubramanian, "Cuckoo searching optimal composition of multicomponent alloys by molecular simulations", *Scripta Mat.* **130**, 292–296 (2017).

[6] C. Niu, W. Windl, and M. Ghazisaeidi, "Multi-cell Monte Carlo relaxation method for predicting phase stability of alloys", *Scripta Mat.* **132**, 9–12 (2017).

[7] O. N. Senkov, J. D. Miller, D. B. Miracle, and C. Woodward, "Accelerated exploration of multi-principal element alloys for structural applications", *Calphad* **50**, 32–48 (2015).

[8] F. Otto, A. Dlouhy, Ch. Somsen, H. Bei, G. Eggeler, and E. P. George, "The influences of temperature and microstructure on the tensile properties of a CoCrFeMnNi high-entropy alloy", *Acta Mat.* **61**, 5743–5755 (2013).

[9] N. D. Stepanov, D. G. Shaysultanov, R. S. Chernichenko, N. Yu. Yurchenko, S. Zherebtsov, M. Tikhonovsky, and G. A. Salishchev, "Effect of thermomechanical processing on microstructure and mechanical properties of the carbon-containing CoCrFeNiMn high entropy alloy", *J. Alloys Compd.* **693**, 394–405 (2017).

[10] A. V. Utkin, "Analysis of parallel molecular dynamics for MPI, CUDA and CUDA-MPI implementation", *Mathematica Montisnigri* **39**, 101–109 (2017).

[11] V. I. Mazhukin, A. A. Samokhin, M. M. Demin, and A. V. Shapranov, "Explosive boiling of metals upon irradiation by a nanosecond laser pulse", *Quantum Electron.* **44**(4), 283–285 (2014).

[12] G. Poletaev, I. Zorya, and R. Rakitin, "Molecular dynamics study of migration mechanism of triple junctions of tilt boundaries in fcc metals", *Comput. Mater. Sci.* **148**, 184–189 (2018).

[13] O. N. Koroleva, A. V. Mazhukin, and V. I. Mazhukin, "Modeling of silicon characteristics in the semiconductor–metal phase transition region", *Mathematica Montisnigri* **41**, 73–90 (2018).

[14] V. Mazhukin, M. Demin, and A. Aleksashkina, "Atomistic modeling of thermophysical properties of copper in the region of the melting point", *Mathematica Montisnigri* **41**, 99–111 (2018).

[15] A. A. Samokhin, V. I. Mazhukin, A. V. Shapranov, M. M. Demin, and A. E. Zubko, "Molecular dynamics modeling of nanosecond laser ablation: transcritical regime", *Mathematica Montisnigri* **38**, 78–88 (2017).

[16] D. S. Kryzhevich, A. V. Korchuganov, K. P. Zolnikov, and S. G. Psakhie, "Role of localized non-equilibrium states in nucleation of plastic deformation in nanocrystalline materials", *Solid State Phenom.* **258**, 21–24 (2017).

[17] J. W. Yeh, "Alloy design strategies and future trends in high-entropy alloys", *JOM* **65**(12), 1759–1771 (2013).

[18] S. Plimpton, "Fast parallel algorithms for short-range molecular dynamics", *J. Comput. Phys.* **117**(1), 1–19 (1995).

[19] W. M. Choi, Y. Kim, D. Seol, and B. J. Lee, "Modified embedded-atom method interatomic potentials for the Co–Cr, Co–Fe, Co–Mn, Cr–Mn and Mn–Ni binary systems", *Comput. Mater. Sci.* **130**, 121–129 (2017).
[20] C. Wu, B. J. Lee, and S. Xuping, "Modified embedded-atom interatomic potential for Fe–Ni, Cr–Ni and Fe–Cr–Ni systems", *Calphad* **57**, 98–106 (2017).
[21] B. J. Lee and M. I. Baskes, "Second nearest-neighbor modified embedded-atom-method potential", *Phys. Rev. B* **62**, 8564–8567 (2000).
[22] A. Stukowski, "Visualization and analysis of atomistic simulation data with OVITO—the open visualization tool", *Modell. Simul. Mater. Sci. Eng.* **18**(1), 015012 (2010).
[23] J. D. Honeycutt and H. C. Andersen, "Molecular dynamics study of melting and freezing of small Lennard-Jones clusters", *J. Phys. Chem.* **91**(19), 4950–4963 (1987).
[24] F. Otto, A. Dlouhy, K. G. Pradeep, M. Kubenova, D. Raabe, G. Eggeler, and E. P. George, "Decomposition of the single-phase high-entropy alloy CrMnFeCoNi after prolonged anneals at intermediate temperatures", *Acta Mater.* **112**, 40–52 (2016).
[25] C. C. Tasan, Y. Deng, K. G. Pradeep, M. J. Yao, H. Springer, and D. Raabe, "Composition dependence of phase stability, deformation mechanisms, and mechanical properties of the CoCrFeMnNi high-entropy alloy system", *JOM* **66**, 1993–2001 (2014).

Received March 10, 2018.

MATHEMATICA MONTISNIGRI
Vol XLII (2018)

# ДВУХПАРАМЕТРИЧЕСКИЙ ЭНТРОПИЙНЫЙ ФУНКЦИОНАЛ ШАРМА−МИТТАЛА КАК ОСНОВА СЕМЕЙСТВА ОБОБЩЕННЫХ ТЕРМОДИНАМИК НЕЭКСТЕНСИВНЫХ СИСТЕМ

**А.В. КОЛЕСНИЧЕНКО**

Институт прикладной математики им. М.В. Келдыша РАН, Москва, Россия
e-mail: kolesn@keldysh.ru, web page: http:.keldysh.ru/kolesnichenko/person.htm

**Ключевые слова:** Принципы неэкстенсивной статистической механики, энтропия Шарма−Миттала, степенной закон распределения.

**Аннотация.** Исследованы свойства семейства обобщённых энтропий, заданного двухпараметрической мерой Шарма−Миттала, которое включает энтропию Тсаллиса, энтропию Реньи, энтропию Ландсберга−Ведрала, энтропию Гаусса и классическую энтропию Больцмана−Гиббса−Шеннона. Построена на базе статистики Шарма−Миттала модифицированная термодинамика неэкстенсивных систем, и показана её взаимосвязь с обобщёнными однопараметрическими термодинамиками, основанными на деформированных энтропиях семейства. Получено обобщение нулевого закона термодинамики для двух независимых неэкстенсивных систем при их тепловом контакте, вводящее в рассмотрение так называемую физическую температуру, отличающуюся от инверсии множителя Лагранжа $\beta$. Этот факт потребовал переопределения термодинамических соотношений, полученных в рамках статистики Шарма−Миттала, которое проведено в работе с учетом обобщённого первого закона термодинамики и преобразования Лежандра. Наконец, на основе двухпараметрической информации различия Шарма−Миттала сформулированы и доказаны теорема Гиббса и $H$-теорема Больцмана об изменении этих мер при эволюции во времени.

# TWO-PARAMETER FUNCTIONAL OF ENTROPY SHARMA-MITTAL AS THE BASIS OF THE FAMILY OF GENERALIZED THERMODYNAMICES OF NON-EXTENSIVE SYSTEMS

**A.V. KOLESNICHENKO**

Keldysh Institute of Applied Mathematics, Russian Academy of Science
e-mail: kolesn@keldysh.ru, web page: http:.keldysh.ru/kolesnichenko/person.htm

**Summary.** The properties of the family of generalized entropies given by the Sharm−Mittal entropy, which includes the entropy of Tsallis, the Renyi entropy , the Landsberg−Vedral entropy, the Gauss entropy, and the classical Boltzmann−Gibbs− Shannon entropy are investigated. Based on the Sharm−Mittal statistics, the two-parameter thermodynamics of non-extensive systems is constructed and its interrelation with generalized one-parameter thermodynamices based on the named deformed entropies of the family is shown.

**2010 Mathematics Subject Classification:** 85A35, 91B50, 82C40.
**Key words and Phrases:** Principles of nonextensive statistical mechanics, Sharma−Mittal entropy, power law of distribution.

A generalization of the zero law of thermodynamics is obtained for two independent non-extensive systems at their thermal contact, introduce into consideration a so-called physical temperature different from the inversion of the Lagrange multiplier $\beta$. This fact has demanded overdetermination of the thermodynamic relations received in frameworks statistics of Sharma−Mittala which is spent in work taking into account the generalised first law of thermodynamics and transformation of Legendre. On the basis of the two-parametric information of Sharm−Mittal's difference, Gibbs's theorem and the *H*-theorem on the change of these measures in the course of time evolution are formulated and proved.

## 1 ВВЕДЕНИЕ

Статистическая энтропия Больцмана−Гиббса−Шеннона и основанная на ней классическая статистическая механика являются чрезвычайно полезным инструментарием при изучении широкого круга простых физических систем. Эти системы, для которых, безусловно, целесообразно использовать классическую статистику и разработанные на её основе теории, можно условно охарактеризовать малым диапазоном пространственно-временных корреляций, эвклидовостью геометрии фазового пространства, марковостью случайных процессов, локальностью силового взаимодействия между элементами системы, эргодичностью динамических процессов и т.п. Такие системы хорошо описываются энтропией Больцмана−Гиббса−Шеннона и, как правило, следуют экспоненциальному закону вероятностных распределений состояния.

Существует, однако, целый круг сложных систем[i)] (природных, искусственных и социальных), которые, в отличие от простых, характеризуются большой дальностью пространственно-временных корреляций, глобальностью силовых взаимодействий между элементами системы, иерархичностью (фрактальностью и мультифрактальностью) геометрии фазового пространства, немарковостью процессов (эредитарностью), неэргодичностью динамических процессов, наличием асимптотически степенных вероятностных распределений. Довольно широкий класс подобных систем (хотя далеко не всех) адекватно описывается неэкстенсивной (неаддитивной) статистической механикой, основанной, в частности, на параметрических энтропиях Тсаллиса[1,2,3] и Реньи[4,5], которые сохраняют гносеологическую структуру (логическую схему построения) классической статистики (см., например,[6-18]). Важным преимуществом неэкстенсивных статистик по сравнению с классической статистикой Гиббса является асимптотический степенной закон распределения вероятностей (проявляющийся при максимизации соответствующих параметрических энтропий), который не зависит от экспоненциального поведения, обусловленного распределением Гиббса.

Неэкстенсивная статистика Тсаллиса успешно применяется ко многим сложным системам начиная от нелинейных диффузионных уравнений[19], обобщенных кинетических уравнений[20,21], систем Фоккера−Планка[22], *H*-теоремы Больцмана[23-27], удельной те-

[i)] Сложные системы состоят из многих элементов, частей, компонентов, подсистем, которые взаимодействуют между собой сложным (нелинейным) образом. В силу характерного для многих сложных систем хаотического поведения, ограничивающего возможности детерминированного описания, моделирование подобных систем возможно лишь в статистических терминах, как то: плотность вероятности, математическое ожидание, дисперсия, ляпуновские показатели и т.п.

плоемкости гармонического осциллятора[28], квантовой статистики[29], до изучения космических систем с дальним силовым взаимодействием[30,31], межзвездной турбулентности[32], эволюции астрофизических дисков[33,34], скорости солнечного звука[35], релаксации спинового стекла[36], городской транспортной системы[37], биофизики, экономики, нейрофизики и т.д.

Энтропия Реньи эффективно используется не только в физике фракталов и в теории информации[7,38-51], но и в различных областях статистической механики, связанных с динамическим поведением сложных хаотических систем. Последнее связано с тем, что между теорией фракталов, опирающейся на геометрию и теорию размерности, с одной стороны, и теорией хаоса существует глубокая связь. Использование статистики Реньи привело к значительному прогрессу в исследованиях ряда аномальных физических явлений, в частности, в теории черных дыр[51], в ядерной физике[52], при изучении фрактальных и мультифрактальных систем в космологии[31,40,41,53], в квантовой статистике[54-56] и т.д. Одновременно, наличие степенного закона в неэкстенсивной статистике позволило сконструировать неаддитивные термодинамики, в частности, на основе энтропии Тсаллиса[7,11,57-60] и энтропии Реньи[53,61,62].

Несколько позднее в статистическую механику был введён новый функционал энтропии − двухпараметрическая энтропия Шарма−Миттала[63] (*SM*), которая, в частности, обобщает энтропии Больцмана−Гиббса−Шеннона, Реньи и Тсаллиса, посредством манипулирования двумя параметрами деформации, тем самым рассматривая эти энтропии как некоторые предельные однопараметрические случаи[64,65-68]. Свойства энтропии Шарма−Миттала были исследованы рядом авторов (см., например,[66,69-73]). Многие неэкстенсивные однопараметрические энтропии, введённые в литературе в рамках обобщённой статистической механики, относятся к семейству *SM* и, таким образом, могут изучаться по единообразной схеме. Среди них, упомянутые выше энтропии Больцмана−Гиббса−Шеннона, Реньи и Тсаллиса, а также энтропия Ландсберга−Ведрала[74], Гауссова энтропия[64] и некоторые другие.

Энтропия Шарма−Миттала, введённая первоначально в теории информации, также была использована для построения термостатистики[64]. В работе[69] были даны точные решения нестационарных уравнений Фоккера−Планка, связанных с энтропиями Реньи и Шарма−Миттала. В работах[66,75] для получения обобщённых термодинамических соотношений на базе энтропии *SM* учитывалась гипотеза мультипликативности вероятностного распределения совместной вероятности двух независимых систем.

Целью данной работы является построение на основе неэкстенсивной статистической механики обобщённых термодинамик, соответствующих однопараметрическим энтропиям, принадлежащим к семейству Шарма−Миттала. При этом осреднённые значения динамических параметров системы получены по нормированному эскортному распределению, которое обычно используется при статистическом рассмотрении хаотических сложных систем, состоящих из большого числа взаимодействующих частей. Однако в отличие от ряда известных работ (см., например,[66,72,76]), в которых подобные исследования по термодмнамике проведены с привлечением двукратно деформированных экспоненты и логарифма (введённых первоначально в теории информации Шарма и Митталем в 1975 г.), особенность данной работы состоит в том, что построение обобщённых неэкстенсивных термодинамик проведено с помощью более простых и хорошо изученных однократно деформированных функций – деформированного логарифма и экспонента Тсаллиса.

## 2 ОДНОПАРАМЕТРИЧЕСКИЕ ТИПЫ ЭНТРОПИЙ СЕМЕЙСТВА ШАРМА−МИТТАЛА

Введённая Шарма и Митталом (1975) двухпараметрическая энтропийная мера случайной величины $p=\{p_j\}$ определяется формулой

$$S_{q,r}^{SM}(p):=k\frac{1-(\sum_j p_j^{\,q})^{(r-1)/(q-1)}}{r-1}, \tag{1}$$

где $r,q>0$, $r\neq 1\neq q$, $r\neq q$. В выражении (1) $p=\{p_j\}_{j=1,\ldots,\mathrm{W}}$ − дискретная функция распределения вероятностей состояния, а $W$ обозначает количество доступных в системе микросостояний; $k$ − постоянная Больцмана.

Энтропийная мера (1) включает как классическую, так и деформированные однопараметрические энтропии, хорошо известные в литературе, в частности:

- энтропию Больцмана−Гиббса−Шеннона

$$S_{q\to 1,r\to 1}^{SM}=S^{BGS}(p):=-k\sum_j p_j\ln p_j; \tag{2}$$

- энтропию Реньи[4,5]

$$S_{q,r\to 1}^{SM}=S_q^R(p):=\frac{k}{(1-q)}\ln(\sum_j p_j^{\,q}),\quad q>0,\ q\neq 1; \tag{3}$$

- энтропию Тсаллиса[1,2,3]

$$S_{q,q}^{SM}=S_q^{Ts}(p):=k\frac{1-\sum_j p_j^{\,q}}{(q-1)}; \tag{4}$$

- энтропию Ландсберга–Ведрала[74]

$$S_{q,2-q}^{SM}=S_q^{LV}:=k\frac{1-(\sum_j p_j^{\,q})^{-1}}{(1-q)}; \tag{5}$$

- энтропию Гаусса[64]

$$S_{q\to 1,r}^{SM}=S_r^G:=k\frac{1-\left\{\exp(r-1)\sum_j p_j\ln p_j\right\}}{(r-1)},\quad q>0,\ q\neq 1. \tag{6}$$

**Экспонента Тсаллиса и деформированный логарифм**. Далее мы будем широко использовать так называемые деформированные функции, в частности, деформированный логарифм $\ln_q(x)$ и деформированную экспоненциальную функцию (экспоненту Тсаллиса) $\exp_q(x)$, которые определяются следующим образом[11]:

$$\ln_q(x) := \frac{x^{1-q}-1}{1-q}, \quad x \in \mathbb{R}^+, \quad q \in \mathbb{R}, \tag{7}$$

$$\exp_q(x) := [1+(1-q)x]_+^{\frac{1}{1-q}} = \begin{cases} 0, & \text{если } q<1 \text{ и } x<-1/1-q; \\ [1+(1-q)x]_+^{1/1-q} & \text{если } q<1 \text{ и } x \geq -1/1-q; \\ [1+(1-q)x]_+^{1/1-q} & \text{если } q>1 \text{ и } x<-1/1-q, \end{cases} \tag{8}$$

где $x \in \mathbb{R}$, $q \in \mathbb{R}$; выражение, стоящее в квадратных скобках, либо положительно, либо равно нулю, $[y]_+ \equiv \max(y,0)$. Из определения деформированной экспоненты Тсаллиса следует, что для $q<1$, экспонента $\exp_q(x)$ исчезает для $x \leq -1/(1-q)$, непрерывна и монотонно увеличивается от $0$ до $\infty$, когда $x$ увеличивается от $-1/(1-q)$ до $\infty$; для $q>1$, функция $\exp_q(x)$ непрерывна и монотонно увеличивается от $0$ до $\infty$, когда $x$ увеличивается от $-\infty$ до $1/(1-q)$, оставаясь расходящейся для $x>1/(q-1)$.

Легко проверить, что в пределе $q \to 1$ деформированные функции принимают стандартный вид:

$$\ln_1(x) = \lim_{q\to 1} \ln_q(x) = \ln(x) \quad (\forall x),$$

$$\exp_1(x) = \lim_{q\to 1+0} \exp_q(x) = \lim_{q\to 1-0} \exp_q(x) = \exp(x) \quad (\forall x), \tag{9}$$

а так же, что

$$\exp_q[\ln_q(x)] = \ln_q[\exp_q(x)] = x, \quad \forall x; \forall q. \tag{9*}$$

Можно также убедиться, что для деформированной экспоненты справедливы следующие соотношения:

$$\frac{1}{\exp_q(x)} = \exp_{2-q}(-x), \quad [\exp_q(x)]^a = \exp_{1-(1-q)/a}(ax), \quad \frac{d}{dx}\mathrm{e}_q^x = (\mathrm{e}_q^x)^q \quad (\forall q),$$

$$\exp_q(x)\cdot\exp_q(y) = \exp_q[x+y+(1-q)xy] \quad (\forall x; \forall q). \tag{10}$$

Соответственно для деформированного логарифма $\ln_q(x)$ имеем:

$$\ln_q\left(\frac{x}{y}\right) = \frac{1}{y^{1-q}}\left(\ln_q x - \ln_q y\right), \quad \ln_q\left(\frac{1}{x}\right) = -\frac{1}{x^{1-q}}\ln_q x, \quad (\forall (x,y); \forall q), \tag{11}$$

$$-\ln_{2-q}(1/x) = \ln_q(x), \quad (x>0; \forall q), \quad \frac{d}{dx}\ln_q x = \frac{1}{x^q} \quad (x>0; \forall q), \tag{11*}$$

$$\ln_q(xy) = \ln_q(x) + \ln_q(y) + (1-q)\ln_q(x)\ln_q(y) \quad (\forall(x,y);\, \forall q). \tag{12}$$

Приведенные соотношения будут использоваться далее.

**Энтропийный функционал Шарма−Миттала, как родоначальник семейства однопараметрических энтропий.** Продемонстрируем теперь, что определяющие формулы для энтропий (1)-(6) связаны равенствами, представляющими чередования обычных ($\ln$, $\exp$) и деформированных ($\ln_q$, $\exp_q$) логарифмов и экспонент, заданных формулами (7) и (8).

Используя обозначение

$$c_q := \sum_j p_j^{\,q} \equiv \langle 1 \rangle_q \tag{13}$$

для так называемой обобщённой статистической суммы, перепишем выражения (3) и (4) для энропий Реньи и Тсаллиса в виде

$$S_q^R = \frac{k}{1-q}\ln\left[\sum_j p_j^{\,q}\right] = \frac{k}{1-q}\ln c_q, \tag{14}$$

$$S_q^{Ts} = k\frac{\left[\left(\sum_j p_j^{\,q}\right)^{1/(1-q)}\right]^{(1-q)} - 1}{1-q} = k\ln_q\left[c_q^{\frac{1}{1-q}}\right]. \tag{15}$$

Сопоставление этих выражений даёт их связь

$$c_q^{\frac{1}{1-q}} = \exp(k^{-1}S_q^R) = \exp_q(k^{-1}S_q^{Ts}), \tag{16}$$

из которой следуют связующие эти энтропии равенства

$$S_q^R(p) = k\ln\left\{\exp_q\left[k^{-1}S_q^{Ts}(p)\right]\right\}, \quad S_q^{Ts}(p) = k\ln_q\left\{\exp\left[k^{-1}S_q^R(p)\right]\right\}. \tag{17}$$

Формула (16) позволяет также получить равенства, связывающие энтропии Шарма−Миттала и Ландсберга–Ведрала с энтропиями Тсаллиса и Реньи:

$$S_{q,r}^{SM}(p) = k\frac{\left[\left(\sum_j p_j^{\,q}\right)^{1/(1-q)}\right]^{(1-r)} - 1}{1-r} = k\ln_r\left[c_q^{\frac{1}{1-q}}\right] =$$

$$= k\ln_r \exp_q[k^{-1}S_q^{Ts}(p)] = k\ln_r\left\{\exp[k^{-1}S_q^R(p)]\right\}, \tag{18}$$

$$S_q^{LV}(p) = -k\frac{\left[(\sum_j p_j^{\,q})^{1/(q-1)}\right]^{1-q} - 1}{1-q} =$$

$$= -k\ln_q\left[c_q^{\frac{1}{q-1}}\right] = -k\ln_q\left\{\exp[-k^{-1}S_q^R(p)]\right\}. \tag{19}$$

Таким образом, $q$-деформированный логарифм и экспонента Тсаллиса позволяют записать все перечисленные меры в компактной форме (16)-(19). Кроме этого, лаконичные соотношения (17)-(19) для энтропий облегчают нахождение предельных значений функционалов (1)-(6), по сравнению с их записью в явном виде. В частности, при использовании формулы (18) и соотношений (9*), легко найти следующие пределы:

$$S_{q,r\to q}^{SM}(p) = k\ln_{r\to q}\exp_q[k^{-1}S_q^{Ts}(p)] = S_q^{Ts}(p), \tag{20}$$

$$S_{q,r\to 1}^{SM}(p) = k\ln_{r\to 1}\left\{\exp[k^{-1}S_q^R(p)]\right\} = S_q^R(p). \tag{21}$$

Поскольку при $q\to 1$ имеем $p_j^{\,q-1} = \exp\left\{(q-1)\ln p_j\right\} \to 1+(q-1)\ln p_j$, то предельное значение энтропии Тсаллиса $\lim\limits_{q\to 1} S_q^{Ts}(p)$ сводится к энтропии Больцмана–Гиббса–Шеннона $S^{BGS}$. Действительно, при $q\to 1$ имеем:

$$S_{q\to 1}^{Ts}(p) = \lim_{q\to 1}\frac{k}{q-1}\sum_j p_j(1-p_j^{\,q-1}) = -k\sum_j p_j\ln p_j) = S^{BGS}(p). \tag{22}$$

Аналогично можно получить следующие предельные значения:

$$S_{q\to 1}^{R}(p) = k\lim_{q\to 1}\frac{\ln[\sum_j p_j p_j^{\,q-1}]}{1-q} = k\lim_{q\to 1}\frac{\ln[\sum_j p_j(1+(q-1)\ln p_j]}{1-q} =$$

$$= k\lim_{q\to 1}\frac{\ln[1+(q-1)\sum_j p_j\ln p_j]}{1-q} \simeq -k\sum_j p_j\ln p_j) = S^{BGS}(p), \tag{23}$$

$$S_{q\to 1}^{LV}(p) = -k\lim_{q\to 1}\left\{\ln_q\exp[-k^{-1}S_q^R(p)]\right\} = S^{BGS}(p). \tag{24}$$

Наконец, используя соотношения (18) и (23), получим формулу для определения энтропии Гаусса

$$S_{q\to 1,r}^{SM}(p) = k\lim_{q\to 1}\ln_r\left\{\exp[k^{-1}S_q^R(p)]\right\} = k\ln_r\exp(k^{-1}S^{BGS}) =$$

$$= k\frac{1-\exp\left\{(r-1)\sum_j p_j\ln p_j\right\}}{(r-1)} = S_r^G(p)\,. \qquad (25)$$

**Псевдоаддитивность энтропии Шарма−Миттала для независимых систем.** Покажем, что подобно энтропии Тсаллиса, энтропия Шарма−Миттала подчиняется псевдоаддитивному закону для двух статистически независимых системы. Пусть общая система характеризуется нормированным распределением вероятностей микросостояний $p_{12} = \{p_{ij}\}_{i,j=1,\ldots,\mathrm{W}}$ и энтропией Шарма−Миттала

$$S_{q,r}^{SM}(p_{12}) = k\ln_r\left\{\exp_q\left[k^{-1}S_q^{Ts}(p_{12})\right]\right\}. \qquad (26)$$

Для двух независимых систем справедливо мультипликативное распределение $p_{12} = p_1p_2$, где $p_1 = \{p_i\}_{i=1,\ldots,\mathrm{W}}$ и $p_2 = \{p_j\}_{j=1,\ldots,\mathrm{W}}$ относятся соответственно, к первой и второй системе. Подставляя распределение $p_{12} = p_1p_2$ в (26) и учитывая формулы (10), (12) и (18), получим равенство

$$S_{q,r}^{SM}(p_{12}) = k\ln_r\left\{\exp_q\frac{1}{k}\left[S_q^{Ts}(p_1)+S_q^{Ts}(p_2)+(1-q)S_q^{Ts}(p_1)S_q^{Ts}(p_2)\right]\right\} =$$

$$= k\ln_r\left\{\exp_q\left[\frac{1}{k}S_q^{Ts}(p_1)\right]\cdot\exp_q\left[\frac{1}{k}S_q^{Ts}(p_2)\right]\right\} = k\ln_r\left\{\exp_q\left[\frac{1}{k}S_q^{Ts}(p_1)\right]\right\}+$$

$$+k(1-r)\ln_r\left\{\exp_q\left[\frac{1}{k}S_q^{Ts}(p_1)\right]\right\}\left\{\exp_q\left[\frac{1}{k}S_q^{Ts}(p_2)\right]\right\}+k\ln_r\left\{\exp_q\left[\frac{1}{k}S_q^{Ts}(p_2)\right]\right\} =$$

$$= S_{q,r}^{SM}(p_1)+S_{q,r}^{SM}(p_2)+\frac{1}{k}(1-r)S_{q,r}^{SM}(p_1)S_{q,r}^{SM}(p_2)\,, \qquad (27)$$

из которого следует свойство псевоаддитивности энтропии Шарма−Миттала для двух независимых систем. Параметр $r$ в (27) определяет степень неаддитивности энтропий из семейства Шарма−Миттала. Из этого выражения видно, что только для энтропий Реньи $(r=1)$ и Больцмана−Гиббса−Шеннона $(r,q=1)$ выполняется закон аддитивности.

## 3 ЭКСТРЕМУМ ЭНТРОПИИ ШАРМА−МИТТАЛА И НЕГИББСОВОЕ РАВНОВЕСНОЕ РАСПРЕДЕЛЕНИЕ

Пусть рассматриваемая статистическая система с мерой Шарма−Миттала реализуется двумя множествами: множеством всех состояний системы, описываемых распреде-

лением вероятностей $p=\{p_1,...,p_W\}$, и множеством динамических параметров $T(p)=\{T_1,...,T_W\}$, характеризующих систему. Будем далее считать, что средневзвешенное каждой случайной величины $T$ в состоянии с распределением $p$ определяется по формуле[ii)]

$$\langle T\rangle_q := \sum_j T_j f_j(q) = c_q^{-1}\sum_j T_j\, p_j^q\,, \tag{28}$$

где

$$f_j(q) := p_j^q/\sum_i p_i^q = p_j^q/\, c_q \tag{29}$$

− эскортное (нормированное) распределение[77], которое обычно используется при рассмотрении хаотических, фрактальных и мультифрактальных систем. Легко показать, что распределения $p_i$ и $f_i$ могут быть записаны в следующих эквивалентных формах

$$p_i = f_i^{1/q}\left[c_q(p)\right]^{1/q} = f_i^{1/q}\,/\sum_j f_j^{1/q}\,,$$

$$f_i(q) = p_i^q \exp\left\{k^{-1}(q-1)S_q^R(p)\right\},$$

Для определения равновесного распределения системы найдём безусловный экстремум энтропии Шарма−Миттала

$$S_{q,r}^{SM}(p) = \frac{k}{r-1}\left(1-c_q^{\,(r-1)/(q-1)}\right) = k\ln_r\left[c_q^{\,1/(q-1)}\right] \tag{30}$$

при заданности среднего значения $E_q$ энергии системы и сохранении нормировки распределения $p$:

$$E_q := \sum_j \varepsilon_j f_j \;= const,\;\; \sum_j p_j = 1\,.$$

Согласно вариационному принципу Джейнса[78], для нахождения вероятного распределения необходимо вычислить безусловный экстремум функционала

$$\Lambda(p) := k\ln_r\left[\sum_j p_j^{\,q}\right]^{1/(q-1)} - \beta\sum_j \varepsilon_j p_j^{\,q}\,/\sum_j p_j^{\,q} - k\alpha\sum_j p_j\,, \tag{31}$$

---

ii) В связи с определением средневзвешенного значения случайной величины $T$ отметим следующее: в неэкстенсивной статистике возможны три способа осреднения по распределениям: $p_i$, $p_i^q$, $f_i \equiv p_j^q/\sum j p_j^q$ (см. Bibliography/ http://tsallis.cat. cbpf. br/biblio.htm). Эти способы осреднения, каждый из которых имеет свои преимущества и недостатки, определяют совершенно разные $q$-термодинамики, соответствующие тем или иным статистически аномальным системам. По этой причине выбор осреднения в физических приложениях носит принципиальный характер, поскольку он оказывается существенным при обработке экспериментальных данных[49,64,66,68].

где параметры $\beta$ и $\alpha$ являются неопределёнными множителями Лагранжа. Из условия равенства нулю первой вариации функционала $\delta\Lambda$, получим равенство

$$\frac{\delta\Lambda}{\delta p_j} = \frac{kq}{1-q} p_j^{\,q-1} c_q^{\frac{r-q}{q-1}} - q\frac{\beta}{c_q} p_j^{\,q-1}(\varepsilon_j - E_q) - k\alpha = 0,$$

из которого следует

$$\tilde{p}_j^{\,q-1}\left[1 - k^{-1}(1-q)\frac{\beta}{\Gamma_{q,r}}(\varepsilon_j - \tilde{E}_q)\right] = \Gamma_{q,r}^{-1}\left(\frac{1-q}{q}\alpha\right). \tag{32}$$

Здесь и далее используется величина $\Gamma_{q,r}$, определяемая соотношением

$$\Gamma_{q,r} := \tilde{c}_q^{\frac{r-1}{q-1}}. \tag{33}$$

Знак «тильды» у параметров системы означает их вычисление для равновесного распределения вероятностей $\tilde{p}_j$. Заметим, что для энтропии Тсаллиса $\Gamma_{q,r=q} = c_q$; для энтропии Реньи $\Gamma_{q,1} = 1$; для энтропии Ландсберга−Ведрала $\Gamma_{q,r=2-q} = 1/c_q$.

Поскольку множители Лагранжа $\beta$ и $\alpha$ имеют произвольные значения то, полагая

$$\alpha \equiv \frac{q}{1-q}\left(\sum_j \tilde{p}_j^q\right)^{\frac{r-1}{q-1}} = \frac{q\Gamma_{q,r}}{1-q}, \tag{34}$$

запишем (32) в виде следующего негиббсового равновесного распределения с параметром $\beta_{q,r}$

$$\tilde{p}_j(\beta_{q,r}) = Z_{SM}^{-1}\left[1 - k^{-1}(1-q)\beta_{q,r}(\varepsilon_j - \tilde{E}_q)\right]_+^{\frac{1}{1-q}} =$$

$$= Z_{SM}^{-1}\exp_q\left[-k^{-1}\beta_{q,r}(\varepsilon_j - \tilde{E}_q)\right], \tag{35}$$

где

$$Z_{SM} = \left[\sum_j \tilde{p}_j^q\right]^{1/(1-q)} = \tilde{c}_q^{\,1/(1-q)} =$$

$$= \sum_j\left[1 - k^{-1}(1-q)\beta_{q,r}(\varepsilon_j - \tilde{E}_q)\right]_+^{\frac{1}{1-q}} = \sum_j \exp_q\left[-k^{-1}\beta_{q,r}(\varepsilon_j - \tilde{E}_q)\right] \tag{36}$$

− статистический интеграл, определяемый из условия нормировки (31); параметр $\beta_{q,r} \equiv \beta/\Gamma_{q,r}$ является обратной физической температурой в статистике Шарма−Миттала (см. ниже).

При условии $r = q$ из (35) следует выражение для равновесного распределения вероятностей состояния $\tilde{p}_j$ в статистике Тсаллиса

$$\tilde{p}_j(\beta_q) = \frac{1}{Z_{Ts}}\left[1 - k^{-1}(1-q)\beta_q(\varepsilon_j - \tilde{E}_q)\right]_+^{\frac{1}{1-q}} = \frac{1}{Z_{Ts}}\exp_q\left[-k^{-1}\beta_q(\varepsilon_j - E_q)\right], \quad (37)$$

где

$$Z_{Ts}(\beta_q) = \sum_j\left[1 - k^{-1}(1-q)\beta_q(\varepsilon_j - \tilde{E}_q)\right]_+^{\frac{1}{1-q}} = \sum_j \exp_q\left[-k^{-1}\beta_q(\varepsilon_j - \tilde{E}_q)\right] \quad (38)$$

− статистический интеграл в статистике Тсаллиса; параметр $\beta_q \equiv \beta / \tilde{c}_q$ является обратной физической температурой системы, $T_{ph} \equiv 1/\beta_q$; $\beta$ − множитель Лагранжа, который связан с ограничением на среднюю энергию в неэкстенсивной статистической механике. При $1 - k^{-1}(1-q)\beta_q(\varepsilon_j - \tilde{E}_q) < 0$ имеем $\tilde{p}_j = 0$, а при $q = 1$ из (37) и (38) следует классическое каноническое распределение Гиббса

$$\tilde{p}_j(\beta) = \exp\left\{-k^{-1}\beta(\varepsilon_j - \tilde{E}_q)\right\} / \sum_j \exp\left\{-k^{-1}\beta(\varepsilon_j - \tilde{E}_q)\right\}. \quad (39)$$

В случае, когда $r = 1$ из (35) следует равновесное распределение в статистике Реньи

$$\tilde{p}_j = \frac{1}{Z_R}\left[1 - k^{-1}\beta(1-q)(\varepsilon_j - \tilde{E}_q)\right]_+^{\frac{1}{1-q}} = \frac{1}{Z_R}\exp_q\left[-k^{-1}\beta(\varepsilon_j - \tilde{E}_q)\right]. \quad (40)$$

Здесь

$$Z_R(\beta) = \tilde{c}_q^{1/(1-q)} = \sum_j\left[1 - k^{-1}\beta(1-q)(\varepsilon_j - \tilde{E}_q)\right]_+^{\frac{1}{1-q}} > 0 \quad (41)$$

− статистический интеграл; $\beta = 1/T$ − обратная температура (изменяющаяся в пределах допустимых значений). Таким образом, распределение вероятностей состояния статистического ансамбля неэкстенсивных систем с мерой Реньи, которые находятся в тепловом равновесии с внешней средой (термостатом) и могут обмениваться с ней энергией при постоянном объёме и постоянном числе частиц, соответствует обобщённому каноническому ансамблю Гиббса (40).

## 4 ТЕРМОДИНАМИЧЕСКИЕ СООТНОШЕНИЯ ОБОБЩЁННОЙ РАВНОВЕСНОЙ ТЕРМОДИНАМИКИ

Приступим теперь к главной цели данной работы – конструированию равновесной термодинамики, основанной на неэкстенсивной статистике Шарма−Мит- тала. Важно иметь в виду, что макроскопический термодинамический уровень описания, использующий немногочисленные статистические средние характеристики системы (параметры состояния), позволяет сжимать огромное обилие статистической информации, подлежащей обработке для получения детального описания поведения сложной системы.

Поскольку соотношение (18) справедливо также и для равновесного распределения $\tilde{p}_j$, то для экстремального значения энтропии $S_{q,r}^{SM}$ имеем

$$S_{q,r}^{SM} = k\frac{\tilde{c}_q^{\,(1-r)/(1-q)} - 1}{1-r} = k\frac{Z_{SM}^{1-r} - 1}{1-r} = k\ln_r Z_{SM}, \tag{42}$$

а для квазиравновесной деформированной свободной энергии Гельмгольца $F_{q,r}$ и обобщённого статистического интеграла $Z_{SM}$ справедливы следующие выражения

$$\tilde{F}_{q,r} := \tilde{E}_q - \frac{1}{\beta}\tilde{S}_{q,r}^{SM} = \tilde{E}_q - \frac{1}{\beta}k\ln_r Z_{SM}, \quad Z_{SM} = \left[\sum\nolimits_j p_0^q\right]^{1/(1-q)}. \tag{43}$$

С учетом (36) и (42) равновесное нормированное распределение (35) может быть переписано в следующем виде:

$$\tilde{p}_j(\beta_{q,r}) = \left\{\frac{1-\omega(q)\beta_{q,r}(\varepsilon_j - \tilde{E}_q)}{\tilde{c}_q}\right\}^{1/(1-q)} =$$

$$= \frac{\left\{1-\omega(q)\beta_{q,r}(\varepsilon_j - \tilde{E}_q)\right\}^{1/(1-q)}}{\left\{1+\omega(r)\tilde{S}_{q,r}^{SM}\right\}^{1/(1-r)}} = \frac{\exp_q\left\{-k^{-1}\beta_{q,r}(\varepsilon_j - \tilde{E}_q)\right\}}{\exp_r\left\{k^{-1}\tilde{S}_{q,r}^{SM}\right\}}. \tag{44}$$

Здесь и далее используются обозначения: $\omega(r) := k^{-1}(1-r)$, $\omega(q) := k^{-1}(1-q)$.

Учитывая соотношения (33) и (36), перепишем статистический интеграл $Z_{SM}$ следующим образом:

$$Z_{SM}(\beta) = \sum\nolimits_j \exp_q\left[-Z_{SM}^{(r-1)}k^{-1}\beta(\varepsilon_j - \tilde{E}_q)\right]. \tag{45}$$

Дифференцируя теперь (45) по параметру $\beta$, с учётом формулы (10) получим

$$\frac{\partial}{\partial\beta}Z_{SM} = -\sum\nolimits_j\left\{\exp_q\left[-Z_{SM}^{(r-1)}k^{-1}\beta(\varepsilon_j - \tilde{E}_q)\right]\right\}^q \times$$

$$\times\left\{Z_{SM}^{(r-1)}k^{-1}(\varepsilon_j - \tilde{E}_q) + k^{-1}\beta(\varepsilon_j - \tilde{E}_q)\frac{\partial Z_{SM}^{(r-1)}}{\partial\beta} - Z_{SM}^{(r-1)}k^{-1}\beta\frac{\partial\tilde{E}_q}{\partial\beta}\right\} =$$

$$= -Z_{SM}^{(r-1)}Z_{SM}^q\sum\nolimits_j\tilde{p}_j^q\left\{k^{-1}(\varepsilon_j - E_q) + k^{-1}\beta(\varepsilon_j - \tilde{E}_q)\frac{\partial\ln Z_{SM}^{(r-1)}}{\partial\beta} - k^{-1}\beta\frac{\partial\tilde{E}_q}{\partial\beta}\right\} =$$

$$= Z_{SM}^{q} Z_{SM}^{(r-1)} \tilde{c}_q k^{-1} \beta \frac{\partial E_q}{\partial \beta} = Z_{SM}^{r} k^{-1} \beta \frac{\partial E_q}{\partial \beta}. \tag{46}$$

Отсюда, с использованием соотношения (11), получим следующее выражение для дифференцированного деформированного логарифма:

$$\frac{\partial \ln_r Z_{SM}}{\partial \beta} = Z_{SM}^{-r} \frac{\partial Z_{SM}}{\partial \beta} = k^{-1} \beta \frac{\partial \tilde{E}}{\partial \beta}. \tag{47}$$

С другой стороны, с учетом (42) и (45), будем иметь

$$\tilde{S}_{q,r}^{SM} = \ln_r \left\{ \sum_j \exp_q \left[ -Z_{SM}^{(r-1)} k^{-1} \beta (\varepsilon_j - \tilde{E}_q) \right] \right\}, \tag{48}$$

откуда следует

$$\begin{gathered} \frac{\partial \tilde{S}_{q,r}^{SM}}{\partial \tilde{E}_q} = k \frac{\partial \ln_r Z_{SM}}{\partial \tilde{E}_q} = \\ = \frac{k}{Z_{SM}^{r}} Z_{SM}^{(r-1)} k^{-1} \beta \sum_j \left( \exp_q \left[ -Z_{SM}^{(r-1)} k^{-1} \beta (\varepsilon_j - \tilde{E}_q) \right] \right)^q = \beta \tilde{c}_q Z_{SM}^{q-1} = \beta. \end{gathered} \tag{49}$$

Таким образом, для равновесной термодинамики, построенной на базе энтропии Шар- ма−Миттала, справедливы следующие соотношения:

$$S_{q,r}^{SM} = k \ln_r Z_{SM}, \quad F_{q,r} = E_q - \frac{1}{\beta} S_{q,r}^{SM} = E_q - \frac{1}{\beta} k \ln_r Z_{SM},$$

$$\beta = \frac{\partial S_{q,r}^{SM}}{\partial E_q} = k \frac{\partial \ln_r Z_{SM}}{\partial E_q}, \quad E_q = \frac{\partial (\beta F_{q,r})}{\partial \beta}, \quad \beta \frac{\partial E_q}{\partial \beta} = k \frac{\partial \ln_r Z_{SM}}{\partial \beta}. \tag{50}$$

(знак «тильды» здесь опущен)

По поводу соотношений (50) важно отметить следующее: Величина $Z_{SM}$ определяется микроскопической энергией $\varepsilon_j$ относительно средней энергии $E_q$ системы (см. (36)). Однако, в случае использования новой величины $\overleftrightarrow{Z}_{SM}$

$$\ln_r \overleftrightarrow{Z}_{SM} = \ln_r Z_{SM} - k^{-1} \beta E_q, \tag{51}$$

(которая определяется микроскопической энергией $\varepsilon_j$ относительно нулевой точки), соотношения равновесной термодинамики (50) принимают почти классическую форму

$$S_{q,r}^{SM} = \beta \left( E_q - F_{q,r} \right), \quad dS_{q,r}^{SM} = \beta dE_q,$$

$$F_{q,r} = -\frac{k}{\beta}\ln_q \overleftrightarrow{Z}_{SM}, \quad E_q = \frac{\partial(\beta F_{q,r})}{\partial\beta}, \quad C_q = -\beta^2\frac{\partial E_q}{\partial\beta}. \tag{52}$$

## 5 ТЕРМОДИНАМИЧЕСКОЕ РАВНОВЕСИЕ ДВУХ НЕЗАВИСИМЫХ СИСТЕМ С ЭНТРОПИЯМИ ШАРМА−МИТТАЛА

Рассмотрим тепловое равновесие двух независимых $q$-систем с энтропиями $S_{q,r}^{SM}\left(p_1\right)$ и $S_{q,r}^{SM}\left(p_2\right)$, представляющих собой общую замкнутую систему с постоянными значениями энтропии $S_{SM}^{12} \equiv S_{SM}\left(p_{12}\right)$ при $p_{12} = p_1 p_2$ и суммарной энергии $E_q(p_{12})$. Согласно свойству неаддитивности (27) энтропий в статистике Шарма−Миттала, энтропию совокупной системы можно переписать в следующем виде:

$$S_{q,r}^{SM}(p_{12}) = S_{q,r}^{SM}(p_1)\left[1+\omega(r)S_{q,r}^{SM}(p_2)\right] + S_{q,r}^{SM}(p_2)\left[1+\omega(r)S_{q,r}^{SM}(p_1)\right] -$$

$$-\omega(r)S_{q,r}^{SM}(p_1)S_{q,r}^{SM}(p_2). \tag{53}$$

Для нахождения осреднённой энергии $E_q(p_{12})$ совокупной $q$-системы воспользуемся равновесным распределением (44)

$$p_j = \frac{\exp_q\left\{-k^{-1}\beta_{q,r}\Delta[\varepsilon_j]\right\}}{\exp_r\left\{k^{-1}S_{q,r}^{SM}\right\}}, \tag{54}$$

где $\Delta[\varepsilon_j] := (\varepsilon_j - E_q)$ — флуктуация энергии частиц. При учёте условия мультипликативности $p_{12} = p_1 p_2$ и формулы (10) будем иметь

$$\frac{\exp_q\left\{-k^{-1}\beta_{q,r}\Delta_{12}[\varepsilon_j]\right\}}{\exp_r\left\{k^{-1}S_{q,r}^{SM}(p_{12})\right\}} = \frac{\exp_q\left\{-k^{-1}\beta_{q,r}\Delta_1[\varepsilon_j]\right\}}{\exp_r\left\{k^{-1}S_{q,r}^{SM}(p_1)\right\}} \cdot \frac{\exp_q\left\{-k^{-1}\beta_{q,r}\Delta_2[\varepsilon_j]\right\}}{\exp_r\left\{k^{-1}S_{q,r}^{SM}(p_2)\right\}} =$$

$$= \frac{\exp_q\left\{-k^{-1}\beta_{q,r}\left(\Delta_1[\varepsilon_j]+\Delta_2[\varepsilon_j]+\omega(q)\Delta_1[\varepsilon_j]\cdot\Delta_2[\varepsilon_j]\right)\right\}}{\exp_r\left\{k^{-1}\left(S_{q,r}^{SM}(p_1)+S_{q,r}^{SM}(p_2)+\omega(r)S_{q,r}^{SM}(p_1)\cdot S_{q,r}^{SM}(p_2)\right)\right\}}. \tag{55}$$

Поскольку знаменатели в правой и левой частях соотношения (55) одинаковы, то можно заключить, что

$$\Delta_{12}[\varepsilon_j] = \Delta_1[\varepsilon_j] + \Delta_2[\varepsilon_j] + \omega(q)\Delta_1[\varepsilon_j]\cdot\Delta_2[\varepsilon_j]. \tag{56}$$

В этом соотношении необходимо использовать условие аддитивности осреднённых энергий

$$E_q^{12} = E_q^1 + E_q^2, \tag{57}$$

поскольку без этого предположения осреднённые величины системы будут зависеть от микроскопических величин, что является неприемлемым[61]. Тогда из (56) для микроскопических энергий получим следующее условие квазиаддитивности микроскопических энергий

$$\varepsilon_{i12} = \varepsilon_{i1} + \varepsilon_{i2} - \omega(q)\beta\Delta_1\left[\varepsilon_i\right]\Delta_2\left[\varepsilon_i\right]. \tag{58}$$

Отметим, что именно наличие этого равенства является, в частности, той причиной, благодаря которой статистику на мере Реньи относят к неэкстенсивной статистической механике.

Варьирование соотношений (53) и (57) для совокупной замкнутой системы с постоянными значениями энтропии $S_{q,r}^{SM}(p_{12})$ и энергии $E_q^{12}$ приводит к равенству

$$\delta S_{q,r}^{SM}(p_{12}) = 0 = \delta S_{q,r}^{SM}(p_1)\left[1 + \omega(r)S_{q,r}^{SM}(p_2)\right] + \delta S_{q,r}^{SM}(p_2)\left[1 + \omega(r)S_{q,r}^{SM}(p_1)\right]$$

для энтропии и равенству

$$\delta E_q^{12} = 0 = \delta E_q^1 + \delta E_q^2$$

для средней энергии. Объединяя их, в итоге получим уравнение

$$\frac{\delta S_{q,r}^{SM}(p_1)/\delta E_q^1}{1 + \omega(r)S_{q,r}^{SM}(p_1)} = \frac{\delta S_{q,r}^{SM}(p_2)/\delta E_q^2}{1 + \omega(r)S_{q,r}^{SM}(p_2)}, \tag{59}$$

из которого, при учёте (33), (42) и (50), вытекает условие

$$\frac{\beta}{1 + \omega(r)S_{q,r}^{SM}(p_1)} = \frac{\beta}{1 + \omega(r)S_{q,r}^{SM}(p_2)} = \frac{\beta}{\Gamma_{q,r}} \equiv \beta_{q,r}, \tag{60}$$

означающее равенство физических температур $\beta_{q,r}$ двух независимых $q$-систем при их тепловом контакте. Отношение эквивалентности (60) является обобщением нулевого закона термодинамики на неэкстенсивные системы, описываемые статистикой Шарма−Миттала. Оно показывает, что в отличие от классического случая $(q,r \to 1)$ физическая температура $T_{ph}$ не является обратной величиной множителя Лагранжа, $\beta^{-1}$, но

$$T_{ph} = 1/\beta_{q,r} \equiv \Gamma_{q,r}/\beta = \left(1 + \omega(r)S_{q,r}^{SM}\right)T = \Gamma_{q,r}T. \tag{61}$$

Важно иметь в виду, что такое переопределение эффективной температуры в статистике Шарма−Миттала противоречит основным принципам классической термодинамики, где абсолютная температура $T$ является интенсивным параметром, а не функ-

ционалом $T_{ph}(p)$. В связи с этим сделаем следующее общее замечание. В большинстве неэкстенсивных систем важную роль играют длинномасштабные пространственно-временные корреляции в фазовом или геометрическом пространстве. Это означает, в частности, что существенное значение имеет та часть внутренней энергии системы, которая связана с силовым взаимодействием отдалённых друг от друга её частей, а именно потенциальная энергия. В классической статистике внутренняя энергия определяется, как правило, суммой кинетических энергий всех молекул совокупной системы. В такой системе «тепловой баланс» достигается в основном за счёт локального теплообмена между близко расположенными её частями, т.е. «тепло» связано с передачей кинетической энергии молекулами.

Поскольку физическая температура $T_{ph}$ отвечает за «глобальный тепловой баланс» между различными частями системы, то её энергетический баланс будет сильно отличаться от локального теплового баланса. Локальный баланс, как известно, можно охарактеризовать абсолютной обратной температурой $\beta = 1/T$, измеряемой термометром. Однако любое измерение физической температуры $T_{ph}$ нереально, что связано с наличием коэффициента $\Gamma_{q,r}$, зависящего, согласно (33), от выбора параметров деформации $q$ и $r$ системы.

Таким образом, обобщённый нулевой закон статистической термодинамики (60) показывает, что физическая температура в статистике Шарма−Миттала отличается от инверсии множителя Лагранжа $\beta$. Этот факт требует переопределения термодинамических соотношений (50) и (52), полученных в рамках статистики Шарма−Миттала. В работе[15,79], в качестве основных предпосылок, взятых за исходный пункт подобного переопределения при построении модифицированной термодинамики Тсаллиса, выбраны первый закон термодинамики и структура преобразования Лежандра. Далее мы используем этот подход для переопределения некоторых термодинамических соотношений при построении модифицированной термодинамики Шарма−Миттала.

## 6 ДЕФОРМИРОВАННЫЕ ТЕРМОДИНАМИЧЕСКИЕ СООТНОШЕНИЯ

Прежде всего введём, по аналогии с физической температурой $T_{ph}$, физическое давление $p_{qh}$ путём рассмотрения механического равновесия двух независимых $q$-систем, представляющих собой общую замкнутую систему с постоянными значениями энтропии $S_{q,r}^{SM}(p_{12})$ и объёма $V_{12} = V_1 + V_2 = const$. В этом случае энтропия совокупной системы должна максимизироваться с фиксацией общего объёма. В результате будем иметь

$$\frac{\delta S_{q,r}^{SM}(p_1)/\delta V_1}{1+\omega(r)S_{q,r}^{SM}(p_1)} = \frac{\delta S_{q,r}^{SM}(p_2)/\delta V_2}{1+\omega(r)S_{q,r}^{SM}(p_2)} = \frac{p_{ph}}{T_{ph}}, \tag{62}$$

где $p_{ph}$ − так называемое физическое давление, которое определяется соотношением

$$p_{ph} := \frac{T_{ph}}{1+\omega(r)S_{q,r}^{SM}}\frac{\delta S_{q,r}^{SM}}{\delta V} = \frac{T_{ph}}{\Gamma_{q,r}}\frac{\delta S_{q,r}^{SM}}{\delta V}. \tag{63}$$

Очевидно, что введённые таким способом физические температура и давление должны привести к модификации определения термодинамической энтропии Клаузиуса.

Чтобы показать это, рассмотрим структуру преобразования Лежандра. Уравнение (50) $\beta = \partial S_{q,r}^{SM} / \partial E_q$ указывает на то, что параметры $\beta$ и $E_q$ образуют пару переменных Лежандра. Это приводит к следующему определению свободной энергии Гельмгольца (изохорно-изотермического потенциала) (см.(43) и (50)):

$$F_{q,r} = E_q - TS_{q,r}^{SM} = E_q - kT\ln_r Z_{SM} = E_q - kT\ln_r\left[c_q^{1/(1-q)}\right]. \tag{64}$$

Это выражение, однако, неудовлетворительно с точки зрения деформированной термодинамики. Свободная энергия должна зависеть от $T_{ph}$, а не от переменной $T = \beta^{-1}$.

По аналогии с подходом, развитым в работе[80], переопределим макроскопическую свободную энергию (64) следующим образом:

$$F_{q,r}(T_{ph}) = E_q - kT_{ph}\ln\left[c_q^{1/(1-q)}\right], \tag{65}$$

что отличается от соответствующего выражения в традиционной термодинамике. Используя соотношения (42), (33) и (61), можно убедиться, что переопределённая таким образом свободная энергия $F_{q,r}$ является функцией $T_{ph}$. Дифференцируя функцию $F_{q,r}$, в результате получим

$$dF_{q,r} = dE_q - \left[\frac{k}{1-q}\ln c_q\right]dT_{ph} - \frac{T_{ph}}{\Gamma_{q,r}}dS_{q,r}^{SM}. \tag{66}$$

Если теперь использовать первый закон термодинамики

$$d'Q_q = dE_q + p_{ph}dV, \tag{67}$$

где $Q_q$ − количество теплоты, подводимое к термодинамической $q$-системе (или отводимое от неё), то (66) можно переписать в виде

$$dF_{q,r} = d'Q_q - p_{ph}dV - \left[\frac{k}{1-q}\ln c_q\right]dT_{ph} - \frac{T_{ph}}{\Gamma_{q,r}}dS_{q,r}^{SM}. \tag{68}$$

Отсюда следует, что определение термодинамической энтропии Клаузиуса модифицируется для неаддитивных систем следующим образом:

$$dS_{q,r}^{SM} = \Gamma_{q,r} d'Q_q \,/\, T_{ph}. \tag{69}$$

Введём теперь в рассмотрение следующие характеристические функции: обобщённую энтальпию $H_q = E_q + p_{ph}V$ и обобщённый термодинамический потенциал $G_{q,r} = F_{q,r} + p_{ph}V$. Заметим, что характеристические функции обладают следующим свойством: если известна характеристическая функция, выраженная через соответствующие (свои для каждой функции) переменные, то из неё можно вычислить любую термодинамическую величину.

В этом нетрудно убедиться. Из уравнений

$$dE_q = \frac{T_{ph}}{\Gamma_{q,r}} dS_{q,r}^{SM} - p_{ph}dV, \quad dH_q = \frac{T_{ph}}{\Gamma_{q,r}} dS_{q,r}^{SM} + VdP_{ph}, \tag{70}$$

$$dF_q = -\left[\frac{k}{(1-q)}\ln c_q\right] dT_{ph} - p_{ph}dV, \quad dG_{q,r} = -\left[\frac{k}{(1-q)}\ln c_q\right] dT_{ph} + Vdp_{ph} \tag{71}$$

следуют обобщённые термодинамические соотношения

$$\left(\frac{\partial E_q}{\partial V}\right)_{S_{q,r}^{SM}} = \left(\frac{\partial F_{q,r}}{\partial V}\right)_{T_{ph}} = -p_{ph}, \quad \left(\frac{\partial E_q}{\partial S_{q,r}^{SM}}\right)_V = \left(\frac{\partial H_q}{\partial S_{q,r}^{SM}}\right)_{P_{ph}} = \frac{T_{ph}}{\Gamma_{q,r}}, \tag{72}$$

$$\left(\frac{\partial H_q}{\partial p_{ph}}\right)_{S_{q,r}^{SM}} = \left(\frac{\partial G_{q,r}}{\partial p_{ph}}\right)_{T_{ph}} = V, \quad \left(\frac{\partial F_{q,r}}{\partial T_{ph}}\right)_V = \left(\frac{\partial G_{q,r}}{\partial T_{ph}}\right)_{P_{ph}} = -\frac{k}{(1-q)}\ln c_q. \tag{73}$$

**Уравнение для теплоёмкостей.** Как известно, в классической термодинамике теплоёмкость вещества в наиболее общем виде определяется следующим образом: $C_z = T\left(\partial S / \partial T\right)_z$. Здесь $C_z$ − теплоёмкость в таком процессе, в котором сохраняется постоянным параметр $z$, где $z$ − любые обобщённые координаты. Наиболее распространёнными являются изобарная и изохорная теплоёмкости:

$$C_p = \frac{T_{ph}}{\Gamma_{q,r}}\left(\frac{\partial S_{q,r}^{SM}}{\partial T_{ph}}\right)_{p_{ph}}, \quad C_V = \frac{T_{ph}}{\Gamma_{q,r}}\left(\frac{\partial S_{q,r}^{SM}}{\partial T_{ph}}\right)_V. \tag{74}$$

Так как в соответствии с формулой $\left(\partial y / \partial x\right)_z = \left(\partial y / \partial u\right)_z \left(\partial u / \partial x\right)_z$ (справедливой для случая двух переменных, когда $y = y(x,z)$ и $u = u(x,z)$) имеем

$$\left(\frac{\partial S_{q,r}^{SM}}{\partial T_{ph}}\right)_{p_{ph}} = \left(\frac{\partial S_{q,r}^{SM}}{\partial H_q}\right)_{p_{ph}} \left(\frac{\partial H_q}{\partial T_{ph}}\right)_{p_{ph}} \text{ и } \left(\frac{\partial S_{q,r}^{SM}}{\partial T_{ph}}\right)_V = \left(\frac{\partial S_{q,r}^{SM}}{\partial E_q}\right)_V \left(\frac{\partial E_q}{\partial T_{ph}}\right)_V, \quad (75)$$

а из (72) и (73) следует, что $\left(\frac{\partial S_{q,r}^{SM}}{\partial H_q}\right)_{p_{ph}} = \frac{\Gamma_{q,r}}{T_{ph}}$, $\left(\frac{\partial S_{q,r}^{SM}}{\partial E_q}\right)_V = \frac{\Gamma_{q,r}}{T_{ph}}$, то соотношения (74) могут быть записаны в виде

$$C_p = \left(\partial H_q / \partial T_{ph}\right)_{p_{ph}}, \quad C_V = \left(\partial E_q / \partial T_{ph}\right)_V. \quad (76)$$

Уравнение, устанавливающее связь между теплоёмкостями $C_p$ и $C_V$, можно получить следующим образом. В соответствии с соотношением[81]

$$\left(\frac{\partial z}{\partial m}\right)_n = \left(\frac{\partial z}{\partial x}\right)_y \left(\frac{\partial x}{\partial m}\right)_n + \left(\frac{\partial z)}{\partial y}\right)_x \left(\frac{\partial y}{\partial m}\right)_n, \quad (77)$$

являющимся следствием выражения для полного дифференциала функции $z = z(x, y)$, можно записать (полагая $m = x$)

$$\left(\frac{\partial S_{q,r}^{SM}}{\partial T_{ph}}\right)_{P_{ph}} = \left(\frac{\partial S_{q,r}^{SM}}{\partial T_{ph}}\right)_V + \left(\frac{\partial S_{q,r}^{SM}}{\partial V}\right)_{T_{ph}} \left(\frac{\partial V}{\partial T_{ph}}\right)_{P_{ph}}. \quad (78)$$

Отсюда, используя уравнение Максвелла $(\partial S_{q,r}^{SM}/\partial V)_{T_{ph}} = (\partial p_{ph}/T_{ph})_V$, получим

$$C_p - C_V = \frac{T_{ph}}{\Gamma_{q,r}^2} \left(\frac{\partial p_{ph}}{\partial T_{ph}}\right)_V \left(\frac{\partial V}{\partial T_{ph}}\right)_{P_{ph}}. \quad (79)$$

Это выражение может быть представлено в другом виде, если использовать связку трёх производных $\left(\frac{\partial z}{\partial x}\right)_y \left(\frac{\partial x}{\partial y}\right)_z \left(\frac{\partial y}{\partial z}\right)_x = -1$ (следствие соотношения (77) при $m = x$, $n = z$), из которой следует

$$\left(\partial p_{ph}/\partial T_{ph}\right)_V = -\left(\partial V/\partial T_{ph}\right)_{p_{ph}} \left(\partial p_{ph}/\partial V\right)_{T_{ph}}. \quad (80)$$

С учётом (80) связь между теплоёмкостями приобретает классический вид:

$$C_p - C_V = -\frac{T_{ph}}{\Gamma_{q,r}^2}\left(\frac{\partial V}{\partial T_{ph}}\right)_{P_{ph}}^2 \Big/ \left(\frac{\partial V}{\partial p_{ph}}\right)_{T_{ph}} . \tag{81}$$

Таким образом, стандартная форма термодинамических соотношений (72), (73) и (81) в термодинамике Шарма−Миттала позволяет заключить, что они остаются инвариантными относительно неаддитивной модификации их классических аналогов. Подчеркнём важный факт, что температуры $T = 1/\beta$ и $T_{ph} = 1/\beta_{q,r}$ не зависят от выбора нуля энергий, и поэтому они допускают физическую интерпретацию. Заметим, что в дополнение к структуре Лежандра различные другие важные теоремы и свойства остаются $q$-инвариантными[11].

## 7 ДВУХПАРАМЕТРИЧЕСКАЯ ИНФОРМАЦИЯ РАЗЛИЧИЯ ШАРМА−МИТТАЛА. ОБОБЩЁННАЯ *H*-ТЕОРЕМА БОЛЬЦМАНА

Наряду с энтропией $S_{q,r}^{SM}$, информация различия Шарма-Миттала[49]

$$K_{q,r}^{SM}(p:u) \equiv -\frac{k}{1-r}\left[\left(\sum_j p_j^q u_j^{1-q}\right)^{\frac{1-r}{1-q}} - 1\right] = -k\ln_r\left(\sum_j p_j^q u_j^{1-q}\right)^{\frac{1}{1-q}} \tag{82}$$

также относится к наиболее существенным статистическим характеристикам неэкстенсивной динамической $q$-системы. Являясь функционалом, она характеризует переход системы от состояния $p$ в состояние $u$, когда статистические наблюдения ведутся относительно состояния $p$.

Заметим, что при $r \to 1$ величина $K_{q,r}^{SM}$ переходит в различающую информацию Реньи[49]

$$K_{q,r=1}^{SM}(p:u) = K_q^R(p:u) := \frac{k}{q-1}\ln\sum_j p_j^q u_j^{1-q},$$

а при $q = r$ величина $K_{q,r}^{SM}$ переходит в различающую информацию Ратье−Каннаппана[49]

$$K_{q,q}^{SM}(p:u) = K_q^{RK}(p:u) := \frac{k}{1-q}\left[1 - \sum_j p_j^q u_j^{1-q}\right] = -k\ln_q\left(\sum_j p_j^q u_j^{1-q}\right)^{\frac{1}{1-q}}.$$

**Выпуклость информации различия Шарма-Миттала**. Различающая инфор-мация $K_{q,r}^{SM}(p:u)$ является вещественным, выпуклым и положительным (или отрицательным) функционалом с минимумом (максимумом) в зависимости от сочетания знаков параметров деформации $r$ и $q$. Покажем это. Для некоторого действительного числа $n > 0$ имеем

$$\frac{n^{q-1}-1}{q-1} \geq 1-\frac{1}{n}, \quad \textit{если } q>0,$$
$$= 1-1/n, \quad \textit{если } q=0, \tag{83}$$
$$\leq 1-1/n, \quad \textit{если } q<0.$$

Поэтому, например, для $q<0$ справедливо неравенство

$$\left(p_j/u_j\right)^{q-1} \geq q+(1-q)(u_j/p_j),$$

при использовании которого получаем

$$K_{q,r}^{SM} = \frac{k}{r-1}\left\{\left[\sum_j p_j\left(\frac{p_j}{u_j}\right)^{q-1}\right]^{\frac{r-1}{q-1}}-1\right\} \leq \frac{k}{r-1}\left\{\left[\sum_j p_j\left(q+(1-q)\frac{u_j}{p_j}\right)\right]^{\frac{r-1}{q-1}}-1\right\}=0, \tag{84}$$

если $r<1$. Легко проверить, что имеют место следующие неравенства

$$K_{q,r}^{SM}(p:u) \leq 0, \text{ если } q<0,\ r<1, \text{ или } q>0,\ r>1;$$
$$K_{q,r}^{SM}(p:u) \geq 0, \text{ если } q<0, r>1, \text{ или } q>0,\ r<1\ . \tag{85}$$

В частном случае, когда $r \to 1$, из неравенств (85) вытекают следующие неравенства для различающей информации Реньи[49] $K_q^R(p:u)$:

$$K_q^R(p:u) \leq 0, \quad (q<0); \quad K_q^R(p:u) \geq 0, \quad (q>0). \tag{86}$$

Важно отметить, что поскольку при $u=p$ имеет место равенство $K_{q,r}^{SM}(p:p)=0$, то различающая информация Шарма−Миттала является функцией Ляпунова[iii)].

Для различающей информации Ратье−Каннаппана $K_q^{RK}(p:u)$ из (85) следует

$$K_q^{RK}(p:u) \geq 0,\ (q>0); \quad K_q^{RK}(p:u)=0,\ (q=0); \quad K_q^{RK}(p:u) \leq 0,\ (q<0), \tag{87}$$

т.е. выражение (87) удовлетворяет такому же основному свойству, что и энтропия Кульбака−Лейблера классической статистики, а потому может использоваться для тех же целей. Однако в данном случае имеется свобода выбора параметра $q$, что позволяет исследовать неэкстенсивные системы.

---

iii) Напомним, что функцией Ляпунова называется знакоопределённая функция, которая обращается в нуль в точке равновесия системы. Состояние равновесия является аттрактором, когда производная по времени от функции Ляпунова имеет знак, противоположный знаку самой функции.

**Обобщённая *H*-теорема в статистике Шарма−Миттала**. Рассмотрим теперь замкнутую систему, для которой распределение $p_j$ является произвольным, а распределение $u_j = \tilde{p}_j$ – равновесным (см. (44))

$$u_j = \tilde{p}_j = \left\{ \frac{1 - \omega(q)\beta_{q,r}(\varepsilon_j - \tilde{E}_q)}{\tilde{c}_q} \right\}^{1/(1-q)} . \tag{88}$$

При использовании соотношений (8), (11), (30), (33) и (36) легко показать, что спонтанный переход между этими состояниями описывается следующей различающей информацией Шарма−Миттала

$$K_{q,r}^{SM}(p:\tilde{p}) \equiv \frac{k}{1-r}\left[1 - \left(\sum_j p_j^q \tilde{p}_j^{1-q}\right)^{\frac{1-r}{1-q}}\right] =$$

$$= -\frac{k}{1-r}\left[\left(\frac{c_q}{\tilde{c}_q}\right)^{\frac{1-r}{1-q}} \left(1 - \omega(q)\tilde{\beta}_{q,r}(E_q - \tilde{E}_q)\right)^{\frac{1-r}{1-q}} - 1\right] =$$

$$= -k \ln_r \left\{ \frac{c_q^{\,1/(1-q)} \exp_q\left[-k^{-1}\tilde{\beta}_{q,r}(E_q - \tilde{E}_q)\right]}{\tilde{c}_q^{\,1/(1-q)}} \right\} =$$

$$\begin{aligned} &= -k\frac{1}{\tilde{c}_q}\ln_r\left\{c_q^{1/(1-q)} \exp_q\left[-k^{-1}\tilde{\beta}_{q,r}(E_q - \tilde{E}_q)\right]\right\} + \frac{k}{\tilde{c}_q}\ln_r \tilde{c}_q^{\,1/(1-q)} = \\ &= Z_{SM}^{q-1}\left\{-\left(S_{q,r}^{SM} - \tilde{S}_{q,r}^{SM}\right) - kc_q \ln_r \exp_q\left[-k^{-1}\tilde{\beta}_{q,r}(E_q - \tilde{E}_q)\right]\right\} \end{aligned} \tag{89}$$

с равенством $K_{q,r}^{SM}(p:\tilde{p}) = 0$ при распределении $p_j = \tilde{p}_j$.

Если $q, r \to 1$, то из (89) вытекает следующее известное выражение для информации различия Кульбака–Лейблера $K^{KL}(p,u) := k\sum_j p_j \ln(p_j / u_j)$ классической статистической механики для случая спонтанного перехода системы от произвольного состояния с распределением $p$ к состоянию с каноническим распределением Гиббса[48] $\tilde{p}_j = Z^{-1}\exp(-k^{-1}\beta\varepsilon_j)$

$$K^{KL}(p:\tilde{p}) = -\left(S^{BGS} - \tilde{S}^{BGS}\right) + \beta(E_q - \tilde{E}_q) \geq 0 \tag{90}$$

характеризующее степень отклонения хаотической системы от полного равновесия.

При выполнении условия Гиббса[82] $E_q = \tilde{E}_q$ и с учётом свойства (85) знакоопределённости информации различия $K_{q,r}^{SM}(p:\tilde{p})$ из (89) следуют два неравенства:

$$K_{q,r}^{SM}(p:\tilde{p})Z_{SM}^{1-q} = -\left(S_{q,r}^{SM} - \tilde{S}_{q,r}^{SM}\right) > 0, \text{ если } q>0,\ r<1, \text{ или } q<0, r>1; \quad (91)$$

$$K_{q,r}^{SM}(p:\tilde{p})Z_{SM}^{1-q} = -\left(S_{q,r}^{SM} - \tilde{S}_{q,r}^{SM}\right) < 0, \text{ если } q<0,\ r<1, \text{ или } q>0,\ r>1, \quad (92)$$

которые обобщают теорему Гиббса на неэкстенсивную статистику Шарма−Миттала. Согласно этой теореме, для замкнутой системы энтропия Реньи $S_{q,r}^{SM} = \tilde{S}_{q,r}^{SM} - \tilde{c}_q K_q^{SM}(p:\tilde{p})$ возрастает (убывает) до экстремального её значения $\tilde{S}_{q,r}^{SM}$ при $q>0$ $(q<0)$ одновременно с уменьшением (увеличением) положительной (отрицательной) информации $K_q^{SM}(p:\tilde{p})$. Таким образом, различающая информация представлена здесь в виде отрицательного вклада в текущую энтропию Шарма−Миттала и потому может быть названа негэнтропией[83].

Поскольку информация различия Шарма−Миттала является знакоопределенной функцией Ляпунова, то для того, чтобы состояние равновесия $\tilde{S}_{q,r}^{SM}$ было устойчивым, необходимо выполнение следующих неравенств

$$\frac{d}{dt}K_{q,r}^{SM}(p:\tilde{p})Z_{SM}^{1-q} = -\frac{d\left(S_{q,r}^{SM} - \tilde{S}_{q,r}^{SM}\right)}{dt} < 0, \text{ если } q>0,\ r<1, \text{ или } q<0, r>1; \quad (93)$$

$$\frac{d}{dt}K_{q,r}^{SM}(p:\tilde{p})Z_{SM}^{1-q} = -\frac{d\left(S_{q,r}^{SM} - \tilde{S}_{q,r}^{SM}\right)}{dt} > 0, \text{ если } q<0,\ r<1, \text{ или } q>0,\ r>1. \quad (94)$$

Из этих соотношений следует неравенство для энтропии Шарма−Миттала:

$$dS_{q,r}^{SM}/dt > 0 \quad \text{при } q<0, r>1, \text{ или } q>0,\ r<1, \quad (95)$$

$$dS_{q,r}^{SM}/dt < 0 \quad \text{при } q<0,\ r<1, \text{ или } q>0,\ r>1, \quad (96)$$

которые выражают $H$-теорему для стохастической $q$-системы, описываемой энтропией Шарма−Миттала: при временной эволюции к равновесному состоянию энтропия замкнутой системы может как возрастать до экстремального её значения $\tilde{S}_{q,r}^{SM}$, так и убывать в зависимости от выбора численных значений параметров неэкстенсивности $q$ и $r$.

## 8 ЗАКЛЮЧЕНИЕ

Исследования в области статистической механики и термодинамики неэкстенсивных систем приобрели в настоящее время значительный общетеоретический интерес в связи с проявлениями неэкстенсивных свойств в аномальных физических явлениях и важностью приложений. В настоящей работе даётся логическая схема построения деформированных термодинамик неэкстенсивных систем, основанная на многопараметрической энтропии Шарма−Миттала. В отличие от ряда известных работ (см., например,[72,76,84]), в которых подобные исследования по термостатике проведены с привлечением двукратно деформированных экспоненты и логарифма (введённых первоначально в теории информации Шарма и Митталем в 1975 г.), особенность данной работы состоит в том, что проведено построение обобщённых неэкстенсивных термодинамик с помощью более простых и хорошо изученных однократно деформированных функций − логарифма и экспоненты Тсаллиса.

В работе функционал Шарма−Миттала рассматривается как форматор семейства классической и деформированных однопараметрических энтропий, состоящего из энтропий Реньи, Тсаллиса, Ландсберга−Ведрала, Гаусса и Гиббса. Все эти энтропии связаны равенствами, представляющими чередования обычных (*ln, exp*) и деформированных ($ln_q$, $exp_q$), логарифмов и экспонент. Показано, что энтропия Шарма−Миттала подчиняется псевдоаддитивному закону для двух статистически независимых систем. Найдено универсальное распределение степенного закона на основе максимизации двухпараметрической энтропии Шарма−Миттала при заданных ограничениях на осреднённые значения параметров системы, полученные по нормированному эскортному распределению вероятностей.

Построена на базе статистики Шарма−Миттала двухпараметрическая термодинамика неэкстенсивных систем и показана её взаимосвязь с обобщёнными однопараметрическими термодинамиками, основанными на указанных выше деформированных энтропиях. Получено обобщение нулевого закона термодинамики для двух независимых неэкстенсивных систем при их тепловом контакте, вводящее в рассмотрение так называемую физическую температуру $T_{ph}(p)$ отличающуюся от инверсии множителя Лагранжа $\beta$. Этот факт потребовал переопределения некоторых термодинамических соотношений, получаемых в рамках статистики Шарма−Миттала. В качестве основных предпосылок, взятых за исходный пункт нахождения деформированных термодинамических соотношений в работе были выбраны первый закон термодинамики и структура преобразования Лежандра. Наконец, на основе двухпараметрической информации различия Шарма−Миттала формулируются и доказываются теоремы Гиббса и *H*-теорема об изменении этих мер при эволюции во времени.

Отметим, что полученные таким образом модифицированные термодинамические соотношения соответствуют различным выражениям однопараметрических энтропий из семейства *SM*, имеют общий вид и могут быть использованы при рассмотрении разнообразных термодинамических процессов (необратимости, устойчивости, самоорганизации, фрактальности и т.п.) в замкнутых и открытых хаотических неэкстенсивных системах.

Работа выполнена при поддержке Программы Президиума РАН № 28 и гранта РФФИ № 18-01-00064.

## REFERENCES


[1] J. Havrda, F. Charvat, "Quantiication method of classiication processes. Concept of structural $\alpha$ - entropy", *Kybernetika,* **3**, 30-35 (1967).

[2] Z. Daroczy, "Generalized information functions", *Inf. Control*., **16** (1), 36-51 (1970).

[3] C. Tsallis, "Possible generalization of Boltzmann−Gibbs statistics" *J. Stat. Phys*. **52** (1-2), 479-487 (1988).

[4] Renyi, "On measures of entropy and information", In: Proceedings of the Fourth Berkeley Symposium on Mathematics*, Statistics and Probability*. University California Press. Berkeley. **1**, 547-561 (1961).

[5] Renyi, *Probability Theory*. Amsterdam: North-Holland Publ. Co., 573 (1970).

[6] E. M. F. Curado, C. Tsallis, "Generalized statistical mechanics: connection with thermo- dynamics", *J. Phys. A : Mathematical and General,* **2**4 (2), L69-72 (1991).

[7] Beck, F. Schlögl, *Thermodynamics of chaotic systems: an introduction.* Cambridge: Cambridge University Press. 286 (1993).

[8] E. Borges, I. Roditi, "A family of nonextensive entropies", *Phys. Lett. A*, **246**. 399-402 (1998).

[9] Tsallis, R. Mendes, A. Plastino, "The role of constraints within generalized nonexten- sive statistics", *Physica A*, **261**, 543-554 (1998).

[10] J. Naudts, "Continuity of a class of entropies and relative entropies" *Rev. Math. Phys*. **16**, 809-822 (2004); *Errata. Rev. Math. Phys*. **21**, 947-948 (2004).

[11] Tsallis, *Introduction to Nonextensive Statistical Mechanics. Approaching a Complex World*, New York: Springer, 382 (2009).

[12] Plastino, A.R. Plastino, "On the universality of thermodynamics' Legendre transform structure", *Phys. Lett. A* . **226** (5), 257-263 (1997).

[13] U. Tirnakli, D.F. Torres, "Exact and approximate results of non-extensive quantum statistics", *Eur. J. Phys. B*. **1**4 (4), 691-698 (2000).

[14] E.K. Lenzi, R.S. Mendes, "Collisionless Boltzmann equation for systems obeying Tsal-lis distribution", *Eur. J. Phys. B*. **21** (3), 401-406 (2001).

[15] S. Abe, "Heat and entropy in nonextensive thermodynamics: transmutation from Tsallis theory to Rényi-entropy-based theory", *Physica A: Statistical Mechanics and its Applications*. **300** (3), 417-423 (2001).

[16] T.Wada, A.M. Scarfone, "A non self-referential expression of Tsallis' probability distri- bution function", *Eur. J. Phys. B*. **47** (4), 557-561 (2005).

[17] M. Scarfone, T. Wada, "Equivalence among different formalisms in the Tsallis entropy framework", *Physica A: Statistical Mechanics and its Applications*. **384** (2), 305-317 (2007).

[18] Hanel R., Thurner S., Tsallis C. "Limit distributions of scale-invariant probabilistic models of correlated random variables with the q-Gaussian as an explicit example", *Eur. J. Phys. B*. **72** (2), 263-268 (2009).

[19] A.R. Plastino, M. Casas, A. Plastino, "A nonextensive maximum entropy approach to a family of nonlinear reaction-diffusion equations", *Phys. A.: Statistical Mechanics and its Applications*. **280** (3), 289-303 (2000).

[20] B. M. Boghosian, "Navier-Stocks Equations for Generalized Thermostatistics", *Bras. J. Phys*. **29** (1), 91-107 (1999).

[21] A.□V. Kolesnichenko, B.□N. Chetverushkin, "Kinetic derivation of a quasihydrodinamic system of equations on the base of nonextensive statistics", *Russian Journal of Numerical Analysis and Mathematical Modellin*g. **28**, 547-576 (2013).

[22] T.D. Frank, A. Daffertshofer, "Multivariate nonlinear Fokker-Planck equations and generalized thermostatistics", *Phys. A.: Statistical Mechanics and its Applications*. **292**. (1), 392-410 (2001).

[23] A.M. Mariz, "On the irreversible nature of the Tsallis and Renyi entropies", *Phys. Lett.A*. **165** (5-6), 409-411 (1992).
[24] J.D. Ramshaw, "*H*-theorems for the Tsallis and Renyi entropies", *Phys. Lett.* A. **175**. (3-4), 169-170 (1993).
[25] J.D. Ramshaw, "Irreversibility and generalized entropies", *Phys. Lett*. A. **175** (3-4), 171- 172 (1993).
[26] M.Shiino, "*H*-theorem with generalized relative entropies and the Tsallis statistics", *J. Phys. Soc. Jpn*. **67** (11), 3658-3660 (1998).
[27] T.D. Frank, A. Daffertshofer, "*H*-theorem for nonlinear Fokker-Planck equations relat-ed to generalized thermostatistics", *Physica A: Statistical Mechanics and its Applicati*ons, **295** (3), 455-474 (2001).
[28] N. Ito, C.Tsallis, "Specific heat of the harmonic oscillator within generalized equilibri-um statistics", *Nuovo Cimento D*. **11** (6), 907-911(1989).
[29] Büyükkılıç, D. Demirhan, A. Güleç, "A statistical mechanical approach to general-ized statistics of quantum and classical gases", *Phys. Lett. A*. **197** (3), 209-220 (1995).
[30] P.H. Chavanis, L. Delfini, "Dynamical stability of systems with long-range interactions: application of the Nyquist method to the HMF model", *Eur. Phys. J. B*. **69** (3), 389-429 (2009).
[31] A.V. Kolesnichenko, "Kriteriy termicheskoy ustoychivosti i zakon raspredeleniy chastits dlya samogravitiruyushchikh astrofisicheskikh sistem v ramkakh statistiki Tsallisa", *Mathematica Montisnigri*, **37,** 45-75 (2016).
[32] Esquivel, A. Lazarian, "Tsallis Statistics as a Tool for Studying Interstellar Turbu- lence", *Astrophys. J*. **710** (1), 125-132 (2010).
[33] A.V. Kolesnichenko, "Modifikatsiya v ramkakh statistiki Tsallisa kriteriev gravitatsi-onnoy neustoychivosti astrofisicheskikh diskov s fraktalnoy strukturoy fazovogo prostranstva", *Mathematica Montisnigri*, **32,** 93-118 (2015).
[34] A.V. Kolesnichenko, M.Ya. Marov, "Modification of the jeans instability criterion for fractal-structure astrophysical objects in the framework of nonextensive statistics", *Solar System Research*. **48** (5), 354-365 (2014).
[35] J. Du, "Test of nonextensive statistical mechanics by solar sound speeds", *Europhys Lett*. **75** (6), 861-867 (2006).
[36] R.M. Pickup, R. Cywinski, C. Pappas, B. Farago, P.Fouquet, "Generalized Spin-Glass Relaxation", *Phys. Rev. Lett*. **102** (9), id. 097202 (2009).
[37] A.□V. Kolesnichenko, "On construction of the entropy transport model based on the formalism of nonextensive statistics", *Mathematical Models and Computer Simulations*. **6** (6), 587-597 (2014).
[38] B.B. Mandelbrot,"Intermittent turbulence in self-similar cascades: divergence of high moments and dimension of the carrier", *J. Fluid. Mech*. **62**, 331-358 (1974).
[39] B.B. Mandelbrot, *Les Objects Fractals. Forms, Hazard et Dimension*, Paris: Flammari-on. 195 (1975).
[40] B.B. Mandelbrot, *Fractals: Form, Change and Dimension*. San Francisco: Freeman. 365 (1977).
[41] B.B. Mandelbrot, *The Fractals Geometry of Nature*. New York: Freeman, 460 (1982).
[42] P. Grassberger, "On the Hausdorff dimension of fractal attractors", *J. Statist. Phys*. **26** (1), 173-179 (1981).
[43] P. Grassberger, "Generalizations of the Hausdorff dimension of fractal measures", *Physics Letters A*. **107** (3), 101-105 (1985).
[44] P. Grassberger, I. Procaccia, "Dimensions and entropies of strange attractors from a fluctuating dynamics approach", *Physica D: Nonlinear Phenomena*. **13** (1-2), 34-54 (1984).
[45] T.C. Halsey, M.H. Jensen, L.P. Kadanoff, I. Procaccia, B.I. Shraiman, "Fractal measures and their singularities: The characterization of strange sets", *Phys. Rev. A*. **33**, 1141-1151 (1986).

[46] H.G.E. Hentschel, I. Procaccia, "The infinite number of generalized dimensions of frac- tals and strange attractors", *Physica D: Nonlinear Phenomena*. **8** (3), 435-444 (1983).
[47] B.B. Mandelbrot, *Fraktalnay geometriy prirody*. Moskva: Institut kompyuternykh issledovaniy. 656 (2002).
[48] R.G. Zaripov, *Samoorganizatsiy i neobratimosty v neekstensivnykh sistemakh*, Kazan: Fen. 251 (2002).
[49] R.G. Zaripov, *Printsipy neekstensivnoy statisticheskoy mekhaniki i geometrii mer besporyadka i poryadka.* Kazan: Izdatelstvo Kazanskogo Gosudarstvennogo tekhnicheskogo universiteta. 404 (2010).
[50] P. Jizba, T. Arimitsu, "Observability of Renyi's entropy", *Physical Review E*. **69** (2), id. 026128 (2004).
[51] Bialas, W. Czyz, "Renyi entropies of a black hole from Hawking radiation", *EPL* (*Europhysics Letters*). **83** (6), 60009 (2008).
[52] Á. Nagy, E. Romera, "Maximum Rényi entropy principle and the generalized Thomas− Fermi model", *Physics Letters A*. **373** (8-9), 844-846 (2009).
[53] A.V. Kolesnichenko, "K razrabotre statisticheskoy termodinamiki i tekhniki fraktalnogo analiza dlya neekstensivnykh system na osnove entropii i razlichayushchey informatsii Renyi", *Keldysh Institute Preprints*, **60**, 44 (2018).
[54] I. Aptekarev, J. S. Dehesa, P. Sanchez-Moreno, D. N. Tulyakov, "Asymptotics of $L_p$-norms of Hermite polynomials and Renyi entropy of Rydberg oscillator states", *Contemp. Math*. **578**, 19-29 (2012).
[55] I. Aptekarev, J. S. Dehesa, P. Sanchez-Moreno, D. N. Tulyakov, "Rényi entropy of the infinite well potential in momentum space and Dirichlet-like trigonometric functionals", *J. Math. Chem*. **50**, 1079-1090 (2012).
[56] I. Aptekarev, D. N. Tulyakov, I. V. Toranzo, J. S. Dehesa, "Renyi entropies of the highly-excited states of multidimensional harmonic oscillators by use of strong Laguerre asymptotics", *Eur. Phys. J. B.* **89**, 85-97 (2016).
[57] Tsallis, "Nonextensive Statistics: Theoretical, Experimental and Computational Evidences and Connections", *Brazilian Journal of Physics*. **29** (1), 1-35 (1999).
[58] Tsallis, "Classical and Quantum Complexity and Nonextensive Thermodynamics", *Chaos, Solitons and Fractals*.**13**, 371-391 (2002).
[59] A.V. Kolesnichenko,"K postroeniyu neadditivnoy termodinamiki slozhnykh sistem na osnove statistiki Kurado−Tsallisa", *Keldysh Institute Preprints,* **25**, 40 (2018).
[60] A.V. Kolesnichenko,"K konstruirovaniyu termodinamiki neadditivnykh sred na osnove statistiki Tsallisa−Mendesa−Plastino", *Keldysh Institute Preprints,* **23**, 28 (2018).
[61] R. Zaripov, "Evolution of the Entropy and Renyi Difference Information during Self- Organization of Open Additive Systems", *Russian Physics Journal*. **48** (3), 267-274 (2005).
[62] A.S. Parvan, T. S. Biro,"Thermodynamical limit in non-extensive Renyi statistics", *Physics Letters A*. **340** (5-6), 375-387 (2005).
[63] B.D. Sharma, D.P. Mittal, "New non-additive measures of relative information:, *J. Comb. Inform. & Syst. Sci*. **2**, 122-133 (1975).
[64] T.D. Frank, A.R. Plastino, "Generalized thermostatics based on the Sharma−Mittal entropy and escort mean value", *Eur. Phys. J. B*. **30**, 543-549 (2002).
[65] A.M. Scarfone, T.Wada, "Thermodynamic equilibrium and its stability for microcanon- ical systems described by the Sharma−Taneja−Mittal entropy", *Physical Review E*. **72** (2), id. 026123 (2005).
[66] M. Scarfone, "Thermal and mechanical equilibrium among weakly interacting systems in generalized thermostatistics framework", *Physics Letters A*. **355** (4-5), 404-412 (2006).
[67] Aktürk, G.B. Bagci, R. Sever, "Is Sharma−Mittal entropy really a step beyond Tsallis and Renyi entropies?", *Eprint arXiv: cond-mat*/0703277 (2007).

[68] O. Aktürk, E. Aktürk, M. Tomak, "Can Sobolev Inequality Be Written for Sharma− Mittal Entropy?", *Intern. J. Theor.l Phys*. **47** (12), 3310-3320 (2008).
[69] T.D. Frank, A. Daffertshofer, "Exact time-dependent solutions of the Renyi Fokker− Planck equation and the Fokker-Planck equations related to the entropies proposed by Sharma and Mittal", *Physica A: Statistical Mechanics and its Applications*. **285** (3), 351-366 (2000).
[70] M. Masi, "A step beyond Tsallis and Renyi entropies", *Phys. Lett. A*. **338**, 3-5 (2005).
[71] K. Lenzi, A. M. Scarfone, "Extensive-like and intensive-like thermodynamical variables in generalized thermostatistics", *Physica A: Statistical Mechanics and its Applications.* **391** (8), 2543-2555 (2012).
[72] Kaniadakis, M. Lissia, A. M. Scarfone, "Two-parameter deformations of logarithm, exponential, and entropy: A consistent framework for generalized statistical mechanics", *Physical Review E*, **71** (4), id. 046128 (2005).
[73] Nielsen, R.Nock, "A closed-form expression for the Sharma-Mittal entropy of exponential families", *J. Phys. A: Mathematical and Theoretical*. **45** (3), id. 032003 (2012).
[74] P.T. Landberg, V. Vedral, "Distributions and channel capacities in generalized statisti- cal mechanics", *Phys. Lett. A*". **247**, 211-217 (1998).
[75] K.S. Fa, E.K. Lenzi, "Thermostatistical aspects of generalized entropies", Chaos, Soli- tons and Fractals", **20** (2), 227-233 (2004).
[76] M. Czachor, J. Naudts, "Thermostatistics based on Kolmogorov-Nagumo averages: unifying framework for extensive and nonextensive generalizations", *Phys. Lett. A*. **298** (5-6), 369-374 (2002).
[77] S. Abe, "Remark on the escort distribution representation of nonextensive statistical mechanics", *Physics Letters A,* **275** (4), 250-253 (2000).
[78] E.T. Jaynes, "Information theory and statistical mechanics", In com.: «Statistical Physics». Brandeis Lectures. **3**, 160 (1963).
[79] S. Abe, Y. Eds. Okamoto, *Nonextensive Statistical Mechanicsand Its Applications, Series Lecture Notes in Physics*. Springer: Verlag, Berlin, New York. 540 (2001).
[80] S. Abe, "Heat and generalized Clausius entropy of nonextensive systems", *Eprint arXiv:cond-mat/0012115*. **3**, 1-14 (2000).
[81] V.V. Sychev, *Differenzialnye uravneniya termodinamiki*, Moskva: Vysshaya. shkola. 224 (1991).
[82] Yu.L. Klimontovich. *Turbulent motion and Structure of Chaos,* Kluwer academic Publishers. Dordrecht. 320 (1991).
[83] Shredinger, *Chto takoe zhizn s tochki zreniya* ? − Moskva: Inostrannaya Literatura, 147 (1947).
[84] A.M. Scarfone, "Legendre structure of the thermostatistics theory based on the Sharma Taneja Mittal entropy", *Physica A: Statistical Mechanics and its Applications*, **365** (1), 63-70 (2006).

Received May 25, 2018

MATHEMATICA MONTISNIGRI
Vol XLII (2018)

# 17TH INTERNATIONAL SCIENTIFIC SEMINAR "MATHEMATICAL MODELS AND MODELING IN LASER-PLASMA PROCESSES & ADVANCED SCIENCE TECHNOLOGIES" (LPPM3-2018)

**V.I. MAZHUKIN**

Keldysh Institute of Applied Mathematics of RAS
Moscow, Russia
e-mail: vim@modhef.ru

**Keywords:** Mathematical modeling, laser-plasma processes, laser technologies, laser plasma, laser action, computational mathematics, Russian space, scientific life

**Abstract.** The results of the Seventeenth International Scientific Seminar "Mathematical Models and Modeling in Laser-Plasma Processes & Advanced Science Technologies" (LPPM3-2018), held from 28 May to 1 June 2018 in Montenegro (Budva), were briefly summarized by the program committee of the seminar.

## 1 INTRODUCTION

From May 28 to June 1, 2018, the 17th International Scientific Seminar "Mathematical Models and Modeling in Laser-Plasma Processes & Advanced Science Technologies" (LPPM3-2018) took place in Montenegro, Budva. Figure 1 presents participants of LPPM3-2018 at the opening day. Seminar organizers: Keldysh Institute of Applied Mathematics of Russian Academy of Sciences, A.M. Prokhorov General Physics Institute of Russian Academy of Sciences, University of Montenegro (Podgorica), Forum of University Professors and Researchers of Montenegro, Scientific Journal "Mathematica Montisnigri".

## 2 MAIN CHARACTERISTICS OF THE SEMINAR

More than 70 well-known scientists from Russia, Montenegro, France, Great Britain took part in the Seminar in 2018. From Russia, scientific results were presented by researchers from five Institutes of the Russian Academy of Sciences, six research centers and universities. Montenegro was represented by researchers at the University of Montenegro. France was represented by the University of Paris-Saclay, Great Britain - Queen Mary's University of London.

The seminar still has the information support of the international scientific journal Mathematica Montisnigri. In 2018, the articles on LPPM3-2018 will be published on the pages of 42th and 43th journal's volumes. The publication in the journal of innovative articles that have scientific novelty and passed approbation at the Seminar, contributes to the development of mathematical science, demonstrates to the scientific community the possibilities of the methodology of mathematical modeling.

All reports were made on the main scientific topics within the framework of two sections.

Section I. Laser-plasma processes, laser action.

- Laser ablation - experiment, theory statement of the problem.
- Continuum and atomistic models.

**2010 Mathematics Subject Classification:** 00B20, 00A66, 97M10, 97M50.
**Key words and Phrases:** Proceedings of conferences of general interest, Mathematical Modeling, Computational Mathematics, Laser Technology, Parallel/Distributed Computing, Heterogeneous Computational Technologies, Russian Space, Advanced Science Technology.

- Simulation of various modes of laser action on materials.
- Generation of nanoparticles and nanostructures by ultrashort laser pulses.
- Non-equilibrium low temperature laser plasma.
- Plasma theory and simulation.
- Mathematical modeling and computer experiment in applied problems.

Section II. Advanced science technologies.

- Models and algorithms for high performance computing.
- Models of mathematical physics and complex analysis.
- Russian space.
- Advanced scientific technologies in humanitarian knowledge.
- Mathematical methods in biology.

The seminar traditionally keeps an interdisciplinary focus, based on the scientific methodology of mathematical modeling, which allows to unite scientists working in different subject areas: mathematics, physics, chemistry, biology, medicine, economics, history.

Fig. 1. Participats of the seminar LPPM3-2018 at the opening day.

The main scientific directions of the seminar were formulated in invited papers. One of the main topics discussed was the problems of short-pulse (nanosecond) laser action on condensed media and methods for their solution. Three invited reports were devoted to this area. The sequence of complex phenomena initiated by short nanosecond laser pulses upon irradiation of metal surfaces was considered in two aspects: theoretical and experimental.

According to the results of theoretical studies, the main tool of which is mathematical modeling, in the report [1], presented by the Keldysh Institute of Applied Mathematics of RAS, (Russia), a complex sequence of events that occur during and after the end of the laser pulse was analyzed. The presented results were obtained within the complex of continuum models: 1D - RGD model, conjugated with the multifront model of phase transformations in the Al target.

The problem of studying nanosecond laser ablation with the help of molecular dynamical modeling was considered in the report [2] presented by the A.M. Prokhorov General Physics Institute of RAS (Russia).

The results of an experimental study of nanosecond ablation by laser pulses and their theoretical analysis were presented in an invited paper [3] presented by the University Paris-Saclay (France).

Another discussed direction of the seminar was the problems of developing numerical methods in the context of improving modeling results in various subject areas. The report [4] is devoted to the construction of exact solutions of equations of hyperbolic type containing a discontinuity. The paper shows the construction of discontinuous solutions for the quasilinear transport equation and the system of shallow water equations with the use of the characteristic approach, the urgency of constructing analytical solutions for complex problems of applied importance is noted.

Recently, the topic "Models and algorithms for high-performance computing", which was reinforced in 2018, was presented by an invited report [5]. The report presents effective technology and software solutions on graphics processors (GPU) of the problem of modern oil and gas engineering related to increasing oil recovery of oil reservoirs by preventing the phenomena of unstable (incomplete) oil displacement. Software solutions of the problem are based on the use of distributed computing and parallelization of graphical calculations using modern shader technologies. The proposed technology includes the construction on the GPU of a polygonal isosurface model, its arbitrary flat section, as well as the visualization of the isosurface model in mono and stereo mode.

The traditional topic is "Russian space" within the framework of the section "Advanced science technologies". In the invited report [6] the retrospective and prospects of space research at the Keldysh Institute of Applied Mathematics of RAS (Russia) since the creation of the Soviet R-7 rocket which brought on the orbit world's first Earth artificial satellite to modern international space research projects. During the sectional discussions, the problems of observing space objects, developing observational systems and statistical processing of the obtained data, and modeling problems of operator-controlled robots were considered.

The problems outlined in the invited papers were discussed during the sessions of the sections. The diagram (Figure 2) shows the quantitative characteristics of the reports submitted by scientific organizations for discussion at the sessions of the sections. Among the scientific centers presenting scientific results at the LPPM3 seminar, the Keldysh Institute of Applied Mathematics of RAS has recently retained the leading position in the number of scientific reports submitted. The share of reports submitted by scientists from the University of Montenegro has increased. A consequence of this was a change in the thematic structure of the reports. As compared to 2017, the number of reports devoted to high-performance computing, molecular dynamics modeling, computational methods, models of mathematical physics has increased significantly.

In the topic "Models of mathematical physics and complex analysis " the problems of numerical methods development in context of improvement of simulation results in various subject areas were discussed. In particular the discontinuous Galerkin method for problems with shock waves is discussed [7]. This method has a number of advantages inherent in both finite-element and finite-difference approximations. It provides a given order of accuracy on smooth solutions and can be used for grids of arbitrary structure. Difference schemes of the method of support operators [8] for the equations of the theory of elasticity in displacements are debated. Such approximations preserve the properties of divergence, self-adjointness and sign-definiteness of differential operators, and applicable to the solution of non-stationary problems of hydrodynamics with allowance for elastic processes.

For the numerical solution of three-dimensional diffusion equations a self-adaptive Chebyshev iterative method is presented [9]. This algorithm is capable of evaluating an unknown lower bound of the discrete operator spectrum. It is shown that adaptive procedure ensures the convergence of the adaptive method with computational costs close to the costs of the Chebyshev method, which uses the exact boundaries of the spectrum.

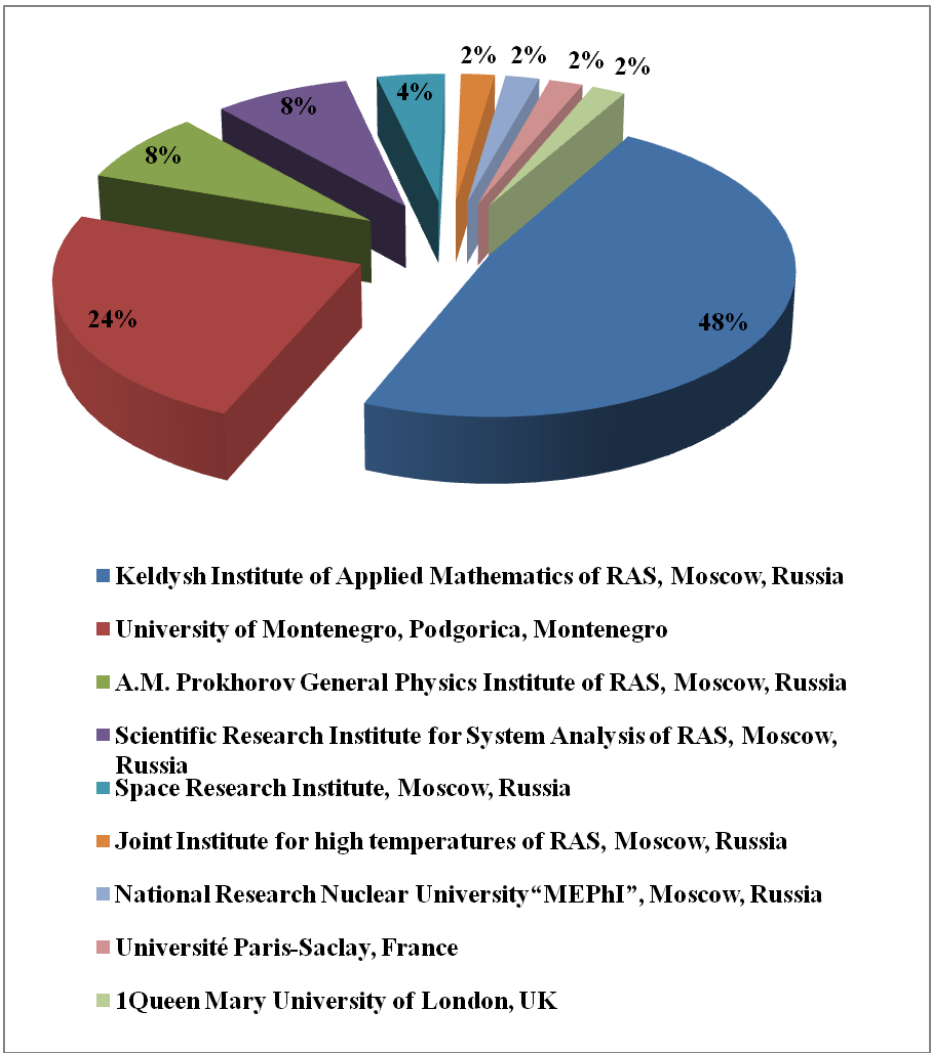


Fig. 2. Structure of reports on scientific organizations of speakers.

The molecular dynamics modeling methodology (MDM) was discussed, and the growing importance in the studies of the atomistic approach associated with the development of computing facilities was noted. A new technique for modeling liquid molecular systems in different spaces and time scales simultaneously with a consistent transition between scales was presented in the report [10]. Within the framework of the molecular dynamics methodology, the results of studies of the properties of metals [11] and semiconductors [12] in the melting range and critical phenomena were presented.

The increase in the share of reports presented by scientists of the University of Montenegro (Fig. 2) reinforced the theme of the fundamental aspects of complex analysis, the n-dimensional bialgebra. The following reports were presented.

- Complex analysis. In this area, the results of studies of various spaces of analytic and harmonic functions were presented [13 - 16];
- Algebra. The results of investigations of various algebraic structures, such as hypernormal rings and semisimple n-dimensional bialgebras, are presented [17, 18];
- Dynamic systems. The results of a study of the motion of particles on a compact Lie group are presented, the swarm model developing on the 3-D sphere [19-21];
- Graph theory. Molecular graphs have been studied in this field [22].

Within the framework of the section "Advanced science technologies" in the topic topic "Mathematical Methods in Biology", the problems of modeling in biomedicine including the problems of multichannel analysis of data, allowing to restore the structure and dynamics of complex systems, such as the human body, including the brain, heart and muscles [23]; modeling of non-stationary processes of infection spread.

Materials of the LPPM3-2018 conference can be found at https://lppm3.ru/historyeng/history-of-programmes .

## 3 SEMINAR DECISIONS

The following decisions were made:

- In every possible way to strengthen and develop international scientific cooperation in the field of application of methods of mathematical modeling;
- To maintain the basic principles of the Seminar, strengthening its interdisciplinary, involving, scientists from various fields of science;
- To hold in 2019 the 18th International Scientific Seminar LPPM3, the 10th held in Montenegro.

Detailed information on the preparation of the seminar, the materials of the speeches and the results of the annual sessions can be found on the website: http://lppm3.ru/.

Chairman of the Program Committee, Professor V.I. Mazhukin.

## 4 REFERENCES

[1] V.I. Mazhukin, M.M.Demin, A.V.Shapranov, A.V. Mazhukin. Dynamics of expansion of a laser-plasma torch during nanosecond ablation of an Al target in an ambient gas. XVII International Seminar Mathematical Model & Modeling in Laser-Plasma Processes & Advanced Science Technologies. Program and Abstracts. Budva, Montenegro, pp.34-36, 2018.

[2] A.A. Samokhin, V.I. Mazhukin, M.M. Demin, A.V. Shapranov, A.E. Zubko. Density fluctuations in nanosecond laser ablation of liquid al film. XVII International Seminar Mathematical Model & Modeling in Laser-Plasma Processes & Advanced Science Technologies. Program and Abstracts. Budva, Montenegro, pp.24-25, 2018.

[3] Semerok, C. Jabbour, J. Simonnet, S.V. Fomichev, J.-L. Lacour, M. Tabarant, F. Chartier. Near-field laser heating of solid samples for nano ablation: modeling and experimental study. XVII International Seminar Mathematical Model & Modeling in Laser-Plasma Processes & Advanced Science Technologies. Program and Abstracts. Budva, Montenegro, p.26, 2018.

[4] V.P. Varin, Yu.A. Kriksin, P.A. Kuchugov, M.E. Ladonkina, O.A. Necliudova, V.F. Tishkin. Construction of exact solutions of some hyperbolic type equations containing discontinuities spread over an uniform background. XVII International Seminar Mathematical Model & Modeling in Laser-Plasma Processes & Advanced Science Technologies. Program and Abstracts. Budva, Montenegro, pp. 32-33, 2018.
[5] M.V. Mikhaylyuk, P.Yu. Timokhin, D.V. Omelchenko. Visualizer of processes of unstable oil displacement from porous media. XVII International Seminar Mathematical Model & Modeling in Laser-Plasma Processes & Advanced Science Technologies. Program and Abstracts. Budva, Montenegro, pp. 37-38, 2018.
[6] G.K. Borovin, A.V. Grushevskii, M.V. Zakhvatkin, G.S. Zaslavsky, V.A. Stepanyantz, A.G. Tuchin, D.A. Tuchin, V.S. Yaroshevsky. Space research in the Keldysh Institute of Applied Mathematics of RAS: past, present, future. XVII International Seminar Mathematical Model & Modeling in Laser-Plasma Processes & Advanced Science Technologies. Program and Abstracts. Budva, Montenegro, pp. 27-31, 2018.
[7] M.E. Ladonkina, O.A. Neklyudova, V.V. Ostapenko, V.F. Tishkin. Research of the accuracy of discontinuous Galerkin method for problems with shock waves. XVII International Seminar Mathematical Model & Modeling in Laser-Plasma Processes & Advanced Science Technologies. Program and Abstracts. Budva, Montenegro, pp. 73-74, 2018.
[8] Yu.A. Poveshchenko, V.A. Gasilov, M.E. Ladonkina, V.O. Podryga. Difference schemes of support operator method for equations of elasticity theory in cylindrical geometry. . XVII International Seminar Mathematical Model & Modeling in Laser-Plasma Processes & Advanced Science Technologies. Program and Abstracts. Budva, Montenegro, pp. 69-70, 2018.
[9] O.B. Feodoritova, V.T. Zhukov, M.M. Krasnov. Self-adaptive Chebyshev iterative method. XVII International Seminar Mathematical Model & Modeling in Laser-Plasma Processes & Advanced Science Technologies. Program and Abstracts. Budva, Montenegro, p. 72, 2018.
[10] I.A. Korotkin, S.A. Karabasov, D.A. Nerukh. Hybrid molecular dynamics – between atomistic and hydrodynamic scales. XVII International Seminar Mathematical Model & Modeling in Laser-Plasma Processes & Advanced Science Technologies. Program and Abstracts. Budva, Montenegro, p. 42, 2018.
[11] V.I. Mazhukin, M.M. Demin, A.A. Aleksashkina. Atomistic modeling of thermophysical properties of copper in a wide temperature range. XVII International Seminar Mathematical Model & Modeling in Laser-Plasma Processes & Advanced Science Technologies. Program and Abstracts. Budva, Montenegro, pp. 40-41, 2018.
[12] O.N. Koroleva, A.V. Mazhukin. Modeling of the silicon thermophysical properties in the region of melting. XVII International Seminar Mathematical Model & Modeling in Laser-Plasma Processes & Advanced Science Technologies. Program and Abstracts. Budva, Montenegro, pp. 43-44, 2018.
[13] Ž. Pavićević. New proof of the theorems picard for analytical and meromorphic function of the complex plane. XVII International Seminar Mathematical Model & Modeling in Laser-Plasma Processes & Advanced Science Technologies. Program and Abstracts. Budva, Montenegro, p. 62, 2018
[14] Romeo Meštrović, Žarko Pavićević. On Privalov spaces on the unit disk as the Hardy-Orlicz classes. XVII International Seminar Mathematical Model & Modeling in Laser-Plasma Processes & Advanced Science Technologies. Program and Abstracts. Budva, Montenegro, p. 80, 2018
[15] Vujadinović Djordjije. Two-sided norm estimate for the Bergman projection on the harmonic Besov space. XVII International Seminar Mathematical Model & Modeling in Laser-Plasma Processes & Advanced Science Technologies. Program and Abstracts. Budva, Montenegro, p. 66, 2018

[16] Marijan Marković. Estimates of harmonic functions. XVII International Seminar Mathematical Model & Modeling in Laser-Plasma Processes & Advanced Science Technologies. Program and Abstracts. Budva, Montenegro, p. 81, 2018
[17] Sanja Jancic Rasovic, Irina Cristea. On a class of d-division hypernear-rings. XVII International Seminar Mathematical Model & Modeling in Laser-Plasma Processes & Advanced Science Technologies. Program and Abstracts. Budva, Montenegro, p. 64, 2018
[18] V.A. Artamonov, B. Zekovich. Pierce decomposition of semisimple n -ary bialgebras. XVII International Seminar Mathematical Model & Modeling in Laser-Plasma Processes & Advanced Science Technologies. Program and Abstracts. Budva, Montenegro, p. 78, 2018
[19] Jacimovic Vladimir. Collective motion of interacting particles on compact Lie groups. XVII International Seminar Mathematical Model & Modeling in Laser-Plasma Processes & Advanced Science Technologies. Program and Abstracts. Budva, Montenegro, p. 65, 2018
[20] Dakić Jelena, Kankaraš Milica. Swarms on the 3-sphere. XVII International Seminar Mathematical Model & Modeling in Laser-Plasma Processes & Advanced Science Technologies. Program and Abstracts. Budva, Montenegro, p. 76, 2018
[21] Kankaraš Milica, Dakić Jelena. Distributed consensus in multi-agent systems on lie groups S3 and SO(3). XVII International Seminar Mathematical Model & Modeling in Laser-Plasma Processes & Advanced Science Technologies. Program and Abstracts. Budva, Montenegro, p. 77, 2018
[22] Goran Popivoda, Žana Kovijanić Vukićević, Vladimir Božović. On some molecular descriptors. XVII International Seminar Mathematical Model & Modeling in Laser-Plasma Processes & Advanced Science Technologies. Program and Abstracts. Budva, Montenegro, p. 88, 2018
[23] S. Rykunov, M. Ustinin. Reconstruction of the functional structure of complex systems by the massive solution of the inverse problems. XVII International Seminar Mathematical Model & Modeling in Laser-Plasma Processes & Advanced Science Technologies. Program and Abstracts. Budva, Montenegro, p. 56, 2018

MATHEMATICA MONTISNIGRI
Vol XLII (2018)

# 17-Й МЕЖДУНАРОДНЫЙ НАУЧНЫЙ СЕМИНАР «МАТЕМАТИЧЕСКИЕ МОДЕЛИ И МОДЕЛИРОВАНИЕ В ЛАЗЕРНО-ПЛАЗМЕННЫХ ПРОЦЕССАХ & ПЕРЕДОВЫХ НАУЧНЫХ ТЕХНОЛОГИЯХ» (LPPM3-2018)

**В.И. МАЖУКИН**

Институт прикладной математики им. М.В. Келдыша РАН
Москва, Россия
e-mail: vim@modhef.ru

**Ключевые слова:** Математическое моделирование, лазерно-плазменные процессы, лазерные технологии, лазерная плазма, лазерное воздействие, вычислительная математика, Русский космос, научная жизнь

**Аннотация.** Результаты Семнадцатого Международного научного семинара «Математические модели и моделирование в лазерно-плазменных процессах & передовых научных технологиях» (LPPM3-2018), проходившего 28 мая по 1 июня 2018 года в Черногории (г.Будва), кратко обобщены программным комитетом семинара.

## 1 ВВЕДЕНИЕ

С 28 мая по 1 июня 2018 года в городе Будва (Черногория) состоялся 17-й Международный научный семинар «Математические модели и моделирование в лазерно-плазменных процессах & Передовых научных технологиях» (LPPM3-2017) На рис.1 представлена фотография участников семинара LPPM3-2018 в день открытия. Организаторы семинара: Институт прикладной математики им. М.В. Келдыша Российской академии наук, Институт общей физики им. А.М. Прохорова Российской академии наук, Университет Черногории (Подгорица), Форум профессоров и исследователей Черногории, Научный журнал «Mathematica Montisnigri».

## 2 ОСНОВНЫЕ ХАРАКТЕРИСТИКИ СЕМИНАРА

В работе Семинара 2018 года приняли участие более 70 известных ученых из России, Черногории, Франции, Великобритании. Из России научные результаты были представлены исследователями пяти Институтов Российской Академии Наук, шести научных центров и университетов. Черногорию представляли исследователи Университета Черногории. Франция была представлена университетом Париж-Саклай, Великобритания – Лондонским университетом королевы Марии.

По-прежнему Семинар получает информационную поддержку научного журнала «Mathematica Montisnigri». По докладам, вызвавшим наибольший интерес участников Семинара в 2018 году, на страницах 42 и 43 томов журнала будут опубликованы статьи. Публикация на страницах журнала инновационных статей, обладающих научной новизной и прошедших апробацию на Семинаре, вносит вклад в развитие

**2010 Mathematics Subject Classification:** 00B20, 00A66, 97M10, 97M50.
**Key words and Phrases:** Proceedings of conferences of general interest, Mathematical Modeling, Computational Mathematics, Laser Technology, Parallel/Distributed Computing, Heterogeneous Computational Technologies, Russian Space, Advanced Science Technology.

математической науки, демонстрирует научному сообществу возможности методологии математического моделирования.

Рис. 1. Участники семинара LPPM3-2018 в день открытия.

Все доклады были сделаны по основным научным темам в рамках двух секций

Секция I. Лазерно-плазменные процессы, лазерное воздействие.

– Лазерная абляция - эксперимент, теория, постановки задач.
– Континуальные и атомистические модели.
– Моделирование различных режимов лазерного воздействия на материалы.
– Генерация наночастиц и наноструктур ультракороткими лазерными импульсами.
– Неравновесная низкотемпературная лазерная плазма.
– Теория плазмы и вычислительный эксперимент.
– Математическое моделирование и вычислительный эксперимент в прикладных проблемах

Секция II. Передовые научные технологии.

– Модели и алгоритмы для высокопроизводительных вычислений
– Модели математической физики и комплексный анализ.
– Русский космос.
– Передовые научные технологии в гуманитарных знаниях.
– Математические методы в биомедицине.

Семинар традиционно сохраняет междисциплинарную направленность, основывающуюся на научной методологии математического моделирования, которая позволяет объединить ученых работающих в различных предметных областях: математике, физике, химии, биологии, медицине, экономике, истории.

Основные научные направления семинара были сформулированы в приглашенных докладах. Одним из основных обсуждаемых направлений стали проблемы короткоимпульсного (наносекундного) лазерного воздействия на конденсированные среды и методы их решения. Этому направлению было посвящено три приглашенных доклада. Последовательность сложных явлений, инициируемых короткими наносекундными лазерными импульсами при облучении металлических поверхностей, была рассмотрена в двух аспектах: теоретическом и экспериментальном.

По результатам теоретических исследований, основным инструментом которых является математическое моделирование, в докладе [1], представленном ИПМ им. М.В. Келдыша РАН (Россия), была проанализирована сложная последовательность событий, которые происходят во время и после окончания лазерного импульса. Представленные результаты были получены в рамках комплекса континуальных моделей: 1D – РГД модели, сопряженной с многофронтовой моделью фазовых превращений в Al мишени.

Проблема исследования наносекундной лазерной абляции с помощью молекулярно динамического моделирования была рассмотрена в докладе [2], представленном ИОФ им. А.М. Прохорова РАН (Россия).

Результаты экспериментального исследования наносекундной абляции лазерными импульсами и их теоретический анализ были представлены в приглашенном докладе [3], представленном Университетом Париж-Саклай (Франция).

Другим обсуждаемым направлением семинара стали проблемы разработки численных методов в контексте улучшения результатов моделирования в различных предметных областях. Построению точных решений уравнений гиперболического типа, содержащих разрыв, посвящен доклад [4]. В докладе показано построение разрывных решений для квазилинейного уравнения переноса и системы уравнений мелкой воды с использованием характеристического подхода, отмечается актуальность построения аналитических решений для сложных задач, имеющих прикладное значение.

Недавно появившееся на семинаре, но усилившееся в 2018 году, направление «Модели и алгоритмы для высокопроизводительных вычислений», было представлено приглашенным докладом [5]. В докладе представлена эффективная технология и программные решения на графических процессорах (GPU) проблемы современного нефтегазового инжиниринга, связанной с повышением нефтеотдачи нефтеносных пластов за счет предотвращения явлений неустойчивого (неполного) вытеснения нефти. Программные решения проблемы основаны на использовании распределенных вычислений и распараллеливании графических расчетов с помощью современных шейдерных технологий. Предлагаемая технология включает в себя построение на GPU полигональной модели изоповерхности, ее произвольного плоского сечения, а также визуализацию модели изоповерхности в моно- и стереорежиме.

Традиционной на семинаре стала тематика «Русский космос». Приглашенный доклад [6], показал ретроспективу и перспективы исследований космической тематики в ИПМ им. М.В. Келдыша РАН (Россия) от периода создания ракеты-носителя Р-7, которая вывела на земную орбиту первый в мире искусственный спутник Земли, до современных международных проектов исследования космоса. В ходе секционных обсуждений рассматривались проблемы наблюдения за космическими объектами, развития систем наблюдения и статистической обработки полученных данных, проблемы моделирования управляемых оператором роботов.

Проблемы, намеченные в приглашенных докладах, обсуждались в ходе заседаний секций. На диаграмме (рис. 2) показана количественная характеристика докладов, представленных научными организациями для обсуждения на заседаниях секций. Первенство по количеству представленных научных докладов на семинаре LPPM3 в 2018 году среди научных центров сохраняет Институт прикладной математики им. М.В. Келдыша РАН. Следствием этого стало изменение тематической структуры докладов. По сравнению с 2017 годом значительно увеличилось количество докладов посвященных высокопроизводительным вычислениям, молекулярно-динамическому моделированию, вычислительным методам, моделям математической физики.

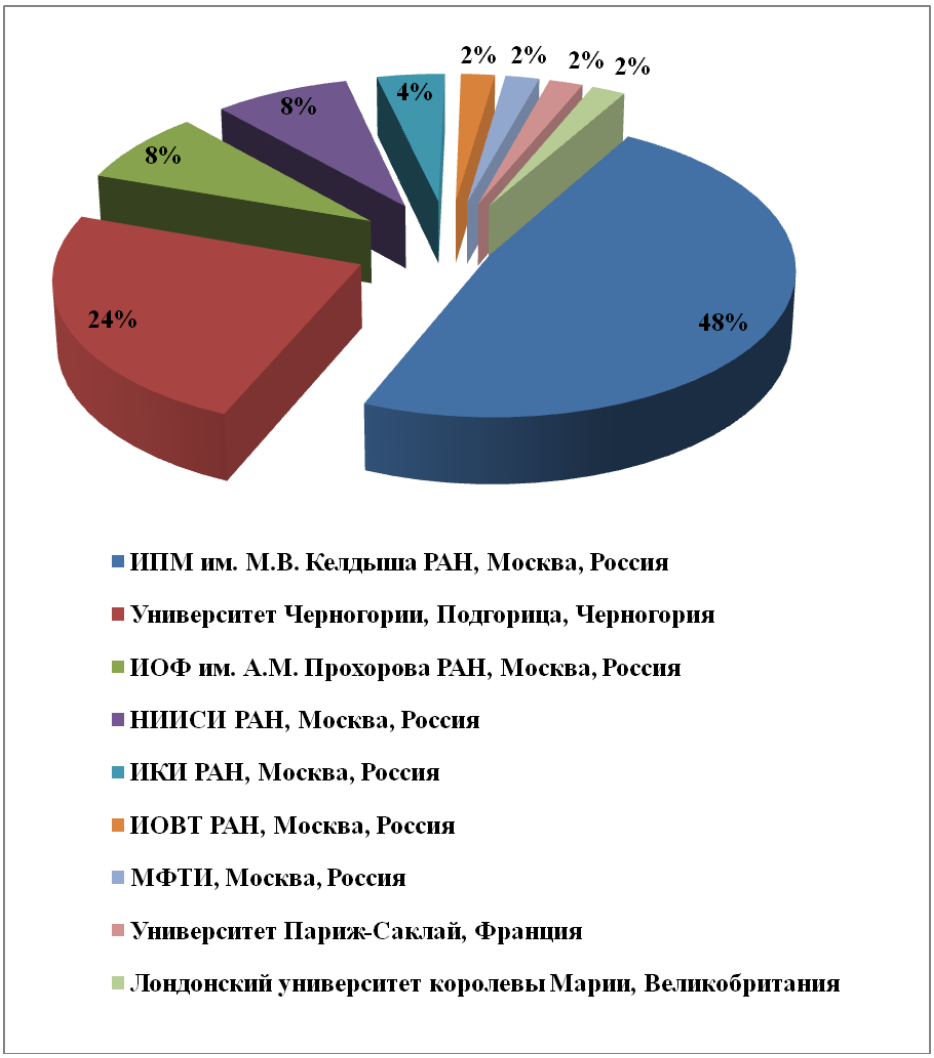


Рис. 2. Структура докладов по научным организациям докладчиков.

В разделе «Модели математической физики и и комплексный анализ» обсуждались проблемы разработки численных методов в контексте улучшения результатов моделирования в различных предметных областях. В частности, обсуждался разрывный метод Галеркина для задач с ударными волнами [7]. Этот метод имеет ряд преимуществ, присущих как конечно-элементным, так и конечно-разностным

приближениям. Он обеспечивает заданный порядок точности на гладких решениях и может использоваться для сеток произвольной структуры. Обсуждались разностные схемы метода опорных операторов [8] для уравнений теории упругости в смещениях. Такие аппроксимации сохраняют свойства расходимости, самосопряженности и знакоопределенности дифференциальных операторов и применимы к решению нестационарных задач гидродинамики с учетом упругих процессов. Для численного решения трехмерных уравнений диффузии представлен самоадаптивный итерационный метод Чебышева [9]. Этот алгоритм способен оценить неизвестную нижнюю границу дискретного спектра оператора. Показано, что адаптивная процедура обеспечивает сходимость адаптивного метода с вычислительными затратами, близкими к затратам метода Чебышева, который использует точные границы спектра.

Обсуждалась молекулярно-динамическая методология моделирования (МДМ), было отмечено возрастающее значение в исследованиях атомистического подхода, связанного с развитием вычислительных средств. Новая методика моделирования жидких молекулярных систем в разных пространствах и временных масштабах одновременно с последовательным переходом между масштабами была представлена в докладе [10]. В рамках молекулярно-динамической методологии были представлены результаты исследований свойств металлов [11] и полупроводников [12] в области плавления и критических явлений.

Увеличение доли докладов, представленных учеными Университета Черногории (рис.2) усилило тематику фундаментальных аспектов комплексного анализа, n-мерной биалгебры. Были представлены доклады по следующим направлениям.

• Комплексный анализ. В этой области были представлены результаты исследований различных пространств аналитических и гармонических функций [13 - 16];

• Алгебра. Представлены результаты исследований разных алгебраических структур, таких как гипернормальные кольца и полупростые n-мерные биалгебры [17, 18];

• Динамические системы. Представлены результаты исследования движения частиц на компактной группе Ли, модель роя развивающуюся на 3-D сфере [19 -21]

• Теория графов. В этой области исследовались молекулярные графы [22].

В рубрике «Математические методы в биологии» рассматривалось проблемы моделирования в биомедицине, в том числе проблемы многоканального анализа данных, позволяющего восстановить структуру и динамику сложных систем, таких как человеческое тело, включая мозг, сердце и мышцы [23]; моделирования нестационарных процессов распространения инфекций.

Материалы выступлений участников конференции LPPM3-2018 можно найти на сайте https://lppm3.ru/en/historyeng/history-of-programmes.

## 3 РЕШЕНИЯ СЕМИНАРА

Были приняты следующие решения:

- всемерно усиливать и развивать международное научное сотрудничество в области применения методов математического моделирования;
- поддерживать основные принципы Семинара, усиливая его междисциплинарность, привлекая для этого ученых из различных областей науки;

– провести в 2019 году 18-й Международный научный семинар LPPM3, десятый в Черногории.

Подробную информацию о подготовке семинара, материалах выступлений и итогах ежегодных сессий можно найти на сайте: http://lppm3.ru/.

Председатель Программного Комитета, профессор В.И. Мажукин.

## 4 REFERENCES


[1] V.I. Mazhukin, M.M.Demin, A.V.Shapranov, A.V. Mazhukin. Dynamics of expansion of a laser-plasma torch during nanosecond ablation of an Al target in an ambient gas. XVII International Seminar Mathematical Model & Modeling in Laser-Plasma Processes & Advanced Science Technologies. Program and Abstracts. Budva, Montenegro, pp.34-36, 2018.

[2] A.A. Samokhin, V.I. Mazhukin, M.M. Demin, A.V. Shapranov, A.E. Zubko. Density fluctuations in nanosecond laser ablation of liquid al film. XVII International Seminar Mathematical Model & Modeling in Laser-Plasma Processes & Advanced Science Technologies. Program and Abstracts. Budva, Montenegro, pp.24-25, 2018.

[3] Semerok, C. Jabbour, J. Simonnet, S.V. Fomichev, J.-L. Lacour, M. Tabarant, F. Chartier. Near-field laser heating of solid samples for nano ablation: modeling and experimental study. XVII International Seminar Mathematical Model & Modeling in Laser-Plasma Processes & Advanced Science Technologies. Program and Abstracts. Budva, Montenegro, p.26, 2018.

[4] V.P. Varin, Yu.A. Kriksin, P.A. Kuchugov, M.E. Ladonkina, O.A. Necliudova, V.F. Tishkin. Construction of exact solutions of some hyperbolic type equations containing discontinuities spread over an uniform background. XVII International Seminar Mathematical Model & Modeling in Laser-Plasma Processes & Advanced Science Technologies. Program and Abstracts. Budva, Montenegro, pp. 32-33, 2018.

[5] M.V. Mikhaylyuk, P.Yu. Timokhin, D.V. Omelchenko. Visualizer of processes of unstable oil displacement from porous media. XVII International Seminar Mathematical Model & Modeling in Laser-Plasma Processes & Advanced Science Technologies. Program and Abstracts. Budva, Montenegro, pp. 37-38, 2018.

[6] G.K. Borovin, A.V. Grushevskii, M.V. Zakhvatkin, G.S. Zaslavsky, V.A. Stepanyantz, A.G. Tuchin, D.A. Tuchin, V.S. Yaroshevsky. Space research in the Keldysh Institute of Applied Mathematics of RAS: past, present, future. XVII International Seminar Mathematical Model & Modeling in Laser-Plasma Processes & Advanced Science Technologies. Program and Abstracts. Budva, Montenegro, pp. 27-31, 2018.

[7] M.E. Ladonkina, O.A. Neklyudova, V.V. Ostapenko, V.F. Tishkin. Research of the accuracy of discontinuous Galerkin method for problems with shock waves. XVII International Seminar Mathematical Model & Modeling in Laser-Plasma Processes & Advanced Science Technologies. Program and Abstracts. Budva, Montenegro, pp. 73-74, 2018.

[8] Yu.A. Poveshchenko, V.A. Gasilov, M.E. Ladonkina, V.O. Podryga. Difference schemes of support operator method for equations of elasticity theory in cylindrical geometry. . XVII International Seminar Mathematical Model & Modeling in Laser-Plasma Processes & Advanced Science Technologies. Program and Abstracts. Budva, Montenegro, pp. 69-70, 2018.

[9] O.B. Feodoritova, V.T. Zhukov, M.M. Krasnov. Self-adaptive Chebyshev iterative method. XVII International Seminar Mathematical Model & Modeling in Laser-Plasma Processes & Advanced Science Technologies. Program and Abstracts. Budva, Montenegro, p. 72, 2018.

[10] I.A. Korotkin, S.A. Karabasov, D.A. Nerukh. Hybrid molecular dynamics – between atomistic and hydrodynamic scales. XVII International Seminar Mathematical Model & Modeling in Laser-Plasma Processes & Advanced Science Technologies. Program and Abstracts. Budva, Montenegro, p. 42, 2018.

[11] V.I. Mazhukin, M.M. Demin, A.A. Aleksashkina. Atomistic modeling of thermophysical properties of copper in a wide temperature range. XVII International Seminar Mathematical Model & Modeling in Laser-Plasma Processes & Advanced Science Technologies. Program and Abstracts. Budva, Montenegro, pp. 40-41, 2018.
[12] O.N. Koroleva, A.V. Mazhukin. Modeling of the silicon thermophysical properties in the region of melting. XVII International Seminar Mathematical Model & Modeling in Laser-Plasma Processes & Advanced Science Technologies. Program and Abstracts. Budva, Montenegro, pp. 43-44, 2018.
[13] Ž. Pavićević. New proof of the theorems picard for analytical and meromorphic function of the complex plane. XVII International Seminar Mathematical Model & Modeling in Laser-Plasma Processes & Advanced Science Technologies. Program and Abstracts. Budva, Montenegro, p. 62, 2018
[14] Romeo Meštrović, Žarko Pavićević. On Privalov spaces on the unit disk as the Hardy-Orlicz classes. XVII International Seminar Mathematical Model & Modeling in Laser-Plasma Processes & Advanced Science Technologies. Program and Abstracts. Budva, Montenegro, p. 80, 2018
[15] Vujadinović Djordjije. Two-sided norm estimate for the Bergman projection on the harmonic Besov space. XVII International Seminar Mathematical Model & Modeling in Laser-Plasma Processes & Advanced Science Technologies. Program and Abstracts. Budva, Montenegro, p. 66, 2018
[16] Marijan Marković. Estimates of harmonic functions. XVII International Seminar Mathematical Model & Modeling in Laser-Plasma Processes & Advanced Science Technologies. Program and Abstracts. Budva, Montenegro, p. 81, 2018
[17] Sanja Jancic Rasovic, Irina Cristea. On a class of d-division hypernear-rings. XVII International Seminar Mathematical Model & Modeling in Laser-Plasma Processes & Advanced Science Technologies. Program and Abstracts. Budva, Montenegro, p. 64, 2018
[18] V.A. Artamonov, B. Zekovich. Pierce decomposition of semisimple n -ary bialgebras. XVII International Seminar Mathematical Model & Modeling in Laser-Plasma Processes & Advanced Science Technologies. Program and Abstracts. Budva, Montenegro, p. 78, 2018
[19] Jacimovic Vladimir. Collective motion of interacting particles on compact Lie groups. XVII International Seminar Mathematical Model & Modeling in Laser-Plasma Processes & Advanced Science Technologies. Program and Abstracts. Budva, Montenegro, p. 65, 2018
[20] Dakić Jelena, Kankaraš Milica. Swarms on the 3-sphere. XVII International Seminar Mathematical Model & Modeling in Laser-Plasma Processes & Advanced Science Technologies. Program and Abstracts. Budva, Montenegro, p. 76, 2018
[21] Kankaraš Milica, Dakić Jelena. Distributed consensus in multi-agent systems on lie groups S3 and SO(3). XVII International Seminar Mathematical Model & Modeling in Laser-Plasma Processes & Advanced Science Technologies. Program and Abstracts. Budva, Montenegro, p. 77, 2018
[22] Goran Popivoda, Žana Kovijanić Vukićević, Vladimir Božović. On some molecular descriptors. XVII International Seminar Mathematical Model & Modeling in Laser-Plasma Processes & Advanced Science Technologies. Program and Abstracts. Budva, Montenegro, p. 88, 2018
[23] S. Rykunov, M. Ustinin. Reconstruction of the functional structure of complex systems by the massive solution of the inverse problems. XVII International Seminar Mathematical Model & Modeling in Laser-Plasma Processes & Advanced Science Technologies. Program and Abstracts. Budva, Montenegro, p. 56, 2018